Cluster synchronization in delayed and multiplex networks

A THESIS

Submitted in partial fulfillment of the requirements for the award of the degree

of

DOCTOR OF PHILOSOPHY

by

Aradhana Singh

DISCIPLINE OF PHYSICS

INDIAN INSTITUTE OF TECHNOLOGY INDORE

February 2015

INDIAN INSTITUTE OF TECHNOLOGY INDORE

CANDIDATE'S DECLARATION

I hereby certify that the work which is being presented in the thesis entitled **"Cluster synchronization in delayed and multiplex networks"** in the partial fulfillment of the requirements for the award of the degree of **DOCTOR OF PHILOSOPHY** and submitted in the **DISCIPLINE OF PHYSICS, Indian Institute of Technology Indore**, is an authentic record of my own work carried out during the time period from January 2011 to February 2015 submission under the supervision of Dr. Sarika Jalan, Associate Professor, Indian Institute of Technology Indore.

The matter presented in this thesis has not been submitted by me for the award of any other degree of this or any other institute.

(Aradhana Singh)

This is to certify that the above statement made by the candidate is correct to the best of my/our knowledge.

(Dr. Sarika Jalan)

Aradhana Singh has successfully given her Ph.D. Oral Examination held on **……………………..**

Signature of Thesis Supervisor
Date:

Convener, DPGC
Date:

Signature of PSPC Member
Date:

Signature of PSPC Member
Date:

Signature of External Examiner
Date:

DEDICATED

TO

MY FAMILY

Acknowledgements

I wish to place on record my deep sense of gratitude and reverence to my supervisor Dr. Sarika Jalan for making me a member of the Complex Systems Lab. I have enjoyed learning physics with her and find myself very lucky for having been associated with such a good researcher.

I thank my PSPC committee members and Convener, DPGC Dr. Rajesh Kumar for their valuable suggestions.

I am very much grateful to Dr. J. Kurths, for his suggestions, which lead to the qualitative improvements in my research work. I take this opportunity to thank Drs. Abhijeet Sen, C. K. Hu and G. Ambika for insightful discussions.

I would like to thank all the faculty members and staff members of the Physics Discipline IIT Indore for their help and support.

My sincere thanks to all the members of the Complex Systems Lab - Sanjiv, Camellia, Aparna, Alok, Amit, Pramod, Saptarshi, Animesh and past members- Ankit, Anagha, Krishna, and Vipin. They were always ready to help me. I specially thank Amit and Camellia, who has helped me a lot in formatting this thesis. I have enjoyed fruitful discussion with all my lab-mates. My best wishes to all of you.

I would also like to thank my friends- Tamalika, Ankita, Raina, Anuradha, Mukta, Veenu, Ankita, Anubha and Fozia for their help and support throughout my PhD tenure at IIT Indore.

Lastly, my life is indebted to my Mammy, Papa, Badi dee, Chhotu and Kuku for their unconditional love and support. I would also like to thank Navin Bhaiya, Arvind and Mahesh for their help and constant motivation. Without them I would have not got the chance to be a part of this research world.

Aradhana Singh

Abstract

The thesis describes the cluster synchronization in undelayed and delayed 1-d lattice, random networks, scale-free, small-world, Cayley tree and complete bipartite networks. Synchronization is an emergent phenomenon where the coupled units adjust their trajectories in some similar manner. Our thoughts, action, motion, perceptions all are controlled by the synchronization of neurons in the brain. Additionally synchronization plays very important role in electric power systems, digital audio, video, inscription in telecommunication, metabolic systems etc and has motivated an intense research in these systems. Synchronization can be global as well as local. The local synchronization leads to the cluster formation which is desired in some cases such as in the neural networks and undesired in some cases such as power grid networks, and thus has drawn tremendous attention the last decade. Furthermore, the finite speed of information transmission leads to time delay, which plays a vital role in synchronization. Additionally, in real world networks, due to signal travelling different distances, rate of information transmission can be different for different units, which leads to the heterogeneity in delay values. A delay may give rise to many new phenomena in dynamical systems such as stabilizing periodic orbits, enhancement or suppression of synchronization, chimera state, etc. The heterogeneous delays being more realistic have shown to maximize the stability of the uniform flow, which is good for traffic dynamics, and show higher-order chaos which can be used to have a more secured communication in chaos based encryption systems. In case of the food web it has been shown that the homogeneous delays lead to destabilization of the system, which may lead to the extinction of a particular species, while the distributed delays are known to yield larger stability regimes, closely resembling to the undelayed systems. The earlier works on the coupled maps have shown two main mechanisms of cluster formation, (1) Driven

(D) and (2) Self-organization (SO). SO synchronization refers to the state when clusters are formed due to intra-cluster couplings, and D synchronization refers to the state when clusters are formed due to inter-cluster couplings. However, none of the studies so far have focused on the impact of delay on cluster synchronization and mechanism behind the cluster synchronization. For the formulation of the facts to achieve the above goal following aims are clarified in this thesis:

Objectives

(a) To study the impact of the network architecture on the mechanism of cluster formation.

(b) To study the role of delay in the mechanism of cluster formation.

(c) To study the impact of heterogeneous delays on the cluster synchronization and mechanism behind the formation of the synchronized clusters.

(d) To study the impact of multiplexing on the cluster synchronizability of a network.

Summary of the Work Done

(1) **Cluster synchronization in networks without delay:**

The first chapter of this thesis presents the impact of network architecture on the mechanism of cluster formation for undelayed coupled maps. In order to explore the relations between dynamical clusters and network clusters, we study coupled maps on various networks generated with a simple rewiring strategy. Starting with a network having two complete sub-graphs, nodes are rewired at each step such that after few rewiring steps, we get a complete bi-partite network. The rewiring strategy is adopted such that the average degree of the networks at each rewiring step remains of the order of N. Coupled dynamical evolution at each rewiring step leads to the different cluster patterns. The smaller coupling strength region shows D clusters independent of the network rewiring strategies, whereas larger coupling strength region depicts a transition from the SO cluster to the D clusters as network connections are rewired to the bi-partite type. The Lyapunov function analysis is performed to understand the dynamical origin of cluster formation. The results provide insights into the relationship between the topological clusters which are based on the direct connections between the nodes and the dynamical clusters which are based on the functional behavior of these nodes.

(2) **Impact of delay on mechanism of cluster formation:**

The second chapter explores an impact of the delayed communication on the cluster synchronization of the coupled maps. This chapter reveals that delay may affect the cluster formation and the mechanism behind the cluster formation in different ways. At the weak couplings, parity of delay value has prominent impact on the mechanism behind the cluster formation, the same parity of delays are associated with the same mechanism of the cluster formation, as well as manifest similar type of the dynamical evolution. As coupling is increased, introducing a delay may destroy self-organized clusters leaving driven synchronization of nodes intact as found for the complete bipartite network or may enhance driven synchronization as is elucidated for other networks. We provide analytical understanding of this behavior using the Lyapunov function analysis. To the end, we relate the results with conflicts and cooperations observed in the family business.

(3) **More heterogeneity, more coherence:**

The third chapter investigates cluster synchronization in the coupled map networks in presence of heterogeneity in delay the values. We find that while the parity of heterogeneous delays plays a crucial role in determining the mechanism of the cluster formation, the cluster synchronizability of the network gets affected by the amount of the heterogeneity. In addition, the heterogeneity in delays induces a rich cluster pattern as compared to the homogeneous delays. The complete bipartite network stands as an extreme example of this richness, where robust ideal driven clusters observed for the undelayed and homogeneously delayed cases dismantle, yielding versatile cluster patterns as heterogeneity in the delay values is introduced. We provide arguments behind this behavior using the Lyapunov function analysis. Further, the interplay between the number of connections in the network and the amount of heterogeneity plays an important role in deciding the mechanism of cluster formation.

Furthermore, heterogeneity in delays leads to the lag synchronization among the siblings lying on the boundary of coupled maps on the Cayley tree network, by destroying the exact synchronization among them. The value of the time lag is equal to the difference in the delay values. To the end we discuss the relevance of these results with respect to their applications in the family business as well as in understanding the occurrence of genetic diseases.

(4) **Cluster synchronization in multiplex networks:**
In this chapter, the impact of interaction of nodes in a layer of the multiplex network on the dynamical behavior and cluster synchronizability of other layers has been explored. We find that interactions in one layer affects the cluster synchronizability of another layer in many different ways. While multiplexing with a sparse network enhances the synchronizability, multiplexing with a dense network suppresses the cluster synchronizability with the network architecture deciding the impact of the enhancement and suppression. Additionally, at weak couplings, the enhancement in the cluster synchronizability, due to the multiplexing, remains of the driven type while for strong couplings, the multiplexing may lead to a transition to the self-organized mechanism.

Keywords : Synchronization, Delay, Networks, Spatio-temporal chaos, Coupled maps.

List of Publications

(1) Singh, A., and Jalan, S., (2012), Transition from the self-organized to the driven dynamical clusters Physica A **391**, 6655-6663 (DOI: 10.1016/j.physa.2012.07.055).

(2) Singh, A., Jalan S., and Kurths, J., (2013), Role of delay in mechanism of cluster formation, Phys. Rev. E **87**, 030902(R)-4 (DOI: 10.1103/PhysRevE.87.030902).

(3) Singh, A., and Jalan, S., (2013), Delay-induced driven patters in coupled Caley tree networks, EPJ-ST **222**, 885-893 (DOI: 10.1140/epjst/e2013-01891-2).

(4) Singh, A., and Jalan, S., (2014), Heterogeneous delays making parents synchronized: A coupled maps on Cayley tree model, AIP Advances **4**, 067111-14 (DOI: 10.1063/1.4881978).

(5) Jalan, S., and Singh, A., (2014), Impact of heterogeneous delay on cluster synchronization, Phys. Rev. E **90**, 042907-9 (DOI: 10.1103/PhysRevE.90.042907).

(6) Jalan, S., Singh, A., Acharyya, S., and Kurths, J., (2015), Impact of leader on cluster synchronization, Phys. Rev. E **91**, 022901-5 (DOI: 10.1103/PhysRevE.91.022901).

(7) Jalan, S., and Singh, A., Cluster synchronization in Multiplex networks, arXiv:1412.5261 (Under Review).

Table of Contents

List of Figures

Chapter 1

Introduction

Synchronization is one of the most important phenomenon shown by many real-world systems. The word synchronization is composed of the Greek words ‘syn’, meaning together and ‘khronos’ which means time. In synchronization, the coupled units adjust their trajectories in a similar manner [1]. This phenomenon was first observed by Christian Huygens in 1665, when he found that two pendulum clocks, suspended by the side of each other, swung in anti-phase with exactly the same frequency [2]. This anti-phase synchronous state caused by the tiny coupling from the imperceptible movements of a common frame, was robust against external perturbations. Here are some examples of the real world system where synchronization is the not only observed but is prime factor for proper functioning of underlying systems.

Different metabolic processes in our body are performed by the synchronization of the cells [3, 4]. In the brain, synchronization of neural assemblies is responsible for our motion, vision, thoughts and perception [5, 6]. Furthermore, in the social systems the synchronization of two individuals can be caused by the synchronization of two individuals brain activities by external stimuli such as viewing a movie or listening to a song [7, 8]. Another system in which synchronization plays a vital role is power grid networks [9]. These networks consist of thousand of power substations and generators which are linked across thousand of kilometres [10, 11]. The synchronization of power generators keeps all connected generators in pace which, is necessary for the stability in the power grid systems. The desynchronization of the generators caused by the disturbances can lead to instability [12, 13].

Synchronization of pedestrian foot steps is another example of synchronization phenomenon in day-today life. Seemingly a very simple phenomenon, it surprised everyone on $10th$ of June 2000 in London on the day of opening ceremony of the London Millennium Bridge. The bridge started oscillating due to the synchronization of pedestrian foot steps [14, 15].

Other examples include blinking behaviour of fireflies. On riverbanks in South-East Asia, the synchronization of the flashes emitted by male fireflies emerges from a seemingly chaotic situation [16]. Furthermore, the coupled lasers can synchronize to lock their optical phases which is desired in communication systems [17–19].

Synchronization has been observed in almost all the fields of science and engineering such as physics, chemistry, biology, ecology, sociology and technology [1, 14, 20–23].

1.0.1 Networks

Starting from a living cell, which is a complex network of chemicals connected by chemical reactions, networks exist everywhere in the universe. The networks can be physical objects in the Euclidean space such as electric power grids, transport networks, neural networks etc, or can be defined in metaphysical space such as the networks of actors [24], collaborations between individuals, networks of citations [25] etc.

Definition: Mathematical properties of networks are described by graphs. A graph is a pair of sets (V, E), where V is a set of vertices (nodes), and E is a set of edges (links) between the vertices [26]. A graph is represented by an adjacency matrix, A_{ij}, which is a matrix in which:

$$A_{ij} = \begin{cases} 1 & \text{if } i \sim j \\ 0 & \text{if } i \nsim j, \end{cases}$$

Following are few basic characterization tools of the networks:

1. **Degree and Degree distribution:** The number of edges a node has in a network is defined as the degree of that node. The probability of a node having degree k is referred as the degree distribution $P(k)$.

2. **Diameter:** The largest of these shortest paths between all the pairs of the nodes is defined as the diameter of the network.

3. **Clustering coefficient:** If node i has degree k_i, then number of neighbors of node i will be k_i and the maximum number of possible cliques of the order of three will be $k_i(1-k_i)/2$. If E_i is actual number of triangles among the neighbors of node i, the clustering coefficient of nodes i can be given as [27]:
$$C_i = \frac{2E_i}{k_i(1-k_i)}. \tag{1.1}$$

In the last two decades an advancement in the direction of the study of real world systems in the complex network framework has been done. The network theory has been very useful to study the origin of various diseases [28], functionally important proteins [29], disease spread in social system [30], virus spread in the Internet networks [31], stability of the ecosystem [26] and pattern formation in the neural networks [5]. Following are some of the major network models:

1.0.1.1 Random network

The algorithm for the random network was given by Hungarian mathematicians Paul Erdős and Alfred Rényi. According to this model, all the pair of the nodes in a network are connected with a probability p. Thus, the total number of connections in the network is approximately $pN(N-1)/2$ [27]. The realization that complex networks such as cell and the Internet are not completely random, has led to other network models.

1.0.1.2 Small-world network

The real world systems possess smaller diameter as small as of the random networks and clustering coefficient as large as found for the regular networks. The social psychologist Stanley Milgram, through his experiment demonstrated that most of the people in the United States of America have six degrees of separation between them [32]. Taking this into consideration, Watts and Strogatz (WS) proposed a model of the small-world network [33]. Following is the procedure to generate the small-world network using WS model: (1) Begin with a 1-d lattice of degree k (each node is connected to its $2k$ nearest neighbors, k neighbors each side). (2) Each link is then removed with a probability p and is rewired to a randomly selected node in the network such that there are no self and multiple connections. The value of p being zero corresponds to a regular graph and $p = 1$ corresponds to the random graph. This random rewiring leads to a network which has diameter as small as that of the random networks and clustering coefficient as large as found that of the 1-d lattice.

1.0.1.3 Scale-free network

Many of the real-world networks such as the citation networks [25], the phone call networks [34], the cellular networks, the Internet networks, and the world wide web [35] show the power law degree distribution ($P(k) \sim k^{-\lambda}$). In order to understand the evolution of the power law degree distribution in these networks, several models have been presented. We consider the model proposed by Barab$\acute{a}$si and Albert in 1999 [36], which is as follows:

(1) Take a small number of nodes (N_0), add a new node having $\langle k\rangle$ edges (where $\langle k\rangle$ is average degree of the network) at each time step.

(2) The newly added node makes connections with the already existing nodes with a probability π_i, which depends on the degree of the node i as:

$$\pi_i = \frac{k_i}{Nc}, \tag{1.2}$$

where N_c is the total number of connections in the network at time t.

The scale-free structure is known to provide robustness to the system against random attacks, while makes it fragile to the targeted attack for example virus spreading in the Internet network, becomes more harmful when the hub nodes get infected [27].

1.0.1.4 Bi-partite network

The bipartite graph consists of two kinds of nodes and edges connect only nodes of different kinds [24]. The complete bipartite networks consists of two sets where each node of one set is connected with all the nodes of other set. Few real world networks such as actor network and collaboration networks can be described by the bipartite graphs. The actor network can be classified into two types of nodes: actors and movies, while in the collaboration networks can be classified into scientists and papers. The metabolic process where two type of nodes can be substrates and reactions, also forms a bi-partite network [27].

1.0.1.5 Cayley tree

The Cayley tree is an infinite dimensional regular graph with an idealized hierarchical structure. These networks have demonstrated their usefulness in the exact analysis of stability of synchronized states [37], modeling of immune network with antibody dynamics, disease spread [38–41] and in the investigation of Bose-Einstein condensation [42]. Tree structures are found everywhere from the real world networks such as the river networks to the technical networks such as power grid networks. The tree structure has also been found in the network of sub-fields of physics [43]. Unlike other networks for Cayley trees branch ratio (denoted by K) and height (denoted by h) are the major network parameters.

The Cayley tree can be divided into two parts inner nodes and the boundary nodes [44]. The boundary nodes (also called leaf) do not have children, but constitute more than 50% of the total nodes ($(K^{h+1}-1)/(K-1)$) in the network. There are total $(K^h-1)/(K-1)$ inner nodes in a tree network. Its idealized hierarchical structure stands as an ideal model network to understand different cluster patterns observed for the coupled maps on delayed networks.

1.0.2 Cluster synchronization:

The synchronization can be global as well as local. In the global synchronization, all the elements of a system exhibit similar behavior in time, while the local synchronization leads to the cluster formation. In the cluster synchronization, the whole system gets divided into groups of synchronized nodes in such a way that any two nodes belonging to the same group are synchronized with each other, whereas, two elements belonging to different groups are not synchronized. If a network of N nodes divides into k clusters, with k_n elements in the n^{th} cluster, the synchronized state can be written as follows :

$$\begin{aligned} x_i(t) = x_j(t); \quad \forall \quad t > t_0, \;\; \text{if } i, \; j \in k_n \\ x_i(t) \neq x_j(t); \quad \forall \quad t > t_0, \;\; \text{if } i \in k_p, \;\; j \in k_q \end{aligned} \tag{1.3}$$

The above definition corresponds to the case of exact synchronization, when the dynamical variables for two subsystems of a system have identical values [45, 46]. Following are other types of the synchronization which have been studied in the context of the cluster synchronization.

1. Lag synchronization (LS): when the state of two maps are nearly identical, but one system lags in time from the other. The state of node may remain almost identical but with a time lag $\triangle$ [47]:
$$x_i(t + \triangle) \approx x_i(t); \; \forall t > t_0, \; i, \; j \in N. \tag{1.4}$$
where $x_i(t)$ is the value of dynamical variable of node i at time t.

2. Phase synchronization (PS): when only phases of the two subsystems are locked and amplitude remain highly uncorrelated [48].
$$|n\phi_i(t) - m\phi_j(t)| < const; \; \forall \; t > t_0 \; , \; i, \; j \in N \tag{1.5}$$

3. Generalized synchronization (GS): When a complicated functional relationship, e.g. $x_i = h(x_j)$ is established between two coupled subsystems $x_i = f_1(x_i)$ and $x_j = f_2(x_j)$ [49].

Examples of the cluster synchronization can be easily seen in nature such as, flocks of birds [50–52], division of the individuals into several groups based on same opinion shared by the members of a group in the social systems [53], splitting of a multi-agent system into several clusters so that the agents synchronize with each other in a same cluster, but differences exist among different clusters [54, 55], and in the neural networks where specific set of neurons response to a specific stimulus.

Cluster synchronization is desired in some cases such as in the neural networks [5–7] and undesired in some cases such as power grid networks [9–11] and thus in last decade, coupled dynamics research got shifted to the investigation of the synchronized clusters [47, 48, 56–58] instead of the global synchronized state.

The cluster synchronization has been proposed a mechanism behind the global synchronization of coupled oscillators [59]. The uncoupled oscillators evolve independently and there is no correlation between the motion of the oscillators. Upon introducing an overall coupling, formation of the phase synchronized clusters was observed as coupling exceeds a critical value [47, 48]. Using mean-field analysis, it has been shown that there exists a transition to the global synchronized state through cluster formation [59]. Further, the critical coupling strength has been shown to depend on the network topology [59, 60].

1.0.2.1 Mechanisms of cluster formation

The earlier works on undelayed coupled network have mainly focused on investigation of partial synchronized state, and did not pay much attention to the coupling configurations. However, networks modelling of real world have some structures and it is important to understand the relation between the connection architecture and the dynamical clusters. The question arises that, "do connections in the dynamical clusters have some specific features ?" Manrubia and Mikhalov in [61] reported that the connections in dynamical clusters do follow a particular configuration, i.e. elements from a cluster generally have more connections inside the cluster than with the elements from other dynamical clusters. This was a very significant observation and more importantly presented the concept of relation between dynamical cluster, and the underlying network, their observation was based on the dynamical units coupled with some particular coupling strength and having random coupling architecture.

Later on, the study of coupled dynamics on various networks, done by Jalan and Amritkar [56] revealed that depending upon the relation between the synchronized clusters and the coupling between the nodes represented by the adjacency matrix, there could be following different phenomena for the cluster formation:

1. **Self-organized (SO) clusters :** The SO synchronization is referred to the case when, nodes of a cluster synchronize due to intra-cluster couplings and the corresponding synchronized clusters are called SO clusters (Fig.4.1(b)). In the ideal SO synchronization, the clusters do not have any connection outside the cluster, except one, which is necessary for a connected network. The state when most of the connections lie inside the cluster except very few outside is referred as the dominant SO synchronization.

2. **Driven (D) clusters :** The D synchronization corresponds to the state when the nodes of a cluster synchronize because of inter-cluster couplings and the corresponding clusters as D clusters (Fig.4.1(a)). Here the nodes of one cluster are driven by the nodes outside the cluster. We refer to this as the driven (D) synchronization . The state when most of the connections lie outside the cluster except very few inside, corresponds to the dominant D synchronization.

3. **Mixed clusters :** The clusters can be formed due to almost equal contribution of the inter- and intra-cluster connections, such clusters are referred as the mixed clusters (Fig.4.1(c)).

The SO and D synchronization has also been investigated in the relevance of brain cortical networks [62].

To have a clear picture of self-organized and driven behavior, f_{intra} and f_{inter} are proposed as measures for intra-cluster and inter-cluster couplings, defined as follows [57] :

$$f_{intra} = \frac{N_{intra}}{N_c}, \quad f_{inter} = \frac{N_{inter}}{N_c} \tag{1.6}$$

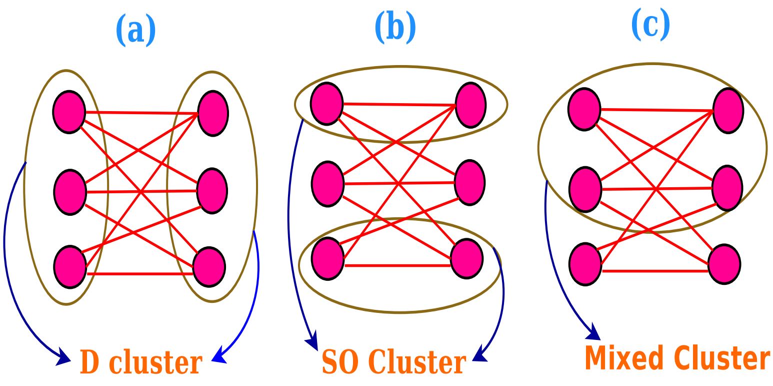

Figure 1.1: Schematic diagram depicting the ideal D (a), ideal SO (b) and mixed (c) clusters. The nodes (closed small circles) in circular region represents that they are synchronized.

where N_{intra} and N_{inter} are the numbers of intra- and inter- cluster couplings, respectively. In N_{inter}, coupling between two isolated nodes are not included.

The criteria for the distinction of different cluster states depending on the value of f_{inter} and f_{intra} is as follows :

1. The state, corresponding to $f_{intra} = 0$ and $f_{inter} > 0$, is defined as the ideal D clusters state as mechanism behind the synchronization is inter-cluster couplings.

2. The state corresponding to $f_{intra} > 0$ and $f_{inter} \sim N_{cl}\langle k\rangle/N_c$, ($N_{cl}$ is the number of clusters) is defined as the ideal SO clusters state as mechanism behind the synchronization between pairs of nodes is due to intra-cluster couplings.

3. If $|f_{intra} - f_{inter}| < th$, clusters are of mixed type. The phase diagram is presented for $th = 0.2$. For the higher values of th, as long as $f_{intra} > f_{inter}$ ($f_{intra} < f_{inter}$), clusters are considered here to be of dominant SO (dominant D) type.

The dynamical evolution of the coupled maps may lead to cluster patterns, defined as follows:

Cluster patterns: A cluster pattern refers to a particular phase synchronized state, which contains information of all the pairs of phase synchronized nodes distributed in different clusters. There can be static or dynamical cluster pattern depending upon the behaviour of nodes. The static pattern has all the nodes, except few floating nodes, fixed in a cluster with respect to the change in the time, delay value or initial condition. The dynamical pattern refers to change in number of nodes with time evolution, or with initial condition or with change in the delay value. Furthermore, a pattern can be of D, SO type or mixed type.

Depending upon the asymptotic dynamical behavior of the nodes, a node can be referred with the following three ways [57].

1. **Cluster node:** A node which synchronizes with other nodes and forms a synchronized cluster. After entering in to a synchronized cluster it remains in that cluster throughout.

2. **Isolated node:** A node which does not synchronize with any other node and remains isolated all the time.

3. **Floating node:** A node that keeps on switching intermittently between an independent evolution and a synchronized evolution attached to a cluster or a set of clusters.

1.0.3 Delay:

In the spatially extended systems, delays are unavoidable due to finite speed of information transmission [63], thus modelling of the real world systems without considering delay is a rather idealistic way. To study a more realistic situation, incorporation of delay is must. The delay in communication primarily depends on the following points [64]:

1. The length signal has to cover

2. Rate of information transmission from one unit to other units

Examples of few real world systems where delay has an important role are given below:

In the neural networks delay arises due to the finite speed of signal conduction such as; speed of signal conduction through unmyelinated axon fibers is of the order of $1m/s$ resulting in time delays up to 80 ms [65, 66]. In the football stadium, the sound of the clapping of fans in one side of stadium reaches to the fans sitting on the other side of stadium after some time due to the finite speed of sound, for example for the distance of $3m$ a time delay of $10ms$ induces [64].

In the Internet networks, the time delay arises due to the delay in processing, queueing, transmission and propagation of data [67]. The delay in the power grid system arises due to the time delay in sending the data through router plus the time delay due to the time taken in the transmission of data over a particular communication medium [68, 69].

In Ecological systems, such as in population dynamics, delay arises due to the retarded reproduction owing to the finite hatching periods, maturation period [70]. Delay in dispersion of a species in a landscape, is known to influence the stability of the ecosystem [70, 71]. In coupled lasers system, delay arises due to finite time taken by the signal in feedback as well as in propagation. Though, the speed of laser beam is very high, the lasers exhibit very fast dynamics and the propagation of few meter distances introduces non-negligible delay time in the coupling [72, 73]. The presence of delay has been shown to enhance the synchronizability of coupled laser system [74]

The delay can be discrete or continuous. For coupled maps model, we consider discrete delays. Discrete delays can be homogeneous or heterogeneous, which are elaborated in the following:

1.0.3.1 Homogeneous delay

For the homogeneous case, delay between all the pair of nodes is same. The homogeneous delay is known to give rise to many new phenomena in dynamical systems such as stabilizing periodic orbits, enhancement or suppression of synchronization, chimera state, etc [75–93].

1.0.3.2 Heterogeneous delay

In this case, the delay between a pair of nodes may be different from the rest of the pairs of nodes in the network. In real world networks, the delay in transmission from all the units may not be the same [94]. Hence, model systems incorporating heterogeneity in delays may provide a better understanding of the behavior of underlying systems. Previous studies considering the heterogeneous delays have shown that they are capable to show all the emerging behaviors as observed for homogeneous delays [95–101]. Heterogeneity in delay may maximize the stability of the uniform flow, which is good for traffic dynamics [102], may lead to a change in cluster patterns and suppression of synchronization [103]. Furthermore, heterogeneous delays show higher-order chaos thus bear a more secured communication in chaos based encryption systems [104].

In case of the food webs, it has been shown that the homogeneous delays leads to destabilization of the system, leading to the extinction of a species [105–107], while the distributed delays yield larger stability regimes, closely resembling to the undelayed systems [70]. The heterogeneous delays also support to the amplitude death, where whole system stabilizes to fixed point [108, 109].

We have considered following discrete heterogeneous delays:

1. **Bi-modal heterogeneous delay:** For generating the bi-modal heterogeneous delays by randomly making a fraction of connections f_{τ_1} conducting with τ_1, and another fraction f_{τ_2} conducting with delay τ_2. These two parameters are defined as $f_{\tau_1} = N_{\tau_1}/N_c$ and $f_{\tau_2} = N_{\tau_2}/N_c$, where N_{τ_1} and N_{τ_2} stand as the number of connections conducting with delay τ_1 and τ_2, respectively. The maximum heterogeneity is exhibited when half of the connections bears τ_1 delay and the other half bears a τ_2 delay. We remark that these definitions do not incorporate the exact values of delay and only take care of the number of connections conducting with different delay values. We consider $h = 1- \mid f_{\tau_1} - f_{\tau_2} \mid$ as a measure of the amount of heterogeneity in the network. The value of h being zero corresponds to the homogeneous delays, whereas $h = 1$

corresponds to $f_{\tau_1} = f_{\tau_2}$, denoting the maximum heterogeneity.

2. **Uniformally distributed:** The heterogeneous delays with the uniform distribution is generated by generating uniform random numbers between range τ_1 and τ_2.

3. **Gaussian distributed:** Gaussian distributed delays are generated as [110], $\tau_{ij} = \bar{\tau} + Near(c\eta)$, where η is Gaussian distributed numbers with mean zero and standard deviation one. The delays are homogeneous ($\tau_{ij} = \tau$) for c = 0 and are Gaussian distributed around $\bar{\tau}$ for $c \neq 0$. The negative values of delays have to be truncated.

4. **Exponentially distributed** $\tau_{ij} = \bar{\tau} + Int(c\eta)$, where η is exponentially distributed with positive, unit mean. The delays are homogeneous ($\tau_{ij} = \tau$) for c =0 and are exponentially distributed with $\bar{\tau}$ for $c \neq 0$ [110].

1.0.4 Model:

In real world systems, the short range connections among the neighbours ($A_{ij} = 1$) and lead to the long range correlations, such as while cooling the water short range interactions among the water molecules lead to the formation of ice crystals. Similarly in the case of the social networks, the local interactions among the people may lead to a revolution. In order to understand the origin of emergence of these long range correlations, many models such as; coupled-oscillator models, coupled map model, cellular automata, transport models and reaction-diffusion systems have been proposed.

1.0.4.1 Coupled map model

The coupled map model was initially proposed by K. Kaneko and others [111–119] as “coupled map lattice (CML)”. This model represents a dynamical system with discrete time and was originally proposed for studying spatiotemporal chaos. Further, many researchers worked on this model due to it simplicity and wide applicability. It has found its applicability in the studies of; crystal growth [120], population dynamics [121], fluid dynamics [122] and stock market [123]. The generalized model for coupled maps on networks is given as :

$$x_i(t+1) = f(x_i(t)) + \frac{\varepsilon}{k_i} \sum A_{ij}[g(x_j(t)) - g(x_i(t))] \tag{1.7}$$

where $x_i(t)$ is the dynamical variable of the ith node at the tth time step, and A is the adjacency matrix with elements taking values one and $zero$ depending upon whether i and j are connected or not, $\varepsilon \in [0, 1]$. Matrix A is a symmetric matrix representing undirected network, and $k_i = \sum_j A_{ij}$ is the degree of node i. Function $f(x)$ defines the local nonlinear map and function $g(x)$ defines the nature of coupling between nodes.

The coupled map model has shown a rich variety of the phenomena such as; pattern formation [124, 125], synchronized chaos [126, 127], spatiotemporal intermittancy [128, 129] etc. Thus, the coupled map model has become a celebrated model to test physical intuitions and concepts for spatiotemporal chaotic systems. We consider chaotic maps for studying the cluster synchronization. In the following, these maps are discussed in detail :

1.0.4.2 Logistic map

Logistic map was introduced by Robert May in 1976 to study the population growth [130, 131]. The population of year $(t+1)$ depends on the population of the previous year (i.e. t) and the rate of population (say μ). Thus population of year $(t+1)$ is linearly proportional to the population of year t (i.e. $z^{t+1} = \mu z^t$). This gives that for $\mu > 1$, population increases exponentially. However, for too large population there can not be enough food supply, consequently the members of the species would start dying. If $\bar{z}$ is the maximum number of population, the number of the members dying will be proportional to $\mu(1 - z^t/\bar{z})$. The final equation for the population dynamics can be written as [131]:

$$x(t+1) = \mu x(t)(1 - x(t)). \tag{1.8}$$

Where $x(t) = z(t)/\bar{z}$. This map depicts an extraordinary transition from an order to the chaos, as the value of parameter μ changes from 0 to 4. As shown by the

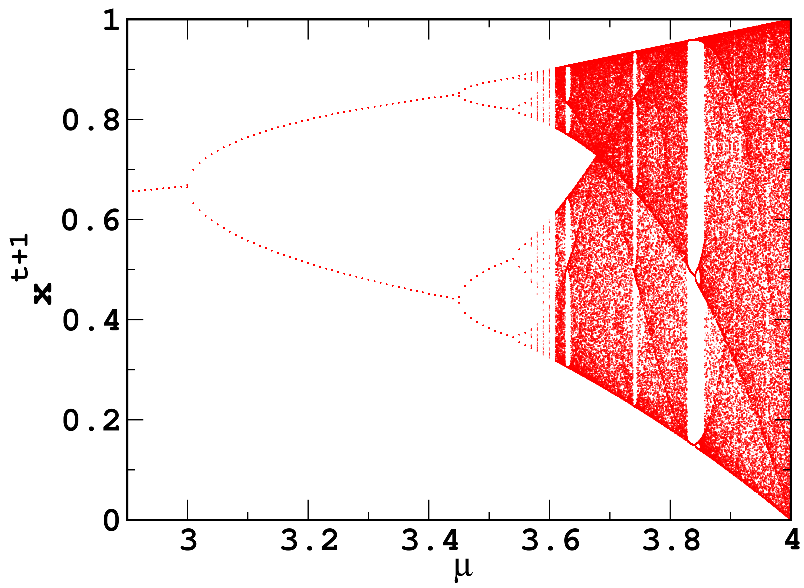

Figure 1.2: Bifurcation diagram of the logistic map, for the logistic map parameter lying in the range $2.9 \lesssim \mu \leqslant 4$. 100 successive iterates of the logistic map are plotted after an initial transient.

Fig.1.2, for $1 < \mu \leqslant 3$ periodic orbit of period-1 is obtained and attractor consists of a single stable fixed point $x = 1 - 1/\mu$. With a further increase in the value of μ there is a sudden change in the behavior as the trajectory does not settle down to a single attractor, instead oscillate back and forth between two values. In terms of the population dynamics, the population fraction is high one year, low next year and so on. This is called the period-2 behavior. At $\mu = 3$, period-doubling bifurcation take place. At $\mu = 3.44948..$ another period-doubling bifurcation take place, and for $\mu > 3.44948..$ the system consists of four attractors. A further increase in the value of μ leads to an orbit of period-8, period-16, and so on. For $\mu = 1 + \sqrt{8}$ periodic orbit of period-3 occurs, after this a period doubling cascade generating the period orbit of period $3(2)^m$, occurs. This continues until chaos appears in three bands. This band is called as *period three window*, which ends up with a situation where the periodic orbit of all the orbits coexist but none of them are stable. In order to quantitatively measure the chaos, the term Lyapunov exponent has been defined [131].

The Lyapunov exponent is the measure of mean rate of exponential separation of neighbouring trajectories [130]. If two nearby trajectories start with two different

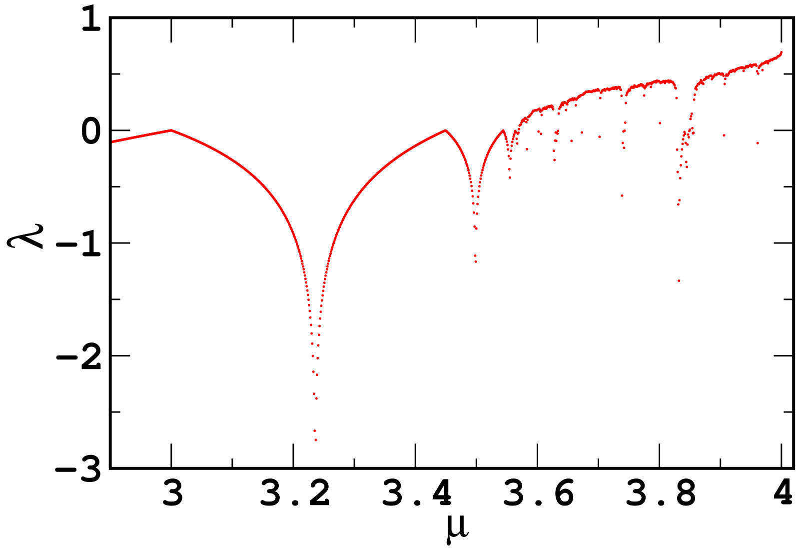

Figure 1.3: Figure depicting average Lyapunov exponent of logistic map, as a function of logistic map parameter μ.

initial conditions, say x_0 and $x_0 + \triangle x_0$, the Lyapunov exponent would be:

$$\lambda = \lim_{\substack{t \to +\infty \\ \|x_0\| \to 0}} \frac{1}{t} \ln \frac{\| \delta x(t) \|}{\| x_0 \|}. \tag{1.9}$$

The positive value of the Lyapunov exponent indicates that two nearby trajectories diverge, i.e the system is chaotic, a negative value of the Lyapunov exponent shows convergence of the two nearby trajectories and zero value indicates of quasi-periodic orbit (motion on a m-torus).

The Fig.1.3 plots the Lyapunov exponent with the increase in the value of μ. The logistic map has been studied extensively due to its computational simplicity and rich dynamical behavior.

For the N coupled maps, there will be N number of Lyapunov exponents.

$$\lambda_1 \geq \lambda_2 \geq \ldots \geq \lambda_n. \tag{1.10}$$

In this case, the positive value of the largest Lyapunov exponent is signature of the chaos.

1.0.4.3 Circle maps

The equation of motion of a periodically forced dynamical system can be given by the following map, called circle map [1]:

$$\phi(t+1) = x(t) + \omega + (p/2\pi)sin(2\pi x(t))\ (mod1). \tag{1.11}$$

Here, p is forcing amplitude and parameter $\omega = \omega_0 T = 2\pi T/T_0$ is proportional to the ratio of the period of force and period of self-sustained oscillations. For $p = 0$ the motion is linear rotation on the circle. For $p > 0$, in case of T/T_0 being rational number, dynamical evolution is on the circle with the period T_0, while for this ratio being irrational, dynamical evolution is quasi-periodic on the circle.

1.0.4.4 Delayed coupled map model:

As discussed earlier, in real-world systems the delay naturally exist due to the finite speed of information transmission. A modified evolution equation incorporating delay needs to be constructed.

For the delayed system the $(t+1)^{th}$ time step behaviour of the i^th node depends on the $(t-\tau_{ij})^th$ time step behaviour of its neighbours, where τ_{ij} is time taken for the information to reach from the j^{th} node to i^{th} node. For the symmetric delays $\tau_{ji} = \tau_{ij}$ and in the case of homogeneous delays $\tau_{ji} = \tau$. The modified coupled map model for the delayed system can be given as:

$$x_i(t+1) = f(x_i(t)) + \frac{\varepsilon}{k_i}\sum A_{ij}[g(x_j(t-\tau_{ji})) - g(x_i(t))], \tag{1.12}$$

This is to be noted that in the above equation, while considering the delay, only the delay in the transmission from one node other nodes has been considered. The delayed coupled map model given by Eq.1.12 is known to exhibit all the behaviors displayed by undelayed model [78, 78, 80, 99], along with the suppression of chaos [110].

1.0.5 Phase synchronization in maps

The uncoupled (i.e. $\varepsilon = 0$) chaotic maps, by definition can not exhibit synchronous behavior. For $\varepsilon > 0$ the interaction of the chaotic maps can lead to the perfect locking of their phases, whereas their amplitudes remain uncorrelated. Further, in

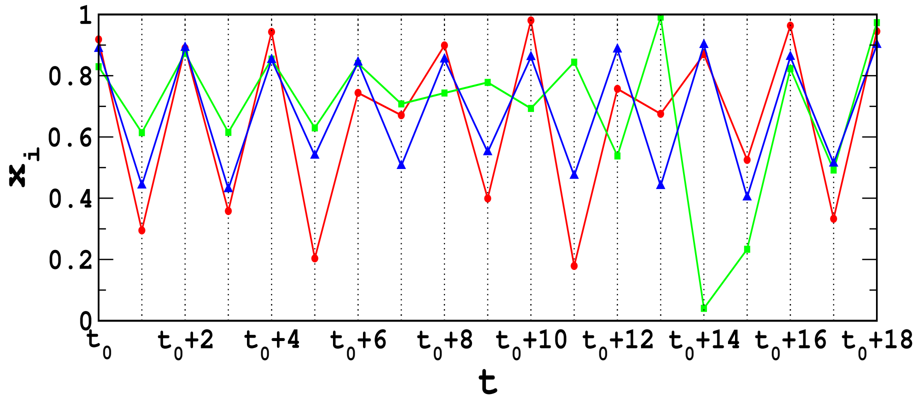

Figure 1.4: Figure shows time series of three nodes.

a phase synchronized state the dynamical variables for different nodes have some definite relation between their phases. In the case of the sparse networks, where the number of connections in the network is small ($N_c \approx N$), the coupled chaotic maps exhibit a very small number of nodes getting exactly synchronized. However, by considering the phase synchronization, synchronized clusters with a larger number of nodes can be obtained. Hence, we have studied the phase synchronization to investigate different cluster patterns in the delayed coupled maps. Phase synchronization considered in this thesis is defined as follows:

Let ν_i and ν_j denote the number of times the dynamical variables $x_i(t)$ and $x_j(t)$, for the nodes i and j, show local minima (maxima) during the time interval T starting from some time t_0. Here, the local minima (maxima) of $x_i(t)$ at time t is defined by the conditions: $x_i(t) < x_i(t-1)$ and $x_i(t) < x_i(t+1)$. Let ν_{ij} denotes the number of times these local minima (maxima) coincide with each other. The phase distance, d_{ij}, between the nodes i and j is given by the following relation [56, 132] :

$$d_{ij} = \frac{(1-\nu_{ij})}{max(\nu_i, \nu_j)}, \tag{1.13}$$

where, $d_{ij} = d_{ji}$ and d_{ij} has been shown to follow the metric properties [57]. When all the minima (maxima) of the variable x_i and x_j match with each other, $d_{ij} = 0$, whereas when none of the minima (maxima) match, $d_{ij} = 1$. Thus, the phase synchronization between two nodes i and j exists if phase distance d_{ij} between them vanishes. Fig.1.4 shows the time evolution of three nodes in a network. For the two nodes (represented with closed circle and triangle) $d_{12} = 0$ (as they have minima (maxima) occurring at the same time), while for the third node (represented with closed square) $d_{13} \neq 0$ and $d_{23} \neq 0$. Nodes 1 and 2 are phase synchronized and consequently fall in the same cluster.

Chapter 2

Cluster synchronization in networks without delay

The interactions in the real world networks are not random. They form various types of modules or community structure. A module represents a group of nodes for which the connections within the group are denser, but between the groups are sparser [133–138]. Depending upon the functional behaviour, a system can be partitioned into a collection of modules and each module is a discrete entity of several components performing an identifiable task, separable from the functions of other modules [138]. This indicates possible relations between dynamical clusters and the network architecture [56, 61], and the question arises that do dynamical clusters reveal organization or module structure of the underlying network as well as what functional clusters are preferred for a given network architecture ? Earlier investigations in this direction [139–141] showed that the collective dynamics of the network follow the network architecture, the nodes of a module getting synchronizing, while no synchronization between the nodes from different modules [142]. Further, the synchronization has been studied to detect the hierarchical organization in coupled networks [143, 144].

In this chapter, we study that dependance of the mechanism of cluster formation on the underlying network architecture. By considering a network of N nodes and N_c connections, we assign each node of the network a dynamical variable $x_i, i = 1, 2, \ldots N$. Evolution of the dynamical variable is written as [111]

$$x_i(t+1) = f(x_i(t)) + \frac{\varepsilon}{k_i} \sum_{j=1}^{N} A_{ij}[g(x_j(t)) - g(x_i(t))] \tag{2.1}$$

where $x_i(t)$ is the dynamical variable of the ith node at the t th time step and A is the adjacency matrix with elements taking values one and $zero$ depending upon whether i and j are connected or not, $\varepsilon \in [0, 1]$ is overall coupling strength. Matrix A is a symmetric matrix representing undirected network, and $k_i = \sum_{j=1}^{N} A_{ij}$ is the degree of node i. Function $f(x)$ defines the local nonlinear map and function $g(x)$ defines the nature of the coupling between nodes. In this chapter, we present results for the local dynamics given by the logistic map $f(x) = \mu x(1-x)$ and $g(x) = f(x)$. We take the value of $\mu = 4$, for which individual un-coupled unit shows chaotic behaviour with the value of Lyapunov exponent being $\ln 2$. As an effect of coupling, the coupled dynamics Eq.2.1 shows various different kinds of coherent behaviour, such as synchronization [111, 118], phase-synchronization [57, 58, 145] and other large scale macroscopic coherence [146] depending upon the coupling architecture and the coupling strength. In this chapter we consider exact synchronization (i.e. $x_i(t) = x_j(t)$ for $i, j \in N$) and phase-synchronization.

The definition of modularity of a network (Q), given by Newman is based on the ratio of intra and inter module connections ($Q = 1/2N_c[\sum_i e_{ii} - \sum_{ijk} e_{ij}e_{ki}]$), where e_{ij} is the fraction of edges in the network connecting nodes in group i to those in the groups j. The modularity of a network is maximum (i.e. one) if it can be divided into sub-graphs such that all the connections lie in the sub-graphs, except those, which are required in order to keep the network connected. These are referred as structural clusters (or community) to distinguish them from the dynamical clusters. The nodes in the same community get synchronized in SO synchronized state, while for the D state, nodes of different sub-graphs synchronize.

In the SO synchronization, the nodes which are connected synchronize with each another. This type of synchronization was studied in [142] in order to find out

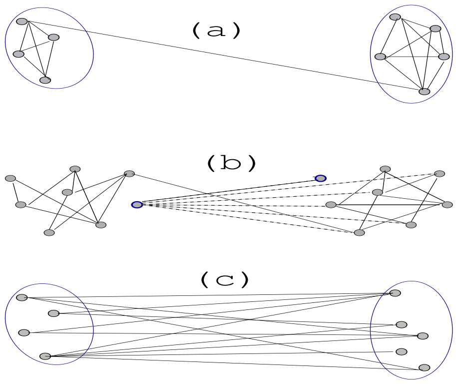

Figure 2.1: Pictorial representation of networks at different rewiring step. (a) Initial network with two complete subgraphs G_1 (left) and G_2 (right) (b) rewired network at $n = 1$, solid lines are the original connections and dotted lines are the new connections which a node from the group G_1 makes with the nodes of G_2, (c) final bipartite graph.

functional hierarchy in cat's cortex network. However, as shown in the earlier works ([56–58]), dynamical clusters could be formed without having even a single connection within the cluster (*ideal D state*). These two types of clusters, self-organized and driven, could be observed irrespective of the dynamical state of the Eq.2.1, i.e. whole dynamics may lie on the chaotic, periodic, quasi-periodic attractor depending upon the coupling strength and the connection architecture. Various different possible states of the coupled dynamics given by Eq. 2.1 are discussed in details in [57]. This chapter describes the relation between different types of clusters and the structure of the coupling matrix A, and subsequently tracks the nature of dynamical clusters with the rewiring of network. In the following, we present results for the coupled maps on networks, as described by the Eq. (1.7), evolved with random initial conditions. First, the rewiring procedure is explained and then various results demonstrating the relation between the dynamical clusters and network structure are presented.

2.1 Evolution of synchronized clusters with network rewiring

We start with a network of size N having two complete sub-graphs, G_1 and G_2 with N_1 and N_2 nodes respectively. Complete sub-graph means, all the nodes in G_1

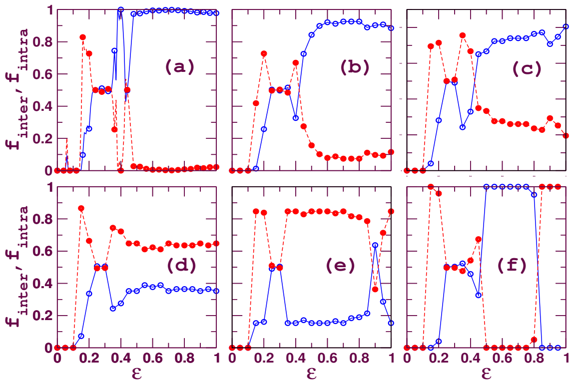

Figure 2.2: Fraction of inter (•) and intra (○) connections as a function of the coupling strength ε. After an initial transient (about 2000 iterates) phase synchronized clusters are studied for $\tau = 100$. The logistic map parameter is $= 4$, and $N_1 = N_2 = 50$. (a) for the original network at rewiring step $n = 0$, (b) $n = 5$, (c) $n = 10$, (d) $n = 20$, (e)$n = 30$, and (f)$n = 50$. All figures are plotted for the average over 20 sets of random initial conditions for the coupled dynamics.

(G_2) are connected with the all other nodes in G_1 (G_2) (Fig. 2.1(a)). There exists one connection between G_1 and G_2, which is necessary to keep the whole graph connected. Now at each rewiring step, we disconnect one node from the sub-graph G_1 (G_2) and connect it to all the nodes in the sub-graph G_2 (G_1) (Fig. 2.1(b)). With this rewiring scheme, average degree of the network remains of the same order (N). After rewiring step N_1, all nodes in G_1 are connected with all the nodes of G_2, and for the case $N_1 = N_2$, the graph is the complete bipartite (Fig. 2.1(c)). At each step of the rewiring we evolve Eq. (1.7) with random initial conditions and study the nature of the dynamical clusters after some initial transient. For small coupling strengths region ($\varepsilon < 0.5$), number of nodes forming synchronized clusters is very small and hence in this region we consider phase-synchronized clusters. For the larger coupling strengths, in general, nodes form exact synchronized clusters. In the following we consider dynamical clusters based on the phase-synchronization. Fig. (2.2) shows behaviour of f_{intra} and f_{inter} as a function of coupling strength ε for the various steps of the network rewiring according to the above strategy.

Fig. (2.2) shows that after an initial turbulent regime, where none of the node synchronizes, nodes form synchronized clusters. For the weak coupling ($\varepsilon \sim 0.2$) the coupled dynamics governed by Eq. 2.1 exhibits partial synchronized state corre-

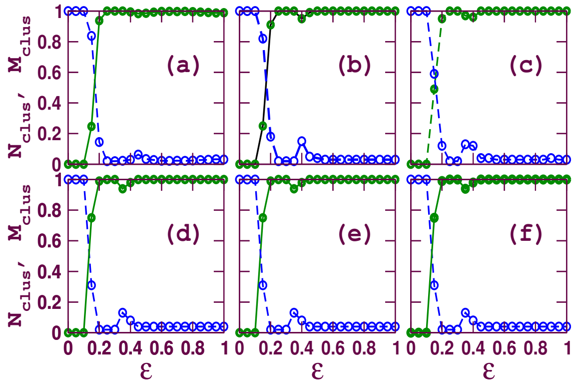

Figure 2.3: The fraction of number of clusters $M_{clus}(\circ)$ and the fraction of the number of nodes forming clusters $N_{clus}(\bullet)$ as a function of the coupling strength ε. The network structure are same as for the Fig. (2) and quantities are plotted for the average over 20 realization of random sets of the initial conditions.

sponding to the many dynamical clusters with f_{inter} and f_{intra} both being nonzero. Sub-figure (a) is plotted for the initial network (Fig. 2.1(a)), sub-figure (b) is plotted for the rewiring stage $n = 5$, which means that 5 nodes from each group are rewired. These nodes break the connections with their communities and make new connections with the nodes of the other communities.

Fig. (2.3) plots the fraction of number of clusters (M_{clus}) and the fraction of number of nodes forming clusters N_{clus}. The first measure M_{clus} counts an isolated node as a separate cluster, and the second measure N_{clus} counts only those nodes which are the part of a cluster and are not isolated. It is clear from the sub-figures that for each rewiring step almost all the nodes form cluster after some coupling strength $\varepsilon > 0.2$ value. Note that for the lower coupling strength region, in general, nodes form phase-synchronized cluster, as defined in the previous section, whereas for the stronger coupling strength region $\varepsilon > 0.5$ they form exact synchronized clusters. For our investigations it does not matter whether nodes are phase-synchronized or exact synchronized, as long as large number of nodes form the clusters we get relevant information regarding dynamical cluster and network structure. It is seen from all the sub-figures of Fig. (2.2), that the nature of synchronized clusters is very much similar in the weaker coupling strength regime ($\varepsilon \sim 0.2$) for all rewiring steps, with (a) and (f) being the extreme cases of the network structure. Hence, for our

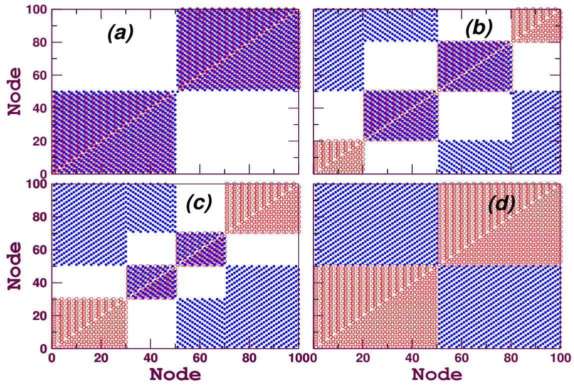

Figure 2.4: Node vs node diagrams illustrating the behaviour of nodes at different step of rewiring. After an initial transient synchronized clusters are studied. The solid circles (●) show that the two corresponding nodes are coupled and the open circles (○) show that the corresponding nodes are (phase) synchronized. In each case the node numbers are reorganized so that nodes belonging to the same cluster are numbered consecutively. All plots are for coupling strength $\varepsilon = 1$. (a) for the network having two complete subgraphs with $N_1 = N_2 = 50$ (b) network at the rewiring step $n = 20$ (c) for $n = 30$ and (d) for $n = 50$ which leads to the complete bipartite network.

study the weaker coupling strength region is not very interesting as in this region one does not seem to get relation between dynamical cluster and network structure. In order to get insight about the relation between dynamical clusters and the network structure we concentrate on the coupling strength region $\varepsilon > 0.5$. Coupled dynamics Eq. (1.7) gives interesting dynamical clusters in this coupling strength region, where connections between the nodes of dynamical clusters differ as structure of the network is varied. In the following, the behavior of coupled dynamics and nature of synchronized clusters for the various coupling strengths in this region are discussed.

Fig. (2.4) plots the synchronized clusters for different networks generated with the above rewiring strategy. The figures are plotted for the coupling strength $\varepsilon = 1$. For this coupling strength the nodes form exact synchronized cluster rather than the phase-synchronized cluster which is the case for weaker coupling strengths. Fig. (2.4)(a) is for the rewiring step $n = 0$, when nodes in the network form two complete sub-graphs. The dynamical behaviour of these nodes show synchronization with two clusters, and these clusters are of self-organized type; i.e. nodes

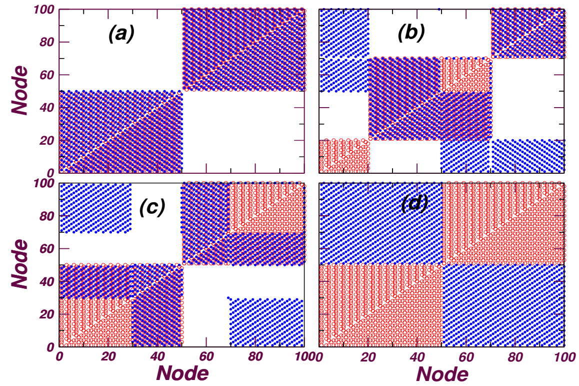

Figure 2.5: Node vs node diagram illustrating the behaviour of nodes (same as Fig. (4)), for the coupling strength $\varepsilon = 0.9$. Network structure remains same as of the Fig. (4). Node numbers are reorganized so that nodes belonging to the same dynamical cluster are numbered consecutively.

belonging to the structural clusters form dynamical clusters. Fig. (2.4)(b) is node-node plot for the network at step $n = 20$, i.e. connections of 20 nodes from each group are rewired such that the 20 nodes from the group G_1 (G_2) get connected with the 30 nodes of the group G_2 (G_1). At this stage mixed dynamical clusters are formed. Two small groups of nodes which are rewired to the different groups loose the synchronization with the nodes in their respective group and are synchronized independently forming two separate clusters. These two clusters, first and fourth cluster from the bottom, are therefore of driven type. Rest of the nodes, which remain fully connected inside their respective groups, remain self-organized type. Fig. (2.5) shows dynamical clusters at the various stage of rewiring for the coupling strength value $\varepsilon = 0.9$. Sub-figure (a) shows the two self-organized clusters for the initial network (Fig. 2.1). Subfigures (b), (c) and (d) are plotted for the $n = 20, 30$ and 50 rewiring steps respectively. For $n = 0$ and $n = 50$, self-organized and driven clusters respectively are the stable configurations, thus coupled dynamics lead to these for both the coupling strengths. For intermediate rewiring states dynamical clusters vary with the value of coupling strengths. Node numbers are reorganized so that nodes belonging to the same cluster are numbered consecutively. Fig. (2.6) plots largest Lyapunov exponent as a function of the rewiring step n, $n = 0$ corresponding to the original network (Fig. 2.1(a)). At each rewiring step one node

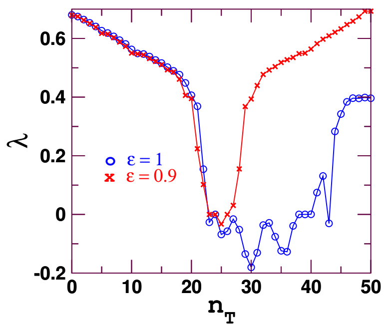

Figure 2.6: The Largest Lyapunov exponent λ as a function of the rewiring step n. Figures are plotted for two different coupling strengths $\varepsilon = 0.9$ and $\varepsilon = 1$. Lyapunov exponents are calculated for the average over 20 realization of the random set of initial conditions.

from each group is rewired. After $n = N_1 = N_2 = 50$, the network becomes like Fig. (2.1)(c). After fixing the coupling strength, Lyapunov exponent λ is: calculated for the coupled dynamics (Eq. 1.7) at each step of the rewiring. Results for $\varepsilon = 0.9$ and $\varepsilon = 1$ show that coupled dynamics may lie on the periodic ($\lambda < 0$), quasi-periodic ($\lambda \sim 0$) or on the chaotic ($\lambda > 0$) attractor, but the nature of the coupled dynamics governed by the Eq. 1.7 remains as shown by the Fig. (2.4) and 2.5, depending upon n.

2.2 Lyapunov function analysis

The Lyapunov function for any pair of nodes i and j can be defined as [147, 148]

$$V_{ij}(t) = (x_i(t) - x_j(t))^2 \tag{2.2}$$

Clearly, $V_{ij}(t) \geq 0$ and the equality holds only when the nodes i and j are exactly synchronized. For the asymptotic global stability of the synchronized state in a region, Lyapunov function should satisfy the following condition in that region:

$$\frac{V(t+1)}{V(t)} < 1$$

For the global synchronous state ($x_i(t) = x_j(t), \forall i, j$), we can write the condition for two synchronized clusters in the self-organized state (i.e. $x_{i_1}(t) = x_{i_2}(t);\ \forall i_1, i_2 \in G_1$ and $x_{j_1}(t) = x_{j_2}(t);\ \forall j_1, j_2 \in G_2$), as;

$$\begin{aligned} V_{i_1 i_2}(t+1) &= \Big[(1-\varepsilon)[f(x_{i_1}(t)) - f(x_{i_2}(t))] \\ &\quad - \frac{\varepsilon}{N_1 - 1}[f(x_{i_1}(t)) - f(x_{i_2}(t))]\Big] \end{aligned} \tag{2.3}$$

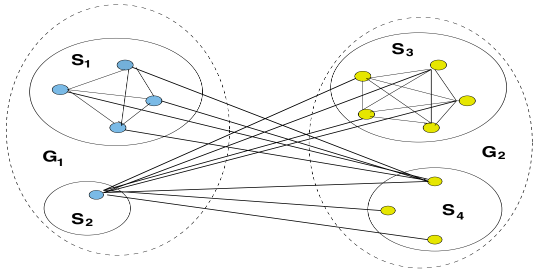

Figure 2.7: Dynamical clusters at a rewiring state n_t. S_1, S_2, S_3 and S_4 are different dynamical clusters as described in the text. G_1 and G_2 are the dynamical clusters for the initial network $n = 0$.

Using Eq. 2.3 and the above equation for coupled dynamics (Eq. 1.7), we get the coupling strength region for which the synchronized clusters state is stable;

$$\frac{N1-1}{N1}(1-\frac{1}{\mu}) < \varepsilon \leq 1 \tag{2.4}$$

With the rewiring, say at rewiring step $n = \nu$, we get ν nodes from each group rewired such that now there are four different types of nodes. One can quickly see by using Lyapunov function test that the following synchronized clusters state would be stable ;

1) Cluster $one(S_1)$ with the nodes which remain unwired in the group G_1, synchronized dynamics of nodes in this cluster is $x_i(t) = X_1(t)$.

2) cluster $two(S_2)$ with nodes from group G_1 which get disconnected with the other nodes in G_1 and get connected with all the nodes in G_2, $x_i = X_2(t)$.

(3) cluster $three(S_3)$ with nodes which remain in group G_2, $x_i = X_3(t)$.

(4) cluster $four(S_4)$, rewired nodes in G_2, $x_i(t) = X_4(t)$.

Lyapunov function for the nodes in the cluster one (and for the cluster $three$) remains same as Eq.2.3, because coupling of the nodes in this group to the groups $three$ and $four$(one and two) cancel out. Lyapunov function for the nodes in group S_2 (S_4) can be written as;

$$V_{ij}(t+1) = [(1-\varepsilon)(f(x_i(t)) - f(x_j(t)))]^2$$

This equation is very simple because the coupling terms for the nodes i and j are same and hence they cancel out. Condition for this state to be stable is given as;

$$\begin{aligned}\frac{V_{ij}(t+1)}{V_{ij}(t)} &= (1-\epsilon)^2 \Big[f'(x_i(t)) + \frac{x_i(t)-x_j(t)}{2}f''(x_j(t)) \\ &\quad +O((x_i(t)-x_j(t))^2)\Big]^2 < 1\end{aligned}$$

For $f(x) = \mu x(1-x)$ and using $0 \leq x_i(t) + x_j(t) \leq 2$ and condition for achieving synchronized state, we get the range of coupling strength as ($(\mu-1)/\mu \leq \varepsilon \leq 1$) for which the synchronized cluster S_2 (as shown in the Fig. (2.7) is stable. Similarly we can write the condition for the nodes in the group G_2 which are rewired and make synchronized cluster as S_4, and nodes which make synchronized cluster as S_3.

2.3 Conclusions and discussions

In order to explore relationships between the dynamical clusters and the network clusters, we studied coupled maps on various networks generated with a simple rewiring strategy. Starting with a network having two complete sub-graphs, nodes are rewired at each step such that after some rewiring steps we get a complete bipartite network. The rewiring strategy is adopted such that average degree of the networks at each rewiring step remains of the order of N. The smaller coupling strength values show phase synchronized clusters of dominant driven type, whereas larger coupling strength region show different mechanisms of synchronized clusters formation depending upon underlying network architecture, and hence provide insight into role of network architecture in the coherent behaviour of the associated dynamical units. Coupled dynamics form self-organized clusters for the network having two complete sub-graphs, and form driven clusters for the bipartite case. At intermediate steps, the nodes receiving similar input form dynamical clusters, and these clusters could be self-organized type, driven type or mixed type depending upon which connection environment they belong to. Lyapunov function analysis shows that for the driven synchronization if any two nodes have similar coupling architecture, the difference of the dynamical variables for these two nodes cancel out. Whereas for the self-organized synchronization, the coupling term corresponding to the direct coupling between the nodes do not cancel out, and other couplings which are common to both the nodes cancel out. The ref. [58] shows that there are two mechanisms of cluster formation in networks, and using the global stability analysis it provides arguments behind the mechanisms by taking globally coupled and complete bipartite as the extreme cases. Here we show that there is a gradual transition from the self-organized to the driven behaviour, as the underlying network is rewired from the two clusters to the bipartite network. The small coupling values do not show any impact of the structural changes on the mechanism of the synchronization, whereas large coupling values show significant signature of the underlying structure on the synchronized clusters. The dense networks ($N_c \sim N^2$) considered here yield all the nodes forming clusters at each rewiring stage, and clusters are of different types depending upon the underlying network structure at that particular rewiring step. Through extensive numerical simulations, we show that the nodes, getting similar coupling environment, are synchronized irrespective of whether they are connected or not. At the intermediate rewiring steps and for the higher coupling values, few clusters are mixed type, and few clusters are of the ideal driven or of the ideal self-organized type. All the nodes in each cluster receive similar coupling environment. Using the Lyapunov function analysis, we get a clear picture of the mechanism governing synchronization for each cluster individually. The stability condition for the synchronization of the nodes in clusters S_2 and S_4 provides an understanding to occurrence of the ideal D cluster. Additionally, the stability range achieved through the Lyapunov function analysis for the dynamical clusters S_1 and S_3 matches with that of the ideal SO cluster observed numerically because of the very simple underlying network model used here, where terms outside these cluster cancel out leading to the condition shown by the globally coupled network in the synchronized state.

The network architecture and rewiring strategies considered here are very simple, whereas real world networks have complicated random structure or have complicated rewiring or connection evolution strategies [149], the results presented here indicates a direct impact of the network connection architecture on the evolution of dynamical units. The main aim of the analysis here is to emphasize that the dynamical clusters *do have* information about the structure. The dynamical clusters do not always comprise the nodes which are directly connected, rather the formation of driven clusters reveals that the nodes which have similar coupling environment show coherent behaviour and form a dynamical cluster.

Chapter 3

Impact of delay on mechanism of cluster formation

The communication delay exists in extended systems due to the finite speed of the information transmission. The presence of delay may lead to qualitative changes in the dynamical evolution [64]. So far, studies on the delayed coupled dynamical systems have concentrated on a global synchronized state, except few recent studies which have focused on pattern formation or clustered states [89, 150–154]. Few recent papers have shown qualitative changes in clustered state on introduction of delay in communication. One of the recent paper [155] has reported that delay plays an important role in formation of two and three clusters states for excitable neurons, while none of the works have explored the mechanisms behind cluster formation in presence of the coupling delays, or the role of delays on the cluster formation.

In this chapter, we present the results pertaining to the impact of delay on the mechanism of formation of phase synchronized clusters in the coupled maps. Through extensive numerical simulations, we investigate the formation of phase synchronized clusters in coupled maps on various networks namely, 1-d lattice, small-world networks, random networks, scale-free networks and bipartite networks.

The results are substantiated by the Lyapunov function analysis, carried out for complete bipartite networks, which explains the impact of delay on the synchronized clusters.

Consider a network of N nodes and N_c connections between the nodes. Let each node of the network be assigned a dynamical variable $x^i, i = 1, 2, \dots, N$. The dynamical evolution is defined by the homogeneous delay coupled maps :

$$x_i(t+1) = (1-\varepsilon)f(x_i(t)) + \frac{\varepsilon}{k_i}\sum_{j=1}^{N} A_{ij}g(x_j(t-\tau)) \tag{3.1}$$

The delay τ is the time it takes for the information to reach from a unit to its neighbors and the other terms are same as discussed in the chapter 1. In this chapter we consider a homogeneous delay and study the phase synchronized clusters [48]. In the present investigation we consider a homogeneous delay, i. e. $\tau_{ij} = \tau$.

In the following, we present results for the local dynamics governed by the logistic map $f(x) = \mu x(1-x)$ at $\mu = 4$, for which it exhibits chaotic behavior, and for coupling $g(x) = f(x)$.

3.1 Numerical results

Starting with the random initial condition, after an initial transient we study the phase synchronized clusters, and calculate values of f_{inter} and f_{intra} as described in the introduction. In the following, we describe phase diagrams depicting the change in the values of f_{inter} and f_{intra}, with ε and τ for 1-d lattice, small-world, scale-free, complete bipartite and Cayley tree networks in detail:

3.1.1 Delayed coupled 1-d lattice

The undelayed 1-d lattice yields dominant D clusters in the range ($0.16 \lesssim \varepsilon \lesssim 0.25$). For higher coupling values, there is no phase synchronization, except towards the end of the coupling ($\varepsilon \gtrsim 0.74$), for which coupled dynamics exhibits mixed clusters with very small values of f_{inter} and f_{intra}.

A delay is introduced for $\tau = 1$ in the evolution Eq.(1.7). For a very small increase in coupling values, for which there is no phase synchronization (black color for the Figs.3.1(a) and (b)), we get self organized phase synchronized clusters in the

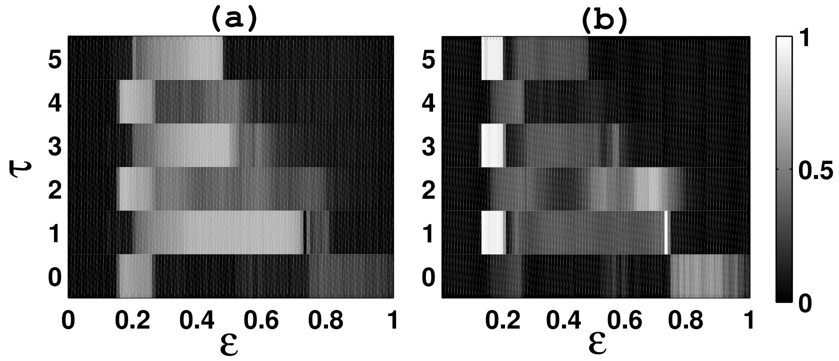

Figure 3.1: Phase diagram demonstrating different values of (a) f_{inter} and (b) f_{intra} in two parameter space of ε and τ for 1-d lattice with $N = 50$, $< k >= 4$. Local dynamics is governed by logistic map $f(x) = 4x(1-x)$ and coupling function $g(x) = f(x)$. The figure is obtained by averaging over 20 random initial conditions. The gray-scale encoding represents values of f_{inter} and f_{intra}. The regions, which are black in both graphs (a) and (b), correspond to states of no cluster formation. The regions, where both subfigures have gray shades, correspond to states where clusters with both inter- and intra-couplings are formed. The regions in (a), which are lighter as compared to the corresponding ε and τ values in (b), refer to dominant D phase synchronized clusters states, and the reverse refer to dominant SO phase synchronized clusters state. White regions in (a) and (b) refer to ideal D or ideal SO cluster states respectively. The regions, which are dark gray in (a) and black in (b) or vice-versa, correspond to states where a much less clusters are formed.

region $0.13 \lesssim \varepsilon \lesssim 0.2$ exhibited by the white region in the Fig.3.1 (b). For most of the coupling values in this region, coupled dynamics exhibits periodic evolution with the period depending upon the value of delay. The undelayed dynamics in this region leads to dominant D clusters of chaotic type. For a further increase in the coupling, there is no cluster formation for the undelayed case, whereas the delayed evolution leads to the formation of dominant D clusters in the coupling range from $0.4 \lesssim \varepsilon \lesssim 0.7$, leading to the light grey shade (almost white) corresponding to very large values of f_{inter} in the gray scale of Fig.3.1(a). The dynamical evolution of the nodes in this phase are quasi-periodic, with the largest Lyapunov exponent being close to $zero$, manifested by the light gray region in the Fig.3.2(a). Towards the end of the coupling $0.81 \lesssim \varepsilon \lesssim 1.0$, the delayed case exhibits a very small (almost negligible) cluster formation compared to the undelayed case.

For $\tau = 2$, the lower coupling range for which $\tau = 1$ shows dominant SO clusters, we get dominant D clusters as observed for the undelayed case. With

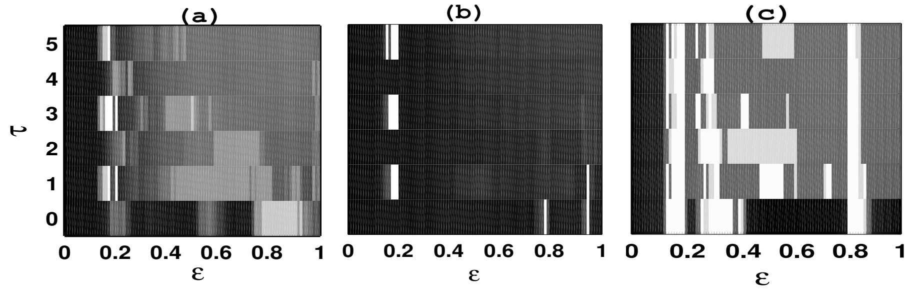

Figure 3.2: Phase diagram showing largest Lyapunov exponent, λ, for two parameter regions ϵ and τ for different networks. (a) 1-d lattice, (b) scale-free network and, (c) complete bi-partite networks. All networks have $N = 50$ and $< k >= 4$, and are plotted for average over 20 realizations of the networks. White and the light gray region correspond to the periodic and the quasi-periodic state respectively. Dark gray and black regions correspond to the chaotic state, with black denoting λ value being higher than the dark gray.

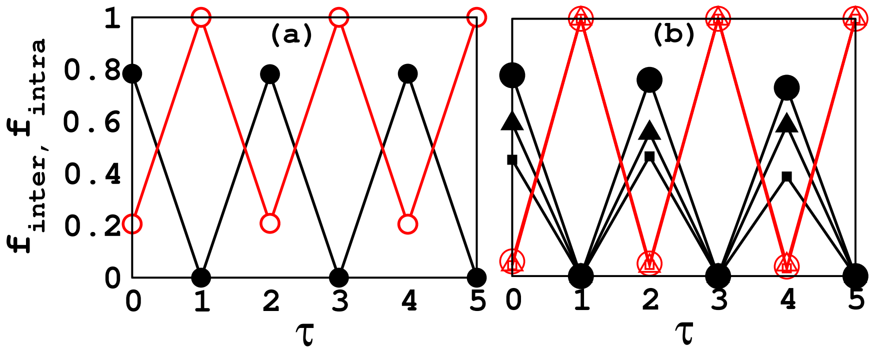

Figure 3.3: Fraction of inter- (closed symbols) and intra- (corresponding open symbols) couplings as a function of τ. (a) 1-d lattice with $N = 50$ and $< k >= 4$ at $\varepsilon = 0.17$, (b) random networks with $N = 50$ at $\varepsilon = 0.16$, and for $< k >= 4$ (rectangle), $k = 8$ (triangle), and $k = 12$ (square). All plots are obtained by averaging over 20 realizations of initial conditions.

increase in the coupling, mixed clusters are observed for the middle range and there is no cluster formation at higher coupling values. Some of the coupling values in the middle range give rise to dominant SO clusters as depicted by the almost white color in Fig.3.1(b). For $\tau = 3$, the lower coupling values leads to a similar behavior as exhibited for $\tau = 1$ case. With a further increase in the delay, at $\tau = 4$, the lower range of coupling exhibits a similar behavior as shown for $\tau = 0$ and $\tau = 2$. In the middle range of coupling, appearance of the gray region in the Fig.3.1(a) depicts the formation of dominant D clusters, similar to the other previous values of τ.

Based on the impact of delay on the formation of phase synchronized clusters, we can divide the coupling range into three parts, a lower coupling region ($0.13 \lesssim \varepsilon \lesssim 0.3$), a middle, and a higher one. In the lower coupling region, the zero and even delays lead to dominant or ideal D phase synchronized clusters, whereas the odd delays lead to dominant or ideal SO phase synchronized clusters. Ideal SO synchronization refers to a state when clusters do not have any connection outside the cluster, except one. The ideal D synchronization refers to the state when clusters do not have any connections within them, and all connections are outside. The middle coupling region exhibits the dominant D clusters for most of the delay values. The larger values of coupling exhibits no cluster formation.

In order to elucidate the drastic effect of the delay on mechanism of synchronization, we plot the fraction of inter-cluster and intra-cluster connections as a function of the delay in the Fig.3.3(a). We start from $\tau = 0$, and calculate f_{inter} and f_{intra} after an initial transient. Once the dynamics gets settled into the stable D clusters state, we change the value of the delay keeping all other parameters same, and calculate these two quantities after the dynamics settles down to a stable state. Fig.3.3(a) manifests that the change in the delay leads to a change in the mechanism of the cluster formation as described earlier. Moreover, the appearance and disappearance of the white window with a change in delay in Fig.3.2(a) reflects that the dynamical evolution changes from a chaotic to a periodic state.

3.1.2 Delayed coupled small-world networks

The delayed coupled maps on small-world networks generated using Watts-Strogatz algorithm [27] do not manifest any distinguishable change compared to the corresponding 1-d lattice results described above.

3.1.3 Delayed coupled scale-free and random networks

Next, we turn our attention to scale-free networks which have completely different structural properties than 1-d lattice and the small-world networks. Scale-free networks are generated using the BA algorithm [27]. The undelayed coupled maps on the scale-free network favor synchronization yielding better cluster formation

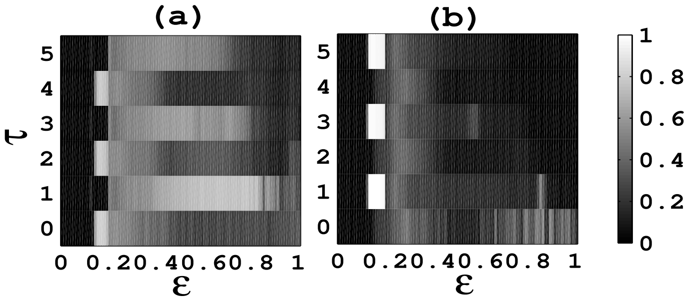

Figure 3.4: Phase diagram presenting (a) f_{inter} and (b) f_{intra} in two parameter space ε and τ for scale-free network. The gray-scale encoding represents values of f_{inter} and f_{intra} as described in the caption of Fig.1.

than the corresponding regular and small-world networks [56]. Fig.3.4 is plotted for $N = 50$ and $< k >= 4$. Again, based on the impact of delay on the nature of phase synchronized clusters, the coupling range can roughly be divided into three different regions similar to the 1-d lattice case as stated above. The lower coupling values exhibit exactly the same behavior as shown by 1-d lattice and small-world networks for all delay values.

Fig.3.5 plots the snapshot of clusters for various delay values at $\epsilon = 0.17$. The undelayed case leads to the formation of dominant D clusters. The introduction of a delay, with $\tau = 1$, leads to formation of SO clusters. Even delay values generate dominant D clusters, whereas odd delays lead to the dominant SO clusters. Moreover, clusters are reorganized in each subfigure, leading to cluster patterns of the different types. The D and the SO patterns respectively, refer to a particular D or SO phase synchronized state, containing information of all the pairs of the phase synchronized nodes distributed in the various clusters. A change in the pattern refers to the state when nodes, being the members of a phase synchronized cluster, get changed with the effect of an external parameter.

The middle range of coupling, for $\tau = 1$, leads to dominant D clusters as seen from the light gray region (with gray code value being close to 0.6) in Fig.3.4(a), and the dark gray region in Fig.3.4(b). The higher coupling values lead to less cluster formation, and for very high values of coupling, there is almost no cluster formation as depicted by the appearance of a dark region in both Figs.3.4(a) and

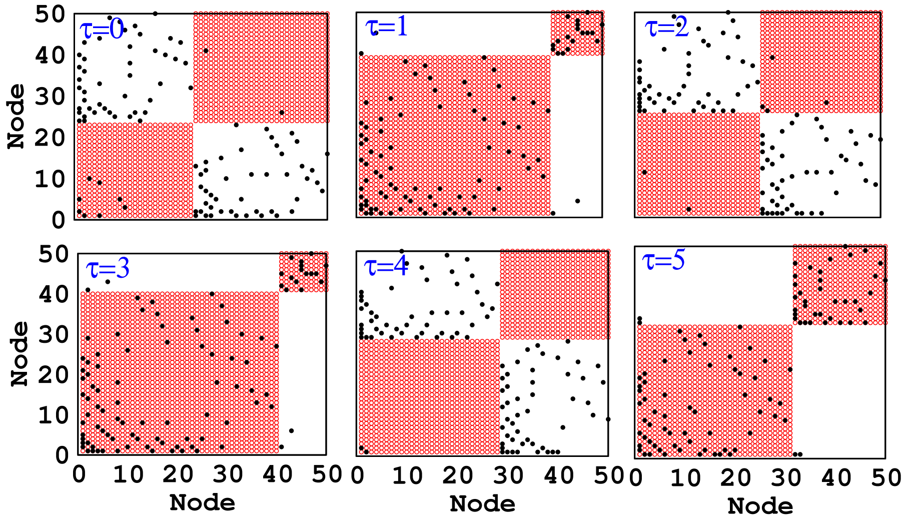

Figure 3.5: Node vs node diagrams illustrating the effect on delay on mechanism of phase synchronization. The examples are for scale-free network with $N = 50$, $< k >= 2$ and $\varepsilon = 0.17$. The closed circles imply that the two corresponding nodes are coupled (i.e. $C_{ij} = 1$), and the open circles imply that the corresponding nodes are phase synchronized. In each case the node numbers are reorganized so that the nodes belonging to the same cluster are numbered consecutively. The D chaotic clusters for $\tau = 0, 2$ and 4. The SO periodic clusters for $\tau = 1, 3$ and 5.

(b).

With a further increase in τ, for the middle range of coupling, the coupled equation exhibits very less or no cluster formation for even values of delay, as depicted by the dark gray, or black regions in the Fig.3.4(b). Whereas odd delay values, Eq.(1.7) leads to dominant D clusters, as seen from the gray region in the Fig.3.4(a). The range of coupling, for which there was no cluster formation for $\tau = 1$, keeps on increasing with the increase in the delay. This behavior is similar to the behavior observed for 1-d lattice and small-world network of the same average degree.

The evolution of the coupled maps on Erdös-Renýi model random network [27] does not exhibit much distinguishable behavior than the corresponding scale-free networks.

3.1.4 Delayed coupled complete bipartite networks

For the lower coupling region, the bipartite network exhibits the same mechanism of cluster formation as for the other networks, marked with the white windows in

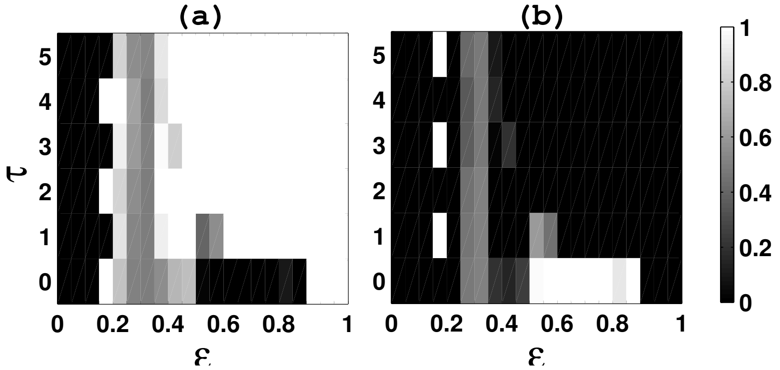

Figure 3.6: Phase diagram presenting (a) f_{inter} and (b) f_{intra} in two parameter space ε and τ for the bipartite network with $N = 50$. Gray-scale coding is similar to as described in the caption of Fig.1.

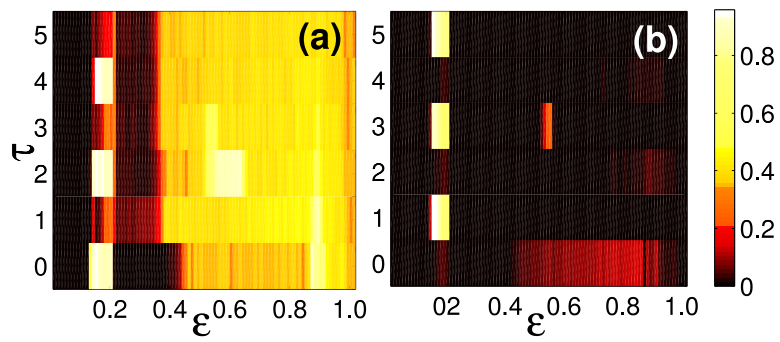

Figure 3.7: Phase diagram demonstrating different values of (a) f_{inter} and (b) f_{intra} for coupled maps on Cayley tree network in two parameter space of ε and τ ((a) and (b)) with $N = 127$, $< k >= 2$. Local dynamics is governed by logistic map $f(x) = 4x(1-x)$ and coupling function $g(x) = f(x)$. The figure is obtained by averaging over 20 random initial conditions.

Fig.3.6(a) and Fig.3.6(b). The dynamical evolution is periodic for all delay values.

For the middle range of coupling, undelayed evolution on other networks investigated here yield one of the following behavior; no cluster formation, mixed or dominant D clusters formation, whereas bipartite networks exhibit global phase synchronization spanning all the nodes leading to SO clusters as implied with the white region in the Fig.3.6(b) for $0.5 \lesssim \varepsilon \lesssim 0.85$. A delayed evolution on this network exhibits ideal D clusters for almost all coupling values and for all delay values we have investigated, which is evident from the white region in Fig.3.6(a) and the corresponding black region in Fig.3.6(b).

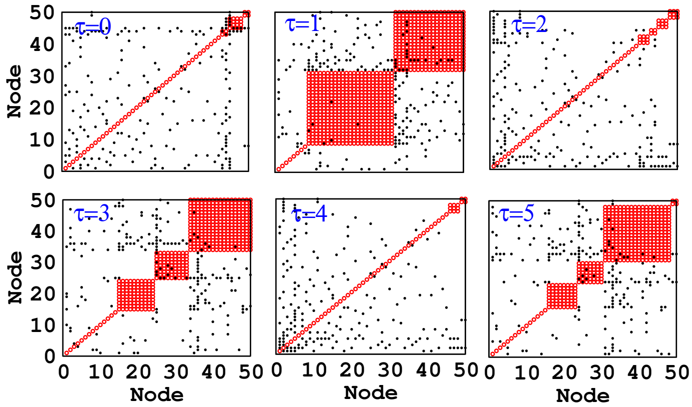

Figure 3.8: A typical behavior of coupled dynamics illustrating D patterns observed with the change in the value of τ. The example presents scale-free network with $N = 50$ and $\varepsilon = 0.6$. For $\tau = 0$, very few nodes are forming cluster. For $\tau = 1, 3$ and 5, nodes form dominant D clusters. For $\tau = 2$ and 4, very few nodes form clusters which is of ideal D type.

3.1.5 Delayed coupled Cayley tree

As, observed for the networks discussed above the undelayed Cayley tree exhibits similar behaviour for the undelayed and delayed evolution at the weak couplings ($0.12 \lesssim \varepsilon \lesssim 0.19$) (Fig. 3.7(a) and (b)). At the intermediate coupling range ($0.36 \lesssim \varepsilon \lesssim 0.42$), where undelayed system exhibits no or very less cluster formation, delayed evolution manifests dominant D clusters as depicted by yellow regions in Fig. 3.7(a). The strong couplings lead to the ideal D clusters, which are robust against change in the delay values, as observed for the complete bipartite networks.

3.2 Delay induced D patterns

In the previous sections, we illustrate that in middle range of coupling, the delayed evolution leads to ideal D clusters for bipartite networks, and dominant D clusters for other networks. In bipartite networks, division of nodes into the ideal D clusters is unique, whereas for the other network structures, there can be various possible ways in which one can distribute nodes to form ideal D (for average degree two) or dominant D (for larger average degree) clusters.

The delayed coupled evolution may lead to various possible patterns, picking up various possible divisions of the underlying network, by only changing the value

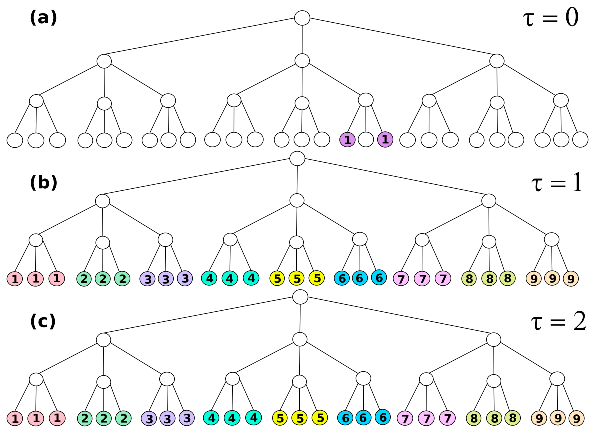

Figure 3.9: Schematic diagrams illustrating delay-induced driven patterns. The examples are for $N = 40, < k >= 3$ and $\varepsilon = 0.37$. The closed circles of same number (same color) imply that the corresponding nodes are phase synchronized (i.e. $A_{ij} = 1$), and the open circles imply that the corresponding nodes are not phase synchronized.The D chaotic clusters for $\tau = 1, 2$

of delay. Fig.3.8 plots snapshots of clusters for different delay values. Note that all the other parameters, i.e., the underlying network structure and the coupling remain the same in all the sub-figures, and only the value of delay is changed. The coupling value is taken from the middle range, for which dominant D clusters have been observed. Fig.3.8 explains that with a change in the delay, the nodes forming clusters and the size of the clusters are changed. The dynamical evolution in this coupling region, may be periodic, quasi-periodic or chaotic. For a particular delay value, the clusters are almost stable with the time evolution, with few nodes of the floating type [56]. But a change of τ has drastic effects on the stability of the cluster, and there could be entirely different sets of nodes forming clusters as the delay is changed, leading to different patterns. The D patterns obtained in this range are dynamic with respect to the change in the value of delay. However the mechanism behind the pattern formation does not change, and the D mechanism is mainly responsible for the cluster formation. Higher average degrees would lead to more intra-cluster connections, and it becomes difficult to have a clear visualization of the phenomena in the middle range where we get dominant D clusters for the delayed case.

Similarly, the coupled Cayley tree shows formation of the D clusters upon the

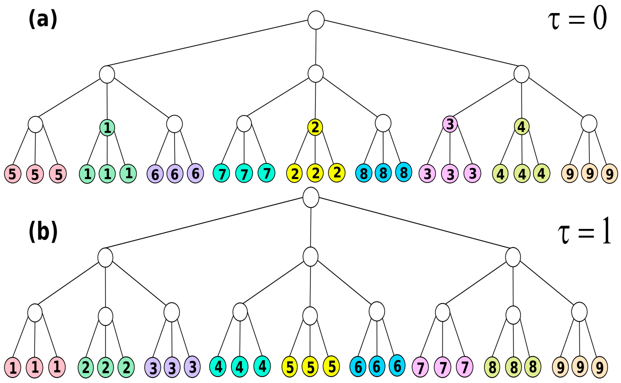

Figure 3.10: Schematic diagrams illustrating the effect on delay on phase synchronized patterns. The examples are for $N = 30, < k >= 3$ and $\varepsilon = 0.7$. The closed circles of same number (same color) imply that the corresponding nodes are phase synchronized (i.e. $A_{ij} = 1$), and the open circles imply that the corresponding nodes are not phase synchronized.

introduction of delay. In order to explain the different dynamical cluster patterns clearly we make schematic representation of dynamical clusters in Fig. 3.9. For undelayed evolution, there is no cluster synchronization as depicted by all empty circles in Fig. 3.9(a). Introduction of delay induces co-ordination between nodes in the same sub-family of the last generation as depicted by different clusters in Fig. 3.9(b).

At the strong couplings regime, delay destroys the co-ordination between the nodes which are connected, giving rise to ideal D patterns with the last generation nodes being synchronized in several clusters. These patterns are too stable with respect to initial condition as well as with respect to the change in the delay value. Fig. 3.10(b) elucidates that nodes belonging to the same sub-family of the last generation are synchronized.

3.3 Change in the mechanism of cluster formation:

Above discussions indicate that at the lower coupling values, change in the delay values are related with the change in mechanism behind the cluster formation. Odd delay values lead to ideal or dominant SO clusters, whereas even delay values are associated with ideal or dominant D clusters. Figs. 3.11(a), (c) and (e) illustrate

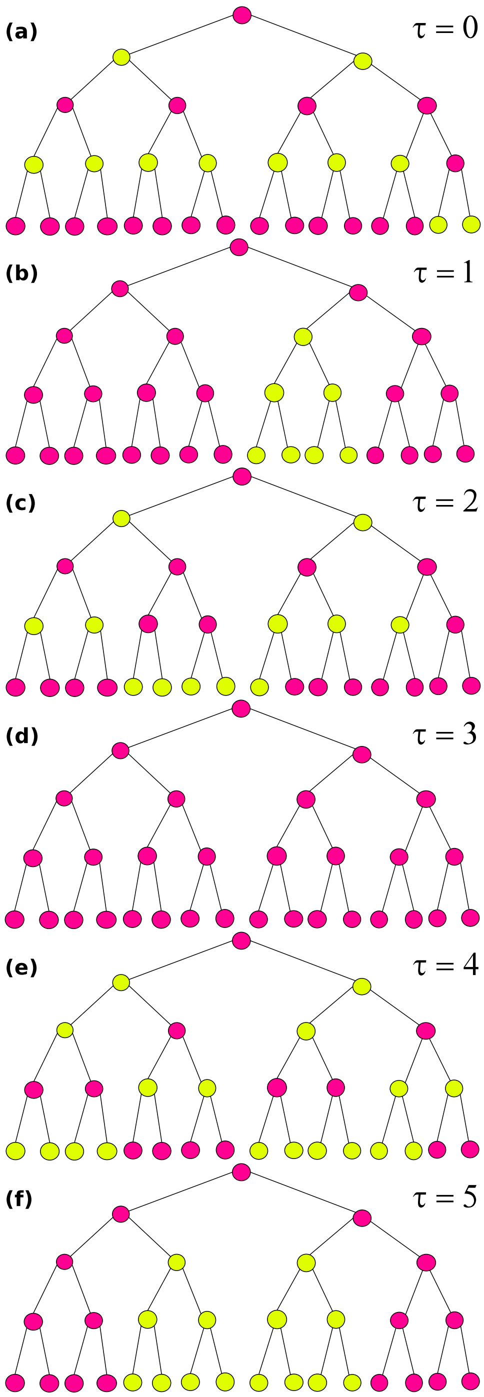

Figure 3.11: Node vs node diagrams illustrating the effect on delay on mechanism of phase synchronization. The examples are for $N = 31, < k >= 2$ and $\varepsilon = 0.16$. The closed circles of same color imply that the corresponding nodes are phase synchronized (i.e. $C_{ij} = 1$), and the open circles imply that the corresponding nodes are not phase synchronized.The D chaotic clusters for $\tau = 0, 2$ and 4. The SO periodic clusters for $\tau = 1, 3$ and 5.

that for $\tau = 0$, $\tau = 2$ and $\tau = 4$, coupled Cayley trees exhibit that the nodes of alternate generations are synchronized with each other, except few cases where nodes in two consecutive generations (parents and children) exhibit synchronization. Figs. 3.11(b), (d) and (f) depict that for $\tau = 1$, $\tau = 3$ and $\tau = 5$, either one cluster is formed spanning all nodes, or several clusters are formed with a cluster consisting of nodes in consecutive generations of same family or different families.

The origin of this behavior can be understood by considering the complete bipartite networks. For the undelayed case, the whole network here gets divided into two parts yielding two D synchronized clusters. Nodes in one cluster take the value p_1 and the nodes in the second one take the value p_2. These two values alternate in time. Upon introduction of delay in the evolution equation for a node, the coupling term having delay part would look like

$$f(x(t-\tau)) = \begin{cases} f(p_1) & \text{if } \tau = 0 \text{ and even} \\ f(p_2) & \text{if } \tau \text{ is odd,} \end{cases}$$

implying that discrete time delay considered here introduces a difference on evolution of nodes (Eq.(1.7)) depending upon the parity of delay, and thus leading to a particular behavior for zero and even delays and a different behavior for odd delays.

3.4 Lyapunov funtion analysis

As discussed in the section 3, D patterns are robust against the change in the delay value. Here we provide understanding to the origin of this behavior using the Lyapunov function analysis. For the complete bipartite networks, the Lyapunov function analysis can easily be carried out for the delayed case in a very similar manner as for the undelayed case described in the previous chapter. The Lyapunov function for a pair of synchronized nodes can be written as:

$$V_{ij}(t+1) = [(1-\epsilon)(f(x_i(t)) - f(x_j(t))) + \frac{2\varepsilon}{N}\sum_{j=N/2+1}^{N} g(x_j(t-\tau)) - \frac{2\varepsilon}{N}\sum_{i=1}^{N/2} g(x_i(t-\tau))]^2$$

For the ideal D synchronized state, the synchronization between two uncoupled nodes is independent of the delay terms as the coupling terms cancel out, and only

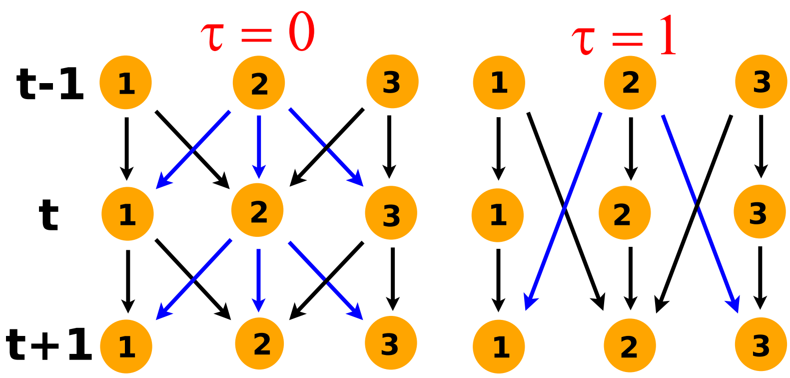

Figure 3.12: Three nodes schematic diagram illustrating impact of delay. Arrows depict direction of information flow as governed by Eq.(1.7). For $\tau = 0$, evolution of all nodes (•) receive information from the second node (left panel), whereas in presence of delay, evolution of connected nodes at a particular time do not involve any common term (right panel). For both panels, first and third nodes are connected with the second node leading to the construction of the smallest possible bipartite network.

depends on the ε value. Hence, delay does not affect synchronization between uncoupled nodes because of the same coupling environment experienced by them, and only renders its presence realized for those which are connected. As a consequence, depending upon ε and τ, it may either enhance or destroy the synchrony between them. For instance, in the lower ε range odd delays lead to an enhancement of coordination between connected nodes yielding a transition to SO clusters. In the middle ε range, delay destroys synchronization between connected nodes yielding D clusters state.

Aforementioned behaviors can be explained further using the example of bipartite networks. For $\tau = 0$, the common term in the evolution equation for all the nodes might be reason for global synchronization. Whereas, for $\tau > 0$, the network gets divided into two parts, one set of nodes have completely different terms in their evolution equations than those of the second set (Fig.3.12). Delayed bipartite networks have already been shown to have pairwise synchronization in the presence of common delayed coupling [150]. The important point in results presented in this chapter is that in the presence of delay, the dynamical evolution identifies the underlying network structure and gives rise to ideal D clusters for almost all the couplings

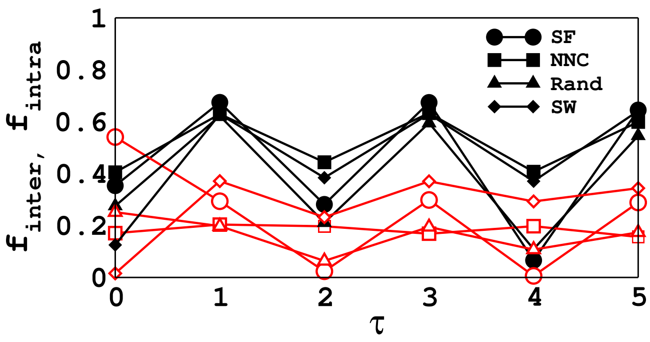

Figure 3.13: Phase synchronized patterns for coupled circle maps on scale-free networks with $N = 50$, $< k >= 2$, $g(x) = x$ and $\varepsilon = 0.24$.

in the range of $\varepsilon \gtrsim 0.4$.

3.5 Coupled cirle maps

In order to demonstrate the robustness of the results for the models, here we demonstrate the impact of delay on coupled circle maps as well.

Let, in Eq.(1.7), local dynamics be defined by circle map, $f(x) = x + \omega + (p/2\pi)sin(2\pi x)$, with parameter values taken in chaotic regime. Fig. 3.13 plots the examples demonstrating transition from one mechnaism to other and pattern formation phenomena in coupled circle maps on scale-free network. The figure depicts that different delay values not only correspond to different types of phase synchronized clusters, but are also associated with change in the pattern of cluster as demonstrated for coupled logistic maps.

3.6 Discussion

We have studied the effect of delay on the mechanism of phase synchronized cluster formation in diffusively coupled logistic map networks. Numerical simulations demonstrate that delay plays a crucial role on the phase synchronization and the mechanism responsible for the formation of clusters.

For lower coupling values, the zero and even delays imply dominant D clusters, whereas odd delays imply ideal or dominant SO clusters. Moreover, odd delays lead to SO clusters with periodic evolution, whereas zero and even delays lead to D cluster with periodic, quasi-periodic or the chaotic evolution. For the case of bipartite networks, a very simple analysis for periodic synchronized state in this lower coupling region provides a basic understanding of the different results exhibited by odd and even delays. Discrete time delay considered here introduces some difference on the evolution of Eq.(1.7) depending upon the parity of delay, thus leading to a particular behavior for zero and even delays and different behavior for odd delays. Differences between the impact of odd and even delays on evolution have been discussed earlier as well, where odd delays have been shown to stabilize unstable periodic orbits [78, 79]. The Ref.[156] presents that change in delay values has a great impact on the stability of a particular state. The results presented in the this chapter imply that change in the value of delay not only affects the stability of a synchronized cluster state, but also changes the phenomena behind these cluster formation.

In the middle range of coupling, for the undelayed case, the cluster formation is dependent on the underlying network structure, whereas the delayed cases lead to either ideal or dominant D clusters for all the networks that we have studied. Phase synchronization is maximum for $\tau = 1$, and decreases with the increase in τ. Earlier investigations have also illustrated that the delay plays a decisive role for the synchronization phenomenon observed in the middle range of coupling [82]. Our studies demonstrate a richer phenomena of cluster formation and D patterns, as we take networks with a less average degree ($N_C \sim N$), leading to the phase synchronized clusters instead of a complete synchronized state which usually spans all the nodes.

At very high coupling values, undelayed evolution for all networks except bipartite, exhibits mixed or dominant D clusters. An introduction of delay here destroys D phase synchronization. Delayed coupled FitzHugh Nagumo oscillators have also been reported to exhibit suppression or enhancement of synchrony [81]. The model and phase synchronization considered here allow us to capture a richer cluster pattern and to investigate the role of delay on the phenomenon of cluster formation. The undelayed bipartite network yields ideal SO behavior in the middle range of coupling, and ideal D behavior for most of the strong couplings. In this coupling range, delay destroys coordination of directly connected nodes as there is no common term in their evolution equations, whereas uncoupled nodes still have common coupling environment, hence leading to a transition from ideal SO behavior to ideal D behavior. This behavior persists for higher values of the coupling till $\varepsilon = 1$.

Moreover, the change in the value of delay leads to a change in the patterns of D and SO clusters. For lower coupling values, any change in the delay value has drastic effect on the pattern. Different values of the delay are not only associated with different mechanisms of cluster formation, but for a given network may lead to an entirely new pattern of the cluster. In the middle coupling range, different delay values lead to different patterns of dominant D type. The SO and D patterns described above are almost stable with time evolution, and hence change in a pattern is only associated with a change in delay value. A recent paper also explains the key role of delay in shaping patterns in nearest neighbor coupled phase oscillators [157].

The results for the Cayley tree networks, which can be correlated withe the family tree provide some interesting insight into the different behaviors shown by the social systems. Coupling strengths can be taken as closeness or bonding among family members, typically lower couplings strength can be considered as members living in nuclear family and do not share much details apart from that they belong to a same big family, where as larger coupling strength can be treated as members living in a joint family [158]. Our work demonstrates that lower coupling strength in general favors synchronization in various members in the family, as indicated by larger cluster size and almost all nodes participating in clusters, while the strong couplings comprise of only last generation siblings. The origin of these stable D clusters for last generation nodes can be very well understood as coupling environment of the last generation nodes belonging to one sub-family is same, and hence gives rise to a stable driven cluster, whereas nodes originated from the same parent in any previous generation can not have same coupling environment unless their children are also synchronized.

While the effect of delay on synchronization is already well investigated in coupled maps models, the role of delay on the formation of phase synchronized clusters and the mechanisms of synchronization were unknown. Delay may enhance the coordination among the connected nodes leading to an enhancement of synchronization identifying the connection topology, which had been the main theme of few recent studies, but observation of D mechanism behind the enhancement of synchronization is a new insight provided by the results presented here. We demonstrate that the delay-induced synchronization may lead to a completely different relation between functional clusters and topology, than the relation observed for the undelayed evolution.

This study may provide a better understanding about the synchronized cluster formation in real world networks such as neural networks, where clusters are formed due to the delayed interaction between the neurons [5] and may be of driven type as reported in the Ref.[159], which shows that two groups of neurons are synchronized via delayed coupling with a third group. Analysis presented here provides an understanding of the possible effect of delay on coupled evolution in such system. Moreover, change in patterns of neural activities are found to be related with brain disorders such as Alzheimers disease [160]. Study of delay induced patterns may help in understanding origin and treatment of these diseases.

Furthermore, the results presented in this chapter provide a possible explanation for conflicts in brothers running family business successfully [161], which on very simple terms can be attributed to the conflict between their children, whereas lower coupling strength keeps a warmer relation or cooperation between distant relatives in the same family [162].

Chapter 4

More heterogeneity, more coherence

In many real world systems such as ecological, nervous, social, coupled semiconductor lasers, and electrical power systems [52, 94, 149–151, 153], the rate of information transmission from all the units may not be the same. Hence, incorporation of the heterogeneity in delay values may provide a better understanding. However, most of the work pertaining to delays has considered a homogeneous delay [78, 78, 80, 87–89, 91–93], except a few previous studies.

The heterogeneous delays have been shown to lead many emerging behaviors as observed for homogeneous delays [99, 110]. A recent work demonstrates that an optimal level of delay heterogeneity may maximize the stability of uniform flow, which has implications in traffic dynamics [102]. Another recent work involving electronic circuits with the heterogeneous delays demonstrates the change in cluster patterns and suppression of synchronization [103]. Furthermore, heterogeneous delays have been shown to lead to a more secured communication in chaos based encryption systems [104].

In this chapter we investigate the impact of heterogeneous delays on the mechanism of cluster synchronization. So far, very few studies have focused on the im-

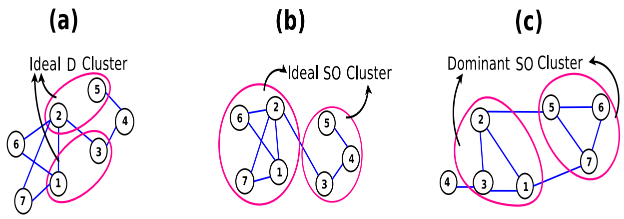

Figure 4.1: Schematic diagram depicting the ideal D (a), ideal SO (b) and dominant SO (c) clusters. The nodes (closed small circles) in circular region represents that they are synchronized.

pact of heterogeneity in delay values on phase synchronized clusters [103, 151, 153, 163]. In addition, further attempts are required to find out the mechanism behind the cluster synchronization in the presence of heterogeneity in the delay values.

We present results for coupled chaotic maps on various networks namely, one-dimensional (1-D) lattice, small-world (SW), Erdös-Rényi (ER) random, scale-free (SF), and the complete bipartite [27].

4.1 Model: Coupled maps with heterogeneous delays

We consider a network of N nodes and N_c connections between the nodes. Let each node of the network be assigned a dynamical variable $x_i, i = 1, 2, \ldots, N$. The dynamical evolution is defined by the well known coupled maps [64, 111] :

$$x_i(t+1) = (1-\varepsilon)f(x_i(t)) + \frac{\varepsilon}{\sum_{j=1}^{N} A_{ij}} \sum_{j=1}^{N} A_{ij} g(x_j(t-\tau_{ji})). \qquad (4.1)$$

The $\tau_{ij} = \tau_{ji}$ is the time it takes for the information to reach from a unit i to its neighbor j, the other terms are similar as discussed in the previous chapters.

In the present investigation we consider networks with two types of delay arrangements: (i) Bimodal heterogeneous delay and (ii) a Gaussian distributed delay. The first arrangement is achieved by randomly making a fraction of connections f_{τ_1} conducting with τ_1, and another fraction f_{τ_2} conducting with delay τ_2. These two parameters are defined as $f_{\tau_1} = N_{\tau_1}/N_c$ and $f_{\tau_2} = N_{\tau_2}/N_c$, where N_{τ_1} and N_{τ_2} stands for the number of connections with delay τ_1 and τ_2, respectively. Maximum heterogeneity is exhibited when half of the connections bear a τ_1 delay and the other half bear a τ_2 delay. We remark that these definitions do not incorporate the exact values of delay and only take care of the number of connections conducting with different delay values. We consider $h = 1- \mid f_{\tau_1} - f_{\tau_2} \mid$ as a measure of the amount of heterogeneity in the network. The value of h being zero corresponds to the homogeneous delays, whereas $h = 1$ corresponds to $f_{\tau_1} = f_{\tau_2}$, denoting maximum heterogeneity.

Also, we define the cluster synchronizability of a network in terms of the number of nodes participating in the clusters. Based on this, we can say cluster synchronizability enhances if the number of nodes participating in the clusters formation increases in the network. Note that some of the earlier works have defined global synchronizability of network in terms of the ratio of the maximum and the first non-zero eigenvalues of the Laplacian of a graph [164, 165]. In the this chapter our definition of the synchronizability is based on cluster synchronization.

We first investigate the arrangement of two delay values in detail and then consider a Gaussian distributed delay arrangement. Depending on the parity of the delay, we classify three types of heterogeneity: (a) odd-odd heterogeneity, (b) odd-even heterogeneity, and (c) even-even heterogeneity. We find that these three types have a distinct impact on the coupled dynamics, and hence may give rise to different patterns of clusters as well as mechanisms behind their origin. We present detailed results for the logistic map as this simple map has been used widely and has exhibited a wide range of emergent behaviors observed so far in the nonlinear dynamics [64]. We also present results for the circle maps in order to demonstrate the robustness of the observed phenomena.

4.2 Coupled maps with bimodal heterogeneous delay

Starting with random initial conditions Eq. (4.1) is evolved and the phase synchronized clusters for T time steps after an initial transient are studied. We considers diffusive coupling ($g(x_i, x_j) = g(x_j) - g(x_i)$) because of its relevance in real world systems [64, 95]. Note that, the other forms of the couplings, such as linear, may yield different results for the same coupling value, but key phenomena observed for diffusive couplings such as different mechanisms of cluster formation would

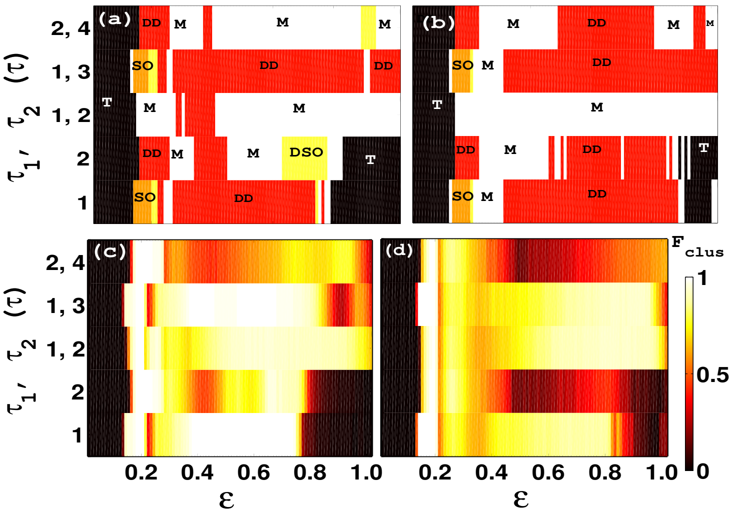

Figure 4.2: Phase diagrams (a) and (b), show different regions in the parameter space of τ_1, τ_2 (τ, for homogeneous delays) and ϵ for $f(x) = 4x(1-x)$. The grey (color) denotes different regions: turbulent (T)(stands for no cluster formation), ideal driven (D), dominant driven (DD), ideal self-organized (SO), dominant self-organized (DSO) and mixed (M). In these phase diagrams, the boundaries of the ideal D and ideal SO clusters do not depend on the threshold value, while the boundaries of the dominant D, SO and mixed clusters depend on the threshold chosen. (c) and (d) show variation in the fraction of nodes forming clusters ($F_{clus} = N_{clus}/N$, where N_{clus} = total number of nodes forming clusters) in the parameter space of τ_1, τ_2 (τ, for homogeneous delays) and ε for $f(x) = 4x(1-x)$. The values on the y axis represent the delay values. Network parameters are $N = 500$ and $\langle k \rangle = 4$. The grey (color) coding represents the variation in the fraction of nodes forming clusters. (a), (c) corresponds to the 1-d lattice and (b), (d) corresponds to the SF networks.

remain same [56, 57]. In the following first we present results for the maximum heterogeneity $f_{\tau_1} = f_{\tau_2}$, followed by the discussions on the impact of amount of heterogeneity on cluster formation.

4.2.1 1-d lattice and SW networks

1-D lattices used in the simulation have circular boundary conditions with each node having $\langle k \rangle$ nearest neighbors. Fig. 4.2(a) plots phase diagram depicting different cluster states based on the values of f_{inter} and f_{intra}, and Fig. 4.2(c) displays the fraction of nodes forming cluster (F_{clus}) for the 1-d lattice. In the absence of any coupling, all the nodes evolve independently in chaotic manner which solely depends upon the value of initial condition. As coupling is introduced ($\varepsilon > 0$), the coupled dynamics displays emerging behavior depending upon the delayed interactions and the strength of the coupling. The even-odd parity (say $\tau_1 = 1$ and $\tau_2 = 2$), for very weak coupling values ($\varepsilon < 0.16$) the local chaotic dynamics dominates over the interaction terms and all the nodes keep evolving in the isolated manner. As coupling is further increased, the coupling range ($0.16 \lesssim \varepsilon \gtrsim 0.25$) leads to the mixed clusters state. As ε increases further, there is an emergence of dominant D clusters (Fig. 4.2(a)) leading to the mixed clusters for strong couplings. For odd-odd parity, the ideal SO or the dominant SO clusters are formed. The snap-shots in the Fig.4.3(a) demonstrate the ideal SO clusters for the 1-d lattice. Note that, here the value of F_{clus} is one as all the nodes participate in the cluster formation, but they distribute in different clusters instead of forming a globally synchronized state. Hence, F_{clus} being one does not provide a criteria for the globally synchronized state.

Further, for the intermediate and strong coupling exhibit a manifestation of the dominant D clusters. Comparison with the homogeneous delays evolution leads to the conclusion that heterogeneous delays cause an enhancement in the synchronization for strong couplings while keeping the D mechanism responsible for the cluster formation. For the even-even parity, the coupled dynamics at weak ε range manifests the formation of the ideal D clusters, as observed for the even homogeneous delays (Fig. 4.2(a)). We remark that the definition of phase synchronization and the phase distance used here assign anti-phase synchronization (minima of one node matching with maxima of the other) into two different clusters as phase distance for this case remains one. However, this particular situation of nodes being anti-phase synchronized [1] is not so often observed for chaotic situation (for example Fig. 4.5 for $t < t_0$). With increase in the coupling strength, at intermediate and strong couplings the mixed clusters are formed (Fig.4.2(a)). At the strong couplings where the undelayed and the homogeneous delays do not lead to the cluster synchronization, for the even-even heterogeneous delays 50% of the nodes participate in cluster formation (Fig.4.2(c)).

The delayed coupled maps on the SW networks, generated using Watts-Strogatz

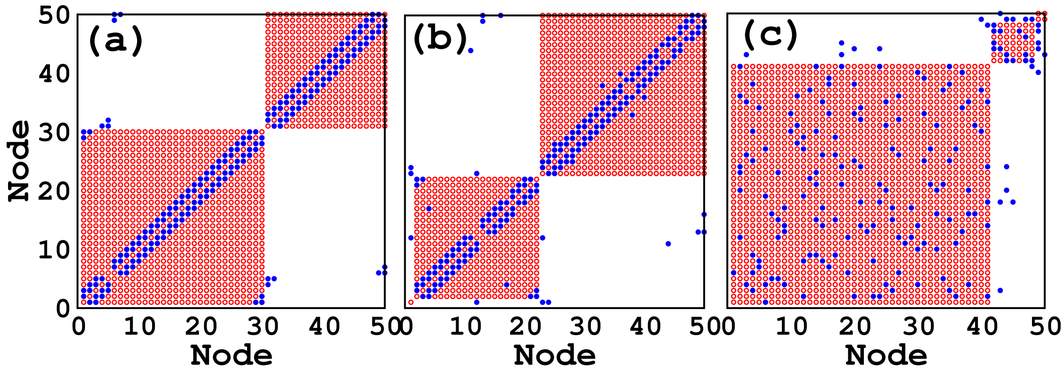

Figure 4.3: The ideal SO clusters for the 1-d lattice (a), SW (b) and random networks (c). Squares represent clusters, diagonal dots represent isolated nodes while off-diagonal dots imply that the two corresponding nodes are coupled (i.e. $A_{ij} = 1$). In each case the node numbers are reorganized so that the nodes belonging to the same cluster are numbered consecutively. The example correspond to the networks with $N = 50$, $\langle k \rangle = 4$ and $\varepsilon = 0.17$. All the graphs correspond to $f_{\tau_1} = f_{\tau_2}$, $\tau_1 = 1$ and $\tau_2 = 3$.

algorithm by rewiring probability p_r [27], do not display any distinguishable changes as compared to the corresponding 1-d lattice described above. Thus for 1-d lattice and SW networks the mechanism behind the cluster formation depends on the parity of delay values. At weak coupling, even heterogeneous delays are associated with the D mechanism, odd heterogeneous delays are associated with the SO mechanism, while mixed heterogeneous delays are associated with the mixed mechanism. Thus, a change in the parity of heterogeneous delay values may give rise to a transition from one phenomenon to the other phenomenon.

4.2.2 SF networks

We further turn our attention to the SF network, which has a completely different structural properties [27] than the 1-d lattice and the SW networks. SF networks are constructed by starting with $\langle k \rangle$ nodes and then adding one node with $\langle k \rangle$ connections at each step [27]. The weak coupling range displays a similar result as for the regular networks described in the previous section for all types of heterogeneity, whereas intermediate couplings do not display the transition from one mechanism to other as observed for the regular networks, which exhibit the transition from the dominant SO clusters state to the dominant D clusters state and instead yield the

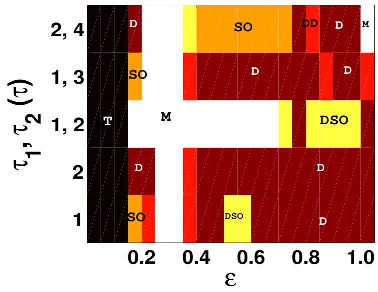

Figure 4.4: Phase diagrams (a) and (b), showing different regions in the parameter space of τ_1, τ_2 (τ for homogeneous delays) and ϵ for complete bipartite network of $N = 500$. The figure description remains same as for 4.2(a) and (b).

D or mixed clusters for all the parities (Fig. 4.2(b)). Comparing the three heterogeneity leads to the conclusion that even-even heterogeneity in delays causes less enhancement in fraction of nodes forming clusters, as compared to the odd-odd and odd-even heterogeneity (Fig. 4.2(d)). The phenomenon of suppression in fraction of nodes forming clusters, for a particular heterogeneity becomes more prominent with the increase in the delay values. At strong couplings, odd-odd heterogeneity in delays manifests better cluster synchronizability of SF networks as compared to the corresponding 1-d lattice and SW networks (Fig. 4.2(c) and (d)).

The random networks display a better synchronization than the corresponding regular networks even for undelayed and homogeneous delays [56, 80]. The interesting finding in the presence of heterogeneous delays is that the enhancement in the cluster synchronizability of the network may be accompanied with the nodes directly connected, as evident from the mixed clusters in Fig. 4.2. We remark that D clusters were already observed for homogeneous delays in intermediate ε range for the SF networks indicating synchronization between nodes which are not directly connected, therefore occurrence of synchronization between these nodes for high coupling range does not impart much surprise. We can fairly conclude that SO mechanism has a major role to play in the enhancement of synchronization in the presence of heterogeneous delays, which further becomes clearly visible for the complete bipartite network.

4.2.3 Complete bipartite networks

The complete bipartite networks consist of two sets where all the nodes of one set (say A) are connected with those of the second (say B). Results are presented for both the sets having equal number of nodes. The simple structure of these networks on one hand makes analytical studies easier to carry, on other hand capability of the network to yield rich cluster patterns such as ideal D, SO and mixed clusters brings it in the same platform of the other random networks. Fig. 4.4 plots phase diagram depicting different cluster states based on the values of f_{inter} and f_{intra} for the complete bipartite networks. Note that for the homogeneous delays itself the coupled dynamics exhibit participation of all the nodes in the cluster formation, and the introduction of heterogeneity in delay does not change this number. The phase diagram Fig.4.4 shows that at the weak couplings, as discussed for the other networks, the complete bipartite networks also exhibit the ideal D clusters for the even delays, while for the odd delays instead of the ideal SO clusters state as exhibited by the other networks discussed above, the complete bipartite networks lead to the globally synchronized sate. We remark that the complete bipartite networks do not show the ideal SO clusters, as due to its topology it is not possible to divide the whole network in the ideal SO clusters, however mixed or dominant SO and D states are possible for instance at the intermediate couplings and the strong couplings where homogeneous delays lead to the robust D clusters, the heterogeneity in delays generates the D, mixed or dominant SO clusters depending upon parity of the heterogeneous delays and coupling strength (Fig. 4.4(a)).

4.3 Analytical insight

In the following, we perform the Lyapunov function analysis in order to have an understanding of destruction of the robust D clusters observed for homogeneous delays and construction of different clusters for the heterogeneous delays. Furthermore, we present some arguments for the transition from the ideal D clusters to SO cluster state upon introduction of heterogeneity in delays at the intermediate and strong couplings.

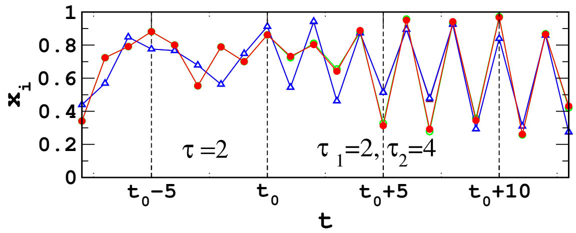

Figure 4.5: Time evolution of few nodes in the complete bipartite network of $N = 500$ (coupling strength is chosen as 0.68 for which network is shown to form two ideal D clusters for homogeneous delay ($\tau = 2$) for $t < t_0$.). At $t = t_0$ the heterogeneity in delay is introduced by randomly making 50% of the connections conducting with $\tau_2 = 4$ and rest keep on conducting with $\tau_2 = 2$

First, we analyze the case of the transition from D clusters to different clusters state. The Lyapunov function for a pair of nodes can be written as [56, 147, 148]

$$V_{ij}(t) = [x_i(t) - x_j(t)]^2. \tag{4.2}$$

$V_{ij}(t) \geqslant 0$ and the equality holds good when nodes i and j are exact synchronized. The Lyapunov function for a pair of nodes on a complete bipartite network in the presence of heterogeneous delays, using Eq.4.1 and Eq.4.2 can be written as:

$$V_{ij}(t+1) = [(1-\epsilon)(f(x_i(t)) - f(x_j(t))) + \frac{2\varepsilon}{N}\sum_{j=N/2+1}^{N} g(x_j(t-\tau_{ji})) - \frac{2\varepsilon}{N}\sum_{i=1}^{N/2} g(x_i(t-\tau_{ij}))]^2. \tag{4.3}$$

Let us consider a pair of nodes of the same set having the homogeneous delays, which leads to the situation where coupling terms having delay values in the Eq.4.3 get cancelled, thereby commencing the D clusters, robust against the change in the delay values [166]. Whereas in the presence of heterogeneity in delay values, the coupling term having delay values does not vanish in Eq.4.3, and thus may or may not emulate the synchronization between these nodes depending upon the delay arrangements of these two nodes, and may be leading to the nodes from the same set organizing into different clusters. Note that for parameter mismatch [167–169], the coupling term bearing the delay values does not vanish and the nodes from the same set may get distributed into different clusters even for undelayed and homogeneously delayed case. The Lyapunov function analysis performed here for the complete bipartite network works for the clusters having exactly synchronized nodes.

Furthermore note that for the undelayed and homogeneously delayed cases, the nodes receiving the same input can be considered as forming a set (say A in Fig. 4.6), similar to the complete bipartite networks, and the nodes which are giving same inputs to these can be considered to form another set (say B in Fig. 4.6). The synchronization criteria for nodes in set A depends whether these nodes are directly connected or not. For the first case, when nodes in set A are not directly connected

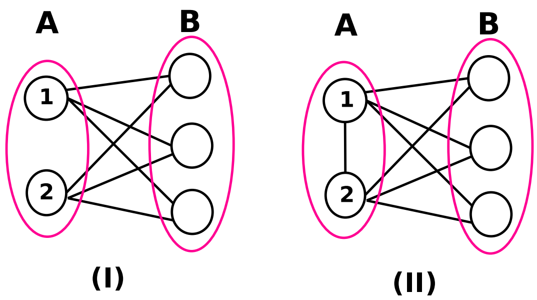

Figure 4.6: Schematic diagram representing two set of nodes, when a pair of nodes in set A receiving same inputs are not directly connected (I) and when they are directly connected (II).

(Fig.4.6 I), for undelayed and homogeneously delayed cases the Lyapunov function between a pair of nodes becomes:

$$V_{12}(t+1) \;=\; [(1-\epsilon)(f(x_1(t)) - f(x_2(t)))]^2.$$

Thus synchronization between the nodes 1 and 2 depends only on the local dynamics of both the nodes and the coupling strength. Whereas, if nodes in set A are directly connected (Fig.4.6 II), in the Lyapunov function all the coupling terms except the one involving the interaction between 1 and 2, cancel out;

$$V_{12}(t+1) \;=\; [(1-\epsilon)(f(x_1(t)) - f(x_2(t))) + \frac{\epsilon}{4}g(x_2(t-\tau)) - g(x_1(t-\tau))]^2.$$

thus yielding different criteria for synchronization of these nodes [58].

Next, using the complete bipartite network, we attempt to understand the parity dependence of the mechanism of cluster formation at weak couplings as observed for all the network architectures. A simple analysis for the periodic synchronized state on the complete bipartite networks provides a basic understanding of different behaviors observed for the lower coupling values. For example, at weak ε range, the homogeneous delays for $\tau_1 = 1$ manifests the globally synchronized state spanning all the nodes for $0.16 \lesssim \varepsilon \gtrsim 0.2$. The dynamical evolution in this range is periodic with periodicity two, say $p1$ and $p2$. As heterogeneity in the delay values is introduced such that $f_{\tau_1} = f_{\tau_2} = 0.5$, say at the $(t+1)^{th}$ time step, it leads to the coupling term having delay part in the evolution equation for the difference variable of i^{th} and j^{th} nodes as,

$$f(x_j(t-\tau_2)) - f(x_i(t-\tau_1)) = \begin{cases} 0 & \text{if } \triangle\tau = 2, 4...., \\ \delta & \text{if } \triangle\tau = 1, 3..... \end{cases}$$

where $\delta = f(p_1) - f(p_2)$ and $\triangle\tau = \tau_2 - \tau_1$. $\triangle\tau$ is even for the odd-odd and the even-even heterogeneity, and odd for the odd-even heterogeneity. Thus the even-even heterogeneity will retain the behavior followed by the even homogeneous delay values, and the odd-odd heterogeneity will retain the behavior followed by the odd homogeneous delay values. Whereas, the odd-even heterogeneity may disturb the behavior manifested by the even homogeneous or odd homogeneous delays and lead to the mixed cluster state. Note that for diffusive coupling, the odd delays leads to mismatch in the parity of delay value of the coupling terms, causing a change in the sign of coupling term. This may cause a significant impact on the dynamics of the coupled system leading to the different phenomena for the odd and even delays [78, 80, 170, 171].

Further, we turn to analyze the origin of mixed and dominant SO clusters for the bipartite networks at the intermediate and strong couplings. A closer look into the time evolution of the coupled nodes in the bipartite networks for the intermediate ε values reveals that the heterogeneity suppresses the exact synchronization between the nodes which are not directly connected while retaining the phase synchronization between them (Fig. 4.5). Whereas all the pairs of nodes which are directly connected experience an occurrence of the phase synchronization producing the globally phase synchronized state. In order to further explain the synchronization between the nodes from two different sets at strong couplings we perform the following analysis. We consider $\varepsilon = 1$, for which all the coupling terms in the difference variable $(x_i(t+1) - x_k(t+1))$ for a pair of nodes in the same set (i.e. nodes are not directly connected) will get cancelled out for the undelayed and the homogeneous delayed case, causing to the synchronization of all the pairs of nodes in the set. Let $x_A(t)$ being the synchronized dynamics of nodes in the first set and $x_B(t)$ being the synchronized dynamics of the nodes in the second set. For homogeneous delay ($\tau_{ij} = \tau$), the difference variable for the nodes from the different sets will be:

$$x_i(t+1) - x_j(t+1) = g(x_B(t-\tau)) - g(x_A(t-\tau)); \tag{4.4}$$

This difference variable will not die for the coupling function $g(x)$ lying in the chaotic regime, if the initial conditions for the nodes in two sets are different. Hence the nodes from different sets does not synchronize ruling out the SO synchronization for the undelayed and homogeneously delayed case for $\varepsilon = 1$. Whereas the heterogeneous delays do not lead to such a simple situation, and the difference variable for the nodes in the different sets takes form

$$\begin{aligned} x_i(t+1) - x_k(t+1) &= \frac{2}{N}[\sum_{i=1}^{N} A_{ik} g(x_k(t-\tau_{ki})) \\ &- \sum_{k=1}^{N} A_{ki} g(x_i(t-\tau_{ik}))]. \end{aligned} \tag{4.5}$$

For the heterogeneous delays, the synchronization between a pair of node from the same set for $g(x) = 4x(1-x)$ at $\varepsilon = 1$, depends on the coupling from other nodes. Thus depending on the heterogeneous delay values, these node may or may not synchronize. Thus, the presence of heterogeneity in delay breaks the restriction (4.8) and gives rise to a possibility of the synchronization of between the nodes in the different sets. Though analysis carried out here is done for the extreme coupling value ($\varepsilon = 1$) and can not be directly applied to other ε values for which another term consisting local dynamics of nodes also appears into the difference variable given by Eq. 4.8 and Eq. 4.5, but at the strong coupling this additional term will have less impact on the dynamical evolution as compared to the coupling term leading to similar effect being responsible.

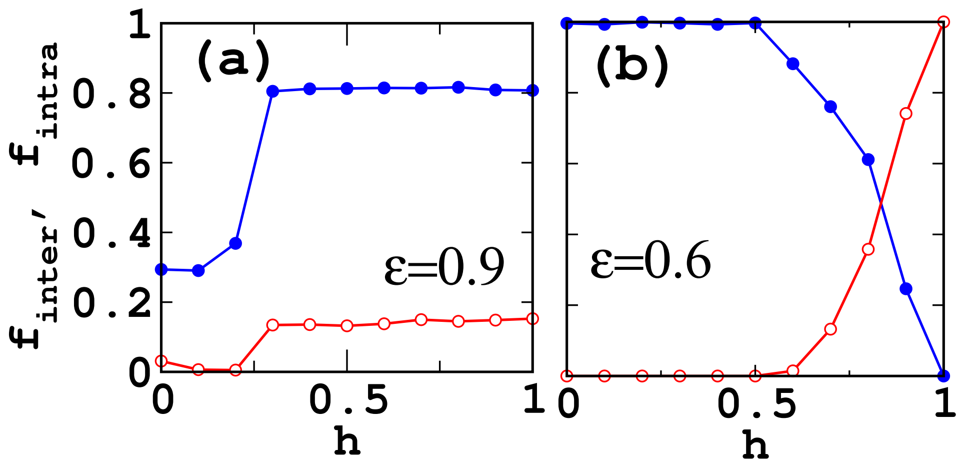

Figure 4.7: Variation of f_{inter} (closed circles) and f_{intra} (open circles) as a function of amount of heterogeneity. (a) SF network with $N = 500$ and $\tau_1 = 1, \tau_2 = 3$, (b) the complete bipartite networks with $N = 200$ and $\tau_1 = 2, \tau_2 = 4$. Both the graphs are for $f(x) = 4x(1-x)$.

4.4 Effect of the change in amount of heterogeneity

So far we have concentrated on the case $h = 1$ corresponding to the maximum heterogeneity. We find that while the amount of heterogeneity plays a crucial role in determining the cluster synchronizability of networks, for some cases even demonstrating a transition from no cluster state to all nodes forming clusters (Fig.4.7(a)), while the mechanism is still governed by the parity except for the complete bipartite networks which show a transition from robust D clusters state to the dominant SO clusters and a single SO cluster state (Fig.4.7(b)). To the end of this section we provide understanding of this behavior. Fig. 4.7(a) demonstrates clear examples of the enhancement in the cluster formation while retaining the mechanism in the presence of the heterogeneous delays with odd-odd parity. For homogeneous delay (say $\tau = 1$), a very less number of nodes form clusters (Fig.4.7). As some connections start conducting with a different delay value τ_2, there is no significant change in the cluster formation as depicted in the Fig.4.7. With a further increase in f_{τ_2}, there is an increment in the number of nodes forming clusters reaching to the all nodes forming cluster for $h \gtrsim 0.4$.

As we have illustrated that the introduction of heterogeneity in delays enhances synchronization and the complete bipartite network already displays 100% nodes participating in formation of the robust D clusters for the homogeneous delay, the only possible way to achieve an enhancement of the synchrony could be via synchronization between nodes of two driven clusters giving rise to the SO clusters. The arguments delivered earlier using difference variable (Eq. 4.8) directs that more heterogeneity in delays will lead to the occurrence of more number of pair of nodes from the same set for which the difference variable does not die, thus destroying synchronization between more pair of nodes belonging to same set, and could be a possible reason behind more heterogeneity inducing more SO synchronization.

4.5 Coupled maps on Cayley tree

Many of the real world networks such as river networks, family networks, computer networks and biological networks reflect the tree structure. Cayley tree provides a very simple model and thus has been widely studied for instance to model some of the real world networks such as immune network [40, 41]. As discussed for the other networks, at the weak couplings the heterogeneous delay leads to the D, SO or mixed clusters depending upon the parity of the heterogeneous delays. In the following we discuss few interesting behaviors shown by the heterogeneous delays, which was not observed for the homogeneous delays.

4.5.1 Synchronization of parent nodes

The earlier work on the Cayley tree unveils that for homogeneous delays the parents are synchronized only when their children are synchronized [172]. We find that the heterogeneous delays lead to the synchronization of the parent nodes, even for situations where their children nodes are not synchronized, a phenomena not observed for the homogeneous delay values. Fig. 4.8 plots a demonstration of synchrony in the parent nodes accompanied with no synchrony among their children nodes. In order to understand the origin of this behavior for heterogeneous delays we study the difference variable for two parent nodes, for example nodes b and c in Fig. (4.10), given as follows:

$$\begin{aligned}
&x_b(t+1) - x_c(t+1) = (1-\varepsilon)(f(x_b(t)) - f(x_c(t))) + \\
&\frac{\varepsilon}{K+1}[\sum_{p\in S_b} f(x_p(t-\tau_{bp})) - \sum_{q\in S_c} f(x_q(t-\tau_{cq})) + \\
&(f(x_a(t-\tau_{ab})) - f(x_a(t-\tau_{ac})))].
\end{aligned} \tag{4.6}$$

where S_b and S_c denote the set of children nodes of b and c respectively. The coupling terms having the delay in the right hand side depend on the behavior of children nodes as well as of immediate ancestor node of b and c, respectively. Since the immediate ancestor of nodes b and c is common (a), for the homogeneous delay the third term in the right hand side cancels out, making the synchronization between b and c depend on the synchronization between the children nodes only. Thus for the homogeneous delay, if the children nodes are synchronized then irrespective of the delay value, depending on the coupling strength the parent nodes will also get synchronized. However, for the heterogeneous delay, the third term in the right hand side of Eq. 4.6 does not vanish, making the synchronization of b and c depend on their parent node a as well. Thus for the heterogeneous delay the synchronization between the parent nodes does not solely depend on the synchronization among their children.

Furthermore, the D clusters induced by the heterogeneity in delays at intermediate couplings are seen to comprise of nodes from the different generations. Note that for these couplings the D clusters observed for the homogeneous delay constitute nodes from the last generation only. The heterogeneity in delays brings nodes from different families together while preserving the underlying mechanism. Fig. 4.8(b) demonstrates the synchronization of different generations for heterogeneous delays. Fig. 4.9 presents the time evolution of the state of few nodes of Fig. 4.8(b). This fugure manifests that for the heterogeneous delay, even when the child nodes are not phase synchronized (Fig. 4.9(b)) their parent nodes are phase synchronized(Fig. 4.9(a)). In order to find the reason behind the synchronization of inner nodes for heterogeneous delay, we study the difference variable for the last generation nodes originated from the different parents, for example nodes d and f

in Fig. (4.10) at $\varepsilon = 1$;

$$x_d(t+1) - x_f(t+1) \quad = \quad (f(x_b(t-\tau_{bd})) - f(x_c(t-\tau_{cf}))). \qquad (4.7)$$

which in case of homogeneous delays for the chaotic evolution of individual nodes never die for the random initial condition, and therefore the synchronization between the last generation nodes from different parent nodes is not possible. As we have already noted that for homogeneous delay synchronization of the parent nodes depends on the synchronization between their children [166], thus the parent nodes of the last generation nodes (for example b and c) can not get synchronized for the homogeneous delay, similarly we can explain that other ancestors also can not get synchronized. Thus for homogeneous delay at $\varepsilon = 1$ the inner nodes can not get synchronized, while for the heterogeneous delays as we explained above that the behavior of the parent nodes is not completely governed by the behavior of the children giving rise to a possibility for the synchronization of the inner nodes.

To conclude, heterogeneity in delay values makes the synchronization of the parent nodes independent of synchronization among their children nodes and at strong coupling where, homogeneous delay does not lead to the synchronization between the inner nodes, heterogeneity in delay paves a way to a more coherent behavior. Although we observe synchronization of the inner nodes in the coupling range $0.55 \lesssim \varepsilon \lesssim 0.9$, and the analysis carried out here is done for extreme coupling value ($\varepsilon = 1$) which can not be directly applied to other ε values for which terms consisting of local dynamics of nodes also appear into the difference variable given by Eq. 4.7, but it would have lesser impact on the dynamical evolution as compared to the coupled terms for the strong coupling range, and hence analysis carried out here may stand valid for this range.

4.5.2 Occurrence of lag synchronization

As discussed in the introduction section, in a tree network more than the 50% of the total nodes lie on the boundary, thus in this section we explain the interesting behavior displayed by these nodes. The study of synchronized patterns in presence of heterogeneity in delays reveals many different emerging behaviors of these nodes,

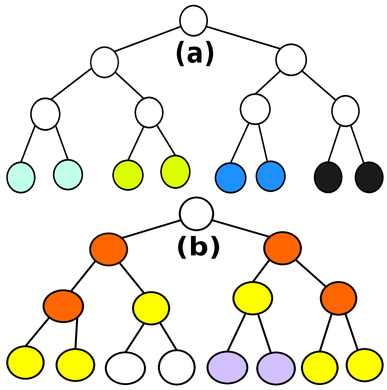

Figure 4.8: (a) synchronization of the last generation siblings for the homogeneous delay ($\tau = 1$), (b) synchronization of the parent nodes for heterogeneous delays ($\tau_1 = 1, \tau_2 = 3$), even though there is no synchronization between their children for Cayley tree networks of $N = 31$, $K = 2$ at $\varepsilon = 0.7$. Shades (colors) denote that corresponding nodes belong to same cluster. Open circles represent that the corresponding nodes are not synchronized.

which are as follows.

In this section we discuss lag synchronization of the last generation nodes originated from the same parent in the presence of heterogeneity in delay values. In order to investigate the lag synchronization we define the variance:

$$\sigma_{g_a}{}^2 = \frac{\langle \sum_{j=a}^{N} A_{aj}(x_j(\tau_{ja}) - \bar{x})^2 \rangle_t}{K};$$

where i, j are the last generation nodes which have originated from a, $\langle\rangle_t$ denotes average over time and:

$$\bar{x} = \frac{\sum_{j=a}^{N} A_{aj} x_j(\tau_{ja})}{K}.$$

Thus $\sigma_{g_a}{}^2 = 0$ for $x_i(t + \triangle\tau) = x_j(t)$, where $\triangle\tau = \tau_1 - \tau_2$. For a network of height h and branch ratio K, there will be K^{h-1} set of last generation siblings (represented by g), thus K^{h-1} number of variance should be calculated, however the behavior of one set of siblings should be same as the other set of siblings. Fig. 4.11 manifests variation of $\sigma_{g_a}{}^2$ vs ε for the dynamics governed by Eq. 4.1. It presents the lag synchronization among the last generation siblings in both lower ($0.18 \lesssim \varepsilon \lesssim 0.38$) and higher ($\varepsilon \gtrsim 0.38$) coupling range.

In order to understand the destruction of exact synchronization and origin of lag synchronization with heterogeneous delay values, we study the difference variable between a pair of last generation nodes originating from the same parent (let i and

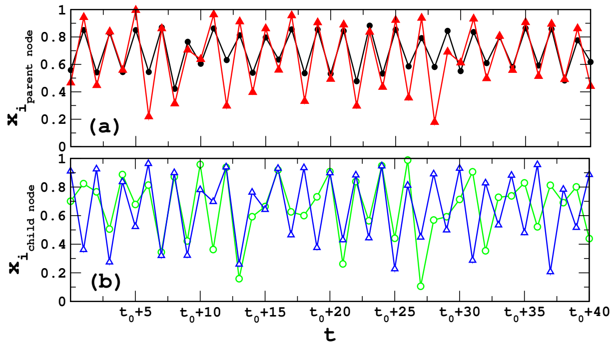

Figure 4.9: (a) time evolution of the two parent nodes(closed circle and closed triangle) (b) time evolution of the child node of parent nodes plotted in (a). The open circle in (b) correspond to the child node of parent node represented by the closed circle in (a), similarly the open triangle in (b) correspond to the child node of parent node represented by the closed triangle in (a). All the parameters are same as taken in Fig. 4.8

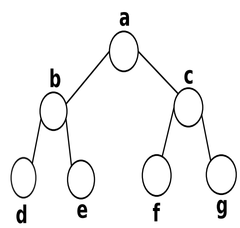

Figure 4.10: Schematic diagram for the tree network for $K = 2$.

j) for the simplest case of $\varepsilon = 1$:

$$x_i(t+1) - x_j(t+1) = g(x_a(t-\tau_{ia})) - g(x_a(t-\tau_{ja})); \quad (4.8)$$

So one can see that for homogeneous delay, the above equation will reduce to :

$$x_i(t+1) - x_j(t+1) = 0;$$

Thus, for the homogeneous delay the last generation nodes originating from the same parent will always get synchronized, while for the heterogeneous delay at $\varepsilon = 1$ a simple calculation gives that the dynamical evolution of the i^{th} and j^{th} last generation nodes will be:

$$x_j(t + \triangle\tau) - x_i(t) = 0; \quad (4.9)$$

where $\triangle\tau = \tau_{ia} - \tau_{ja}$.

Thus, the introduction of heterogeneity in delay destroys the exact synchronization between a pair of last generation nodes and leads to the lag synchronization with time lag being equal to the difference of delay values for the two nodes.

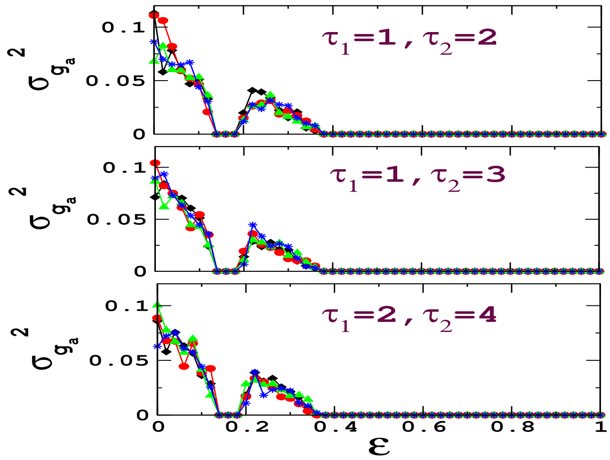

Figure 4.11: ${\sigma_{g_a}}^2$ as a function of ε for the last generation nodes for $N = 21$, $K = 4$ and for 20 random initial conditions. The different symbols correspond to the different set of last generation siblings. The local dynamics of the nodes is governed by the logistic map($x_i(t+1) = 4x_i(t)(1 - x_i(t))$).

Fig 4.12 represents the time evolution of the last generation nodes from the same parent.

4.6 Coupled circle maps

In order to demonstrate the robustness of the results, in this section we present results for the coupled circle maps. The local dynamics is given by:

$$f(x) = x + \omega + (p/2\pi)sin(2\pi x) \ \ (mod1). \tag{4.10}$$

Here we discuss results with the parameters of circle map in the chaotic region ($\omega = 0.44$ and $p = 6$). As discussed for the logistic map, the coupled circle maps also lead to: (i) dependance of mechanism behind cluster formation on the parity of delays, (ii) the enhancement in the synchronization by introduction of heterogeneity in delay, (iii) change in the cluster patterns with the change in the heterogeneous delays and (iv) occurrence of lag synchronization among last generation siblings in Calyley tree network. Fig. 4.13 demonstrates the change in the mechanism behind the cluster formation with change in the parity of heterogeneous delay values as well as exhibit the change in the cluster patterns. These snapshots depict the formation of the SO clusters for the odd heterogeneous delays, mixed clusters for the mixed parity of the heterogeneous delays and D clusters for the even heterogeneous delays.

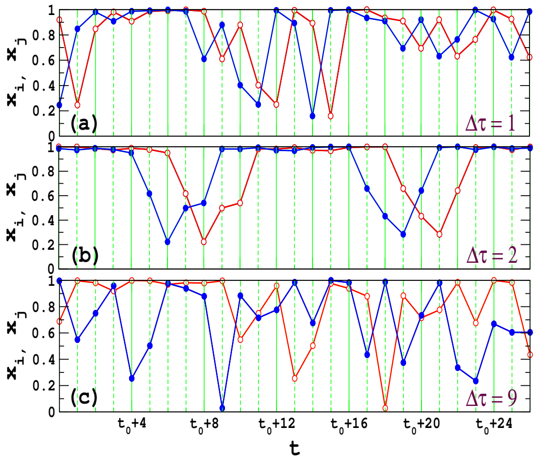

Figure 4.12: Time evolution of the boundary nodes originated from the same parent for a Cayley tree network with $N = 21$, $K = 4$ and $\varepsilon = 1$. The diagram exhibits that there is time lag synchronization between the two nodes i (open circle) and j (closed circle) with time lag being 1, 2 and 9 for (a), (b) and (c) respectively. The local dynamics is governed by the logistic map $(x_i(t+1) = 4x_i(t)(1 - x_i(t)))$.

Figs. 4.15(a) and (b) plot examples demonstrating the transition from the ideal D to the globally synchronized state for the coupled circle maps on the complete bipartite networks.

4.7 Gaussian distributed delays

In order to see robustness of the phenomena, such as enhancement in cluster synchronization and change in the mechanism for the two delays case, we consider the Gaussian distributed delays as [110], $\tau_{ij} = \bar{\tau} + Near(c\eta)$, where η is Gaussian distributed with mean zero and standard deviation one. The delays are homogeneous ($\tau_{ij} = \tau$) for c =0 and are Gaussian distributed around $\bar{\tau}$ for $c \neq 0$. We choose example of SF networks in order to capture a better overview of the mechanism behind cluster synchronization as they are known to exhibit good synchronizability for undelayed and delayed evolution. We find that the distributed delays breaks dominance of any of the two mechanisms, clearly visible for homogeneous and two delays case, leading to the mixed clusters state for $\varepsilon \gtrsim 0.15$ (Fig. 4.16(a)). The other networks, except the complete bipartite networks, we have considered, manifest the similar results as for the SF networks. The complete bipartite networks for

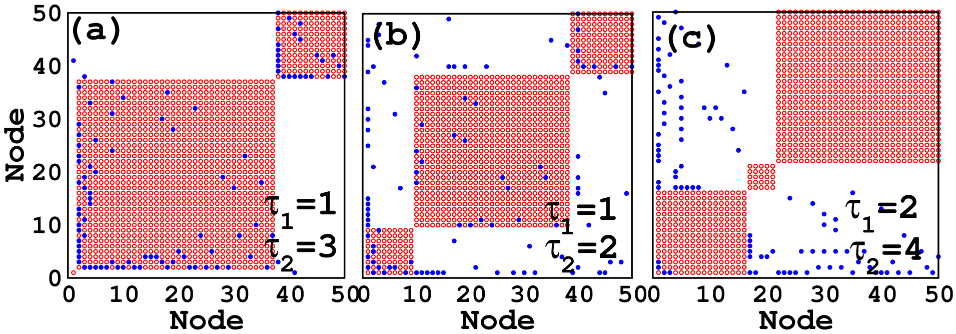

Figure 4.13: A typical behavior of coupled dynamics illustrating different cluster patterns for change in parity of heterogeneous delays. Figure description remains same as in Fig.4.3. The example presents a scale-free network with $N = 50$, $\langle k \rangle = 4$ and $\varepsilon = 0.02$. All the graphs correspond to $f_{\tau_1} = f_{\tau_2}$.

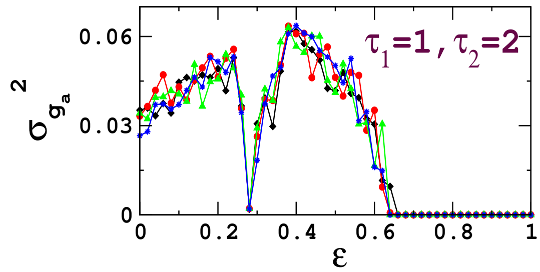

Figure 4.14: ${\sigma_{g_a}}^2$ as a function of coupling strength for the last generation nodes for circle map. The figure is plotted for $N = 21$, $K = 4$ and for 40 random initial conditions. The different symbols correspond to the different set of last generation siblings. The local dynamics of the nodes is governed by Eq. 4.10.

the Gaussian distributed delays are capable of displaying all the mechanism of cluster synchronization as observed for the two delays case (Fig. 4.16(b)), leading to the rich cluster patterns depending on the coupling strength. Comparison with the Fig. 4.2(a) and (b) indicate that the Gaussian distributed delays reveals no further phenomena than already observed for the two delays heterogeneity.

4.8 Effect of average degree

Previous studies demonstrate that undelayed and the homogeneously delayed evolution of all the networks with high average degree leads to the globally synchronized state after a critical ε value, whereas the introduction of the odd-even heterogeneity leads to the multi-cluster state. Note that for this multi-cluster state there is no significant suppression in the overall synchronization in the network, as still almost

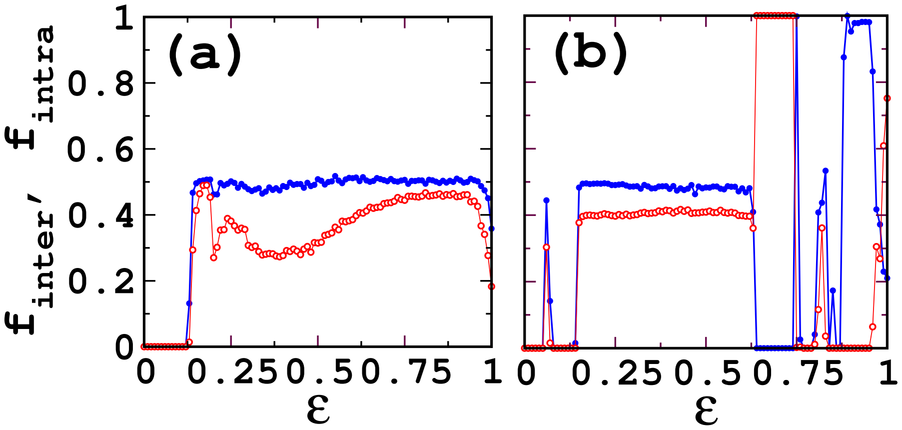

Figure 4.15: Node versus node diagram demonstrating various clusters state for (a) and (b) for coupled circle maps on the complete bipartite networks of $N = 50$ at $\varepsilon = 0.85$, (c) and (d) for coupled logistic maps on globally connected network of $N = 200$ at $\varepsilon = 1.0$. (a) and (c) $\tau = 0$/ $\tau = 1$ indicate that exactly same patterns are obtained for the undelayed ($\tau = 0$) and the homogeneous delayed ($\tau = 1$) cases. Circles and dotes remain same as in Fig.4.3. All the graphs correspond to $f_{\tau_1} = f_{\tau_2}$.

all (95%) the nodes participate in the cluster formation. The only difference is that the heterogeneity in delays breaks the globally synchronized cluster, distributing its nodes into the different clusters (Fig.4.15). The Gaussian distributed delays at strong couplings also generates the multi-cluster state as observed for the two delays odd-even heterogeneity.

For the coupled dynamics, there exists a trade off between the local dynamics and the coupling term resulting in various emerging behaviors. At strong coupling values, the coupling term dominates over the local dynamics. Again as explained earlier, for $\varepsilon = 1$, the Lyapunov function for a pair of nodes (Eq. 4.2) in the globally connected networks would depend only on the term $(g(x_j(t-\tau)) - g(x_i(t-\tau)))$ while other terms cancel out. Whereas for the heterogeneous delays, the Lyapunov function would contain all the coupling terms (4.3), thereby making the stability of the synchronized state dependent on the neighbors thereby disturbing the synchronization between the nodes for the homogeneous delay case. Therefore, for the heterogeneous delays, a pair of nodes i and j may or may not get synchronized depending on the delays connecting to all the neighbors, thereby leading to different cluster patterns such as multi-cluster state for globally coupled network against

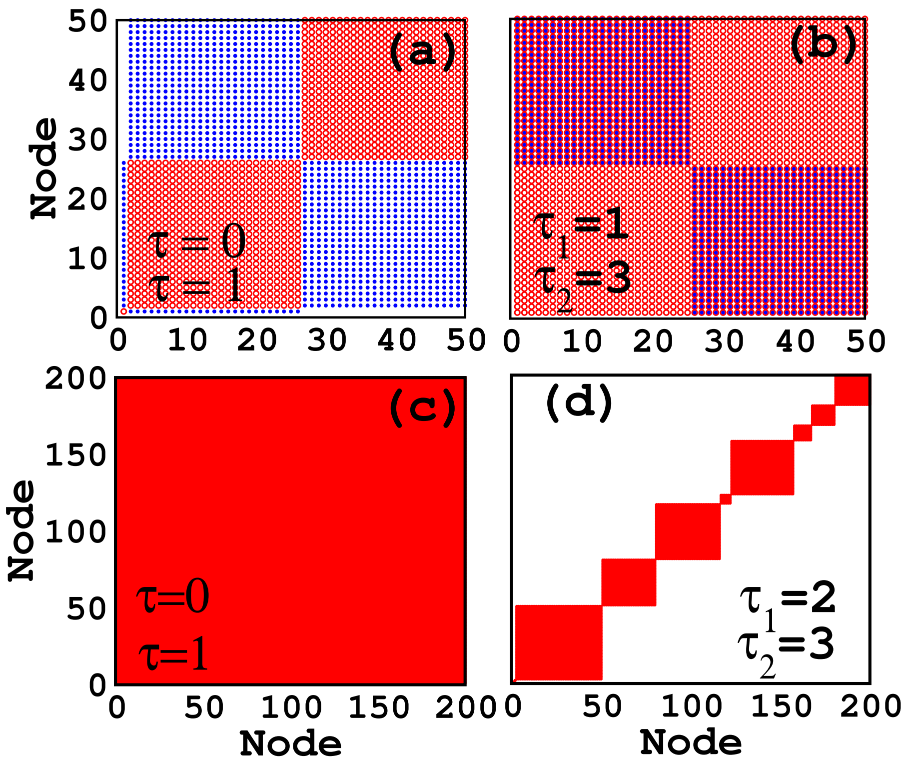

Figure 4.16: Variation of f_{inter} (closed) and f_{intra} (open) circles as a function of ε for SF (left) and complete bipartite (right) networks with $N = 500$ and for Gaussian distributed delays with mean $\bar{\tau} = 10$ and variance $c = 9$.

global synchronized state for the homogeneous delays.

4.9 Discussion and conclusion

We study the impact of heterogeneity in delay values on cluster synchronization and present the results for two different delay arrangements; (i) the heterogeneity with two different delay values, and (ii) the heterogeneity with the Gaussian distributed delays. For the first case, the cluster synchronization exhibits a dependence on the amount of heterogeneity in delays. Our results suggest that the heterogeneous delays accomplish an enhancement in the cluster synchronization for which we provide arguments using simple network structures. The enhancement in the cluster synchronization with enhancement in the heterogeneity in delays at the strong couplings indicates that heterogeneity in delay may simplify the coupled dynamics.

Next, we find that at weak couplings the different parities impose different constraints on the coupled dynamics, thereby inducing the different mechanism of cluster formation for which we provide an explanation by considering a simple case of periodic evolution. For intermediate and strong couplings, we find that more amount of heterogeneity in delays is associated with enhanced cluster synchronizability of the network. Thus, the amount of heterogeneity can be used as a tool to improve or reduce the cluster synchronizability of the model networks [151, 152] and can be used to understand versatile cluster patterns observed in the real world network [103]. The Gaussian distributed delays exhibit similar results as observed for the odd-even delays displaying the mixed clusters at the weak, intermediate and strong couplings. All the numerical results indicate that the heterogeneity in delays favor SO mechanism of synchronization for achieving a better synchrony in network as connections in the network increase. This is more evident in case of odd-odd heterogeneity, which advances the ideal D clusters for network having less number of connections and manifests a transition to the SO cluster as connections are increased. Note that for these high average degrees all the networks (except the complete bipartite networks) with homogeneous or zero delay display the globally synchronized state at strong enough coupling strength, while the networks with heterogeneous delays yield the multi-clusters state keeping SO mechanism responsible for the synchronization intact.

Using the Lyapunov function analysis, we furnish the argument that the heterogeneity in delays wreaks a different couplings environment for nodes directly connected, which for strong coupling regime, where coupling term dominates over the local evolution, is responsible for disrupting the global cluster. We further substantiate that for the complete bipartite networks, at the strong couplings, in the presence of heterogeneity in delays, the combined effect of the two postulates: (i) destruction of the ideal D cluster state and (ii) possibility of the SO synchronization, leads to the formation of different cluster patterns such as mixed, dominant D, dominant SO and ideal SO.

To conclude, using extensive numerical simulations for various model networks accompanied with the analytical understanding using the Lyapunov function for the completely bipartite networks we demonstrate that in the presence of heterogeneity in delays, the mechanism for cluster synchronization can be completely different from the homogeneous delayed evolution. In brain, the time of information transmission lie in a range exhibiting a heterogeneity in time delay [94], the results presented in this Letter can be used to gain insight into the synchronized activities of such systems. Furthermore, the heterogeneous delays have been shown to display the regular chaotic patterns in the brain networks [173–175]. Our results may be further extended to study the mechanism behind the origin of these patterns. Furthermore, since our definition of phase synchronization is based on the study of matching local maxima (minima) in the time evolution of the coupled nodes and recently local maxima (minima) has been found useful in understanding dynamical behavior of stock market [176, 177], our work may be further extended to investigate the cluster patterns in the stock market.

Chapter 5

Cluster synchronization in multiplex networks

A complex system may consist of a superposition of various interacting networks [178–180], such as a social system which may be composed of different sub-networks consisting family, friends, colleagues, work collaborators and hence forming a multiplex network. The multiplex network presents a more realistic representation of real world interactions [178] leading to a spurt in the activities of modelling real world complex systems under this framework.

Most of the studies on multiplex networks have concentrated on the investigation of various structural properties or emergence of spectral properties [181–183]. A recent work, considering dynamical properties of the multiplex networks reports that the synchronizability of a multiplex network is maximum for the small-world - random regular topology [184] as well multiplexing reduces the rate of the global synchronization [184].

In this chapter, we present the dynamical behavior of nodes in a layer upon multiplexing with other layers. Particularly, we investigate the impact of nodes interactions in one layer on the cluster synchronizability of the same nodes in the other layer. In a realistic situation, the connection density as well as degree of distribution of two layers can be different, for instance in a social system a family network can be denser than a counter friendship network. Similarly, the friendship network can be denser than a corresponding business network.

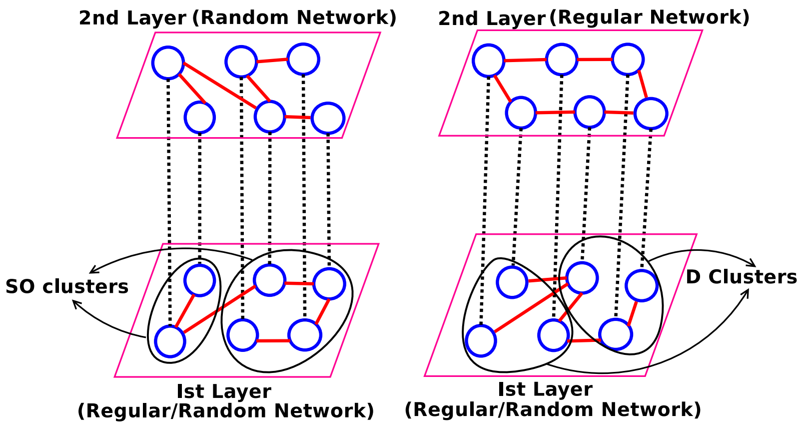

Figure 5.1: Schematic diagram depicting a multiplex network with two layers. The dashed lines indicate the inter-layer connections. The density of connections in the different layers can be different and is defined as $\langle k_1 \rangle$ for the first layer and $\langle k_2 \rangle$ for the second layer.

We consider the well known coupled maps model [111] to investigate the phase synchronized clusters in the multiplex networks. We consider the phase synchronization instead of complete synchronization as for sparse networks number of nodes exhibiting the complete synchronization is very less and with an increase in the connection density there is a transition to the globally synchronized state [178], whereas the prime motive of the current work is to study cluster synchronization. The phase synchronization reveals interesting cluster patterns as well as dependence of mechanism of cluster formation in one layer on the network structure of other layer. Let each node of the network be assigned a dynamical variable $x_i, i = 1, 2, \ldots, N$. The dynamical evolution is defined by,

$$x_i(t+1) = (1-\varepsilon)f(x_i(t)) + \frac{\varepsilon}{k_i}\sum_{j=1}^{n} NA_{ij}g(x_j(t)) \tag{5.1}$$

Here, A is the adjacency matrix with elements A_{ij} taking values 1 and 0 depending upon whether there is a connection between i and j or not and n is the number of layers in the multiplex network. We consider simplest case of two layer multiplex network. The matrix A for a two layer multiplex network can be given as:

$$A = \begin{pmatrix} A^1 & I \\ I & A^2 \end{pmatrix},$$

where, A^1 and A^2 are the adjacency matrix corresponding to the layer 1 and layer 2. $k_i = (\sum_{j=1}^{N} A_{ij})$ is the degree of the i-th node and N is total number of nodes in a layer. The average degree of the different layers may be different and are indicated as $\langle k_1 \rangle$ and $\langle k_2 \rangle$. We consider the local nonlinear map ($f(x)$) as well as the coupling function ($g(x)$) governed by the logistic map for $\mu = 4$.

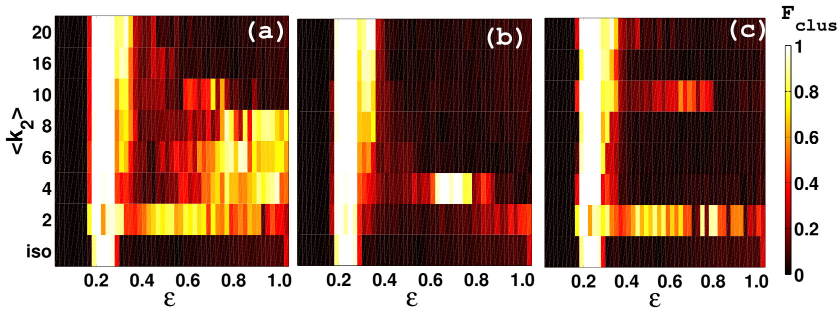

Figure 5.2: Phase diagram depicting the variation of f_{clus} with respect to the ε and the average degree ($\langle k_2 \rangle$) of 1-d lattice multiplexed with the (a) random network, (b) SF network and (c) 1-d lattice. The average degree of the first layer ($\langle k_1 \rangle = 4$) remains same for all three cases. The label 'iso' on the y axis represents that the corresponding row represents the values of f_{clus} for the isolated network. For all the layers $N = 100$ and phase diagrams are plotted for average over 20 random realizations of the networks and initial conditions.

5.1 Numerical Results

Starting from a set of random initial conditions we evolve Eq. 5.1 and study the phase synchronized clusters after an initial transient. We present detailed results of cluster synchronization for simplest multiplex network consisting of two layers. First layer can be represented by a regular or a random network, similarly the second layer can also be modelled by a regular or random network. Here, we present results for all the possible combinations, such as random-random, random-regular, regular-regular and regular-random.

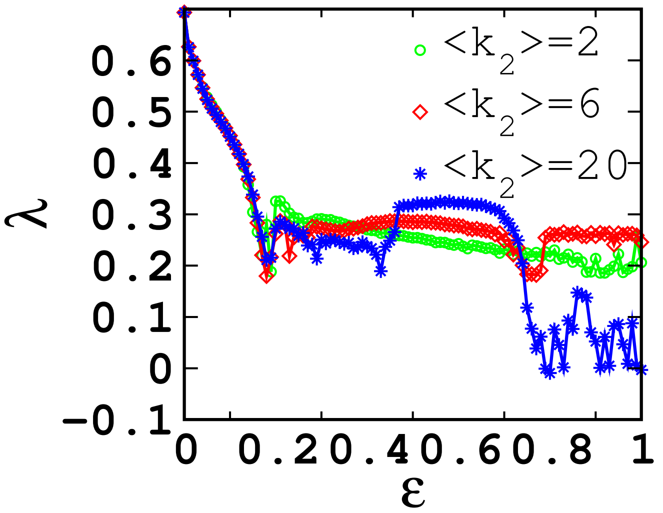

Figure 5.3: (Color online) The largest Lyapunov exponent for a multiplex network consisting of two layers, one represented with the ER random ($\langle k_1 \rangle = 4$) network and another with 1-d lattice for various average degree $\langle k_2 \rangle$. Number of nodes in each layer is $N = 100$.

5.1.1 Cluster synchronizability of regular networks upon multiplexing

First, we discuss the cluster synchronizability of a regular network represented by 1-d lattice upon multiplexing with a ER random network [27].

We find that the isolated sparse 1-d lattice at weak couplings leads to the phase synchronized clusters with all the nodes participating in the clusters, whereas strong couplings lead to a very few nodes forming clusters (Fig. 5.2(a)). Multiplexing with a sparse ER network enhances the cluster synchronizability of the 1-d lattice at all the couplings . Multiplexing with a denser ER network while enhances the cluster synchronizability as weak couplings, leaves the cluster synchronizability unchanged with few nodes keep forming synchronized clusters at the intermediate and strong couplings. Fig. 4.2(a) demonstrates that cluster synchronizability of 1-d lattice enhances at the weak couplings irrespective of the value of $\langle k_2 \rangle$, whereas at the intermediate coupling, for $\langle k_2 \rangle = 2$, there is an enhancement in the cluster synchronization, which for the higher values of $\langle k_2 \rangle$ gets vanished. At strong couplings synchronization enhances for $\langle k_2 \rangle \lesssim 8$. Additionally, the multiplex network yields the chaotic dynamics for almost all the coupling values for the layers

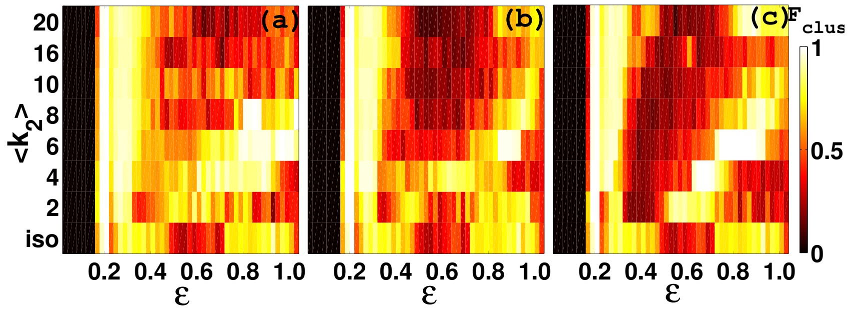

Figure 5.4: (Color online) Phase diagram depicting the variation of f_{clus} with respect to the ε and the average degree ($\langle k_2 \rangle$) for SF network, multiplexed with (a) random network, (b) SF network, and (c) 1-d lattice. The average degree of the first layer ($\langle k_1 \rangle$) remains same for all three cases. For all the layers $N = 100$ and phase diagrams are plotted for average over 20 random realizations of the networks and initial conditions.

being represented by sparse networks. Additionally, multiplex network yields the chaotic dynamics for almost all the coupling values for the layers being represented by sparse networks (Fig. 5.3). Note that the synchronizability of the second layer, represented as the ER random network, always increases with an increase in the average degree as observed for the isolated networks.

Next we discuss the cluster synchronizability of the 1-d lattice upon multiplexing with various other network architectures. At the weak couplings, multiplexing with the SF networks and 1-d lattice lead to an enhancement in the cluster synchronizability as observed for the multiplexing with the ER random network. At the strong couplings, there is an enhancement in the synchronization for sparse networks as observed for the multiplexing with the random networks but the connection density for which this enhancement occurs becomes lower. For example, a 1-d lattice with $\langle k_1 \rangle = 4$, exhibits no enhancement in the cluster synchronization upon multiplexing with the 1-d lattice and SF networks with $\langle k_2 \rangle \gtrsim 4$ and $\langle k_2 \rangle \gtrsim 6$ respectively (Fig. 5.2(c),(b))). Thus the enhancement in the cluster synchronizability of the 1-d lattice is least favourable when it is multiplexed with the 1-d lattice and favourable being multiplexed with the random networks.

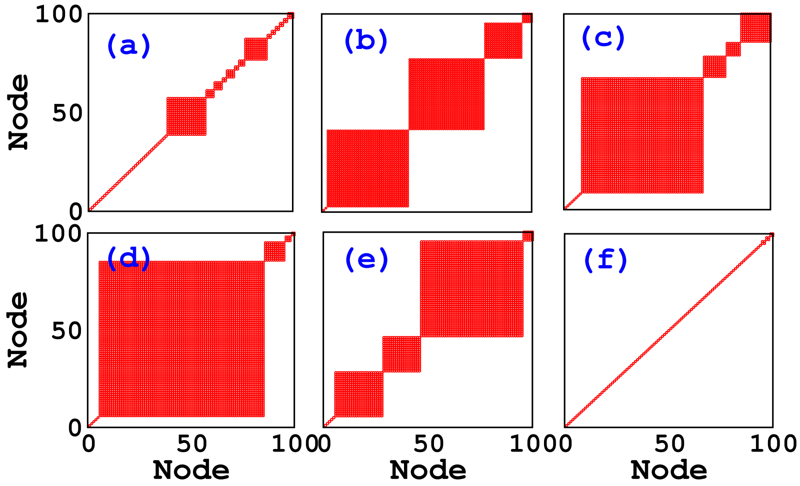

Figure 5.5: (Color online) Node versus node diagram (a) for the isolated SF network with $N = 100$ and $\langle k_1 \rangle = 2$, (b), (c), (d), (e) and (f) after multiplexing with a layer represented by ER random network with $\langle k_2 \rangle = 4, 6, 8, 10, 16$ respectively at $\varepsilon = 0.8$. In each case nodes numbers are reorganized so that the nodes belonging to the same cluster are numbered consecutively.

5.1.2 Cluster synchronizability of random networks upon multiplexing

Further, we study cluster synchronizability of SF networks upon multiplexing with various network architecture. The isolated sparse SF networks are known to exhibit a better cluster synchronizability as compared to the sparse regular or random networks (Fig. 5.4).

At the weak couplings, the multiplexing with another network only changes the cluster pattern and does not bring any enhancement in the cluster synchronization. For example the isolated SF networks with $\langle k_1 \rangle = 4$ and $N = 100$ lead to the participation of about 50% nodes in the cluster formation. After multiplexing, the same fraction of the nodes keep participating in the cluster formation as shown by the reappearance of the grey shade in the Fig. 5.4(b). At the intermediate and strong couplings, there is an enhancement in the synchronization for multiplexing with the sparse networks whereas impact of multiplexing with the dense networks is largely depend on the network architecture. For example, the cluster synchronizability of SF networks with $\langle k_1 \rangle = 4$ enhances upon the multiplexing with random and SF networks up to a certain limit of $\langle k_2 \rangle$. The multiplexing with the random and SF

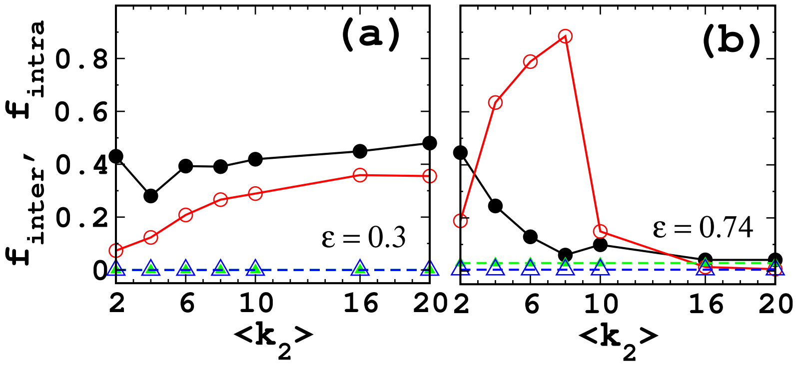

Figure 5.6: (Color online) Variation of f_{inter} and f_{intra} with $\langle k_2 \rangle$ for isolated 1-d lattice (closed and open triangles) with $N = 100$ and $\langle k_1 \rangle = 4$ and after multiplexing with a random network (closed and open circles) with various average degrees ($\langle k_2 \rangle$). Value of ε are chosen such that they exhibit an enhancement in the D synchronization and enhancement in the SO synchronization followed by a suppression at the strong couplings with an increase in $\langle k_2 \rangle$. All the graphs are plotted for average over 20 different realizations of network and initial conditions.

networks enhances the cluster synchronizability for $\langle k_2 \rangle \lesssim 40$ (Fig. 5.4(a) and (b)), while in the case of multiplexing with the 1-d lattice the enhancement occurs for $\langle k_2 \rangle \lesssim 10$ (Fig. 5.4(c)). For the higher connection density there is a suppression in the synchronization. This shows that the cluster synchronizability of the SF network is more favorable when it is multiplexed with the random and SF networks. The multiplexing also completely changes the cluster pattern. For example that at $\varepsilon = 0.8$ the isolated network exhibits few less nodes forming the cluster with the sizes of all the clusters being very small (Fig. 5.5(a)). The size of the largest cluster is 20. Multiplexing with the random networks of $\langle k_2 \rangle = 4, 6, 8, 10$, enhances the number of nodes forming the cluster as well as the size of the clusters (Figs. 5.5(b), (c), (d) and (e)). For $\langle k_2 \rangle \gtrsim 16$ synchronization suppresses completely (Figs. 5.5(f)). Furthermore, multiplexing of ER random networks with different network architectures at the weak couplings exhibit the similar behavior as observed for the 1-d lattice, whereas the strong couplings lead to the similar behavior as discussed for the SF networks. What follows that multiplexing of random (SF and ER) networks with 1-d lattice favours more to the cluster synchronizability as compared to multiplexing with the random networks.

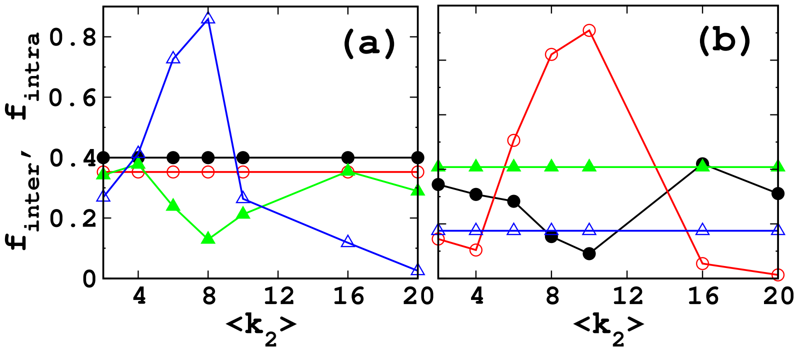

Figure 5.7: (Color online) Variation of f_{inter} and f_{intra} with $\langle k_2 \rangle$ for isolated SF network (closed and open triangles) with $N = 100$, $\langle k_1 \rangle = 4$ and for SF network after multiplexing (closed and open circles) with random networks at $\varepsilon = 0.74$ (a) and $\varepsilon = 1.0$ (b). All the graphs are plotted for an average over 20 different realizations of network and initial conditions.

5.2 Analytical understanding

In the following, we explore the reasons behind the impact of change in the density of connections in the second layer on the cluster synchronizability of first layer at strong couplings by using a simple case. The difference variable, of two nodes in the first layer at $\varepsilon = 1$, can be written as,

$$\begin{aligned} x_i^1(t+1) - x_j^1(t+1) = \frac{1}{k_i^1+1}(\sum_{j=1}^{N}(A_{ij}^1 f(x_i^1(t)))) - \\ \frac{1}{k_j^1+1}(A_{ji}^1 f(x_j^1(t))) + (\frac{1}{k_i^1+1} f(x_i^2(t) - \\ \frac{1}{k_j^1+1} f(x_j^2(t)))), \end{aligned} \tag{5.2}$$

where superscripts 1 and 2 stand for the first and second layer respectively. If global synchronization is achieved in the second layer, due to its denseness, in the above variable the coupling term having contribution from the second layer will get cancel out provided these pair of nodes have same degree ($k_i = k_j$). Consequently the synchronization between two nodes will depend only on the properties of isolated network. For example, the sparse 1-d lattice upon multiplexing with dense random networks exhibits no cluster synchronization at the strong couplings upon multiplexing, as observed for the isolated network (Fig. 5.2(a)).

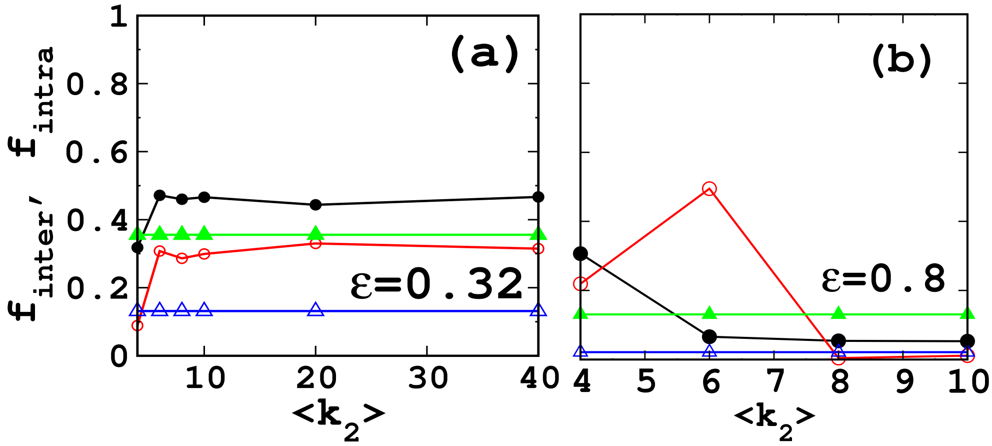

Figure 5.8: (Color online) Variation of f_{inter} and f_{intra} with $\langle k_2 \rangle$ for random networks with $N = 500$, $\langle k_1 \rangle = 4$ (a) and 1-d lattice with $N = 500$, $\langle k_1 \rangle = 6$ (b). The closed and open triangles represent values of f_{inter} and f_{intra} respectively for the isolated random network (a) and for isolated 1-d lattice (b). The closed and open circles represent values of f_{inter} and f_{intra} respectively for the random network after multiplexing with the SF network (a) and 1-d lattice after multiplexing with the random network (b). All the graphs are plotted for average over 20 different realizations of network and initial conditions.

5.3 Mechanism of cluster formation upon multiplexing

Furthermore, we study the change in the mechanism behind the cluster formation due to multiplexing. At weak couplings, the D synchronization remains the prime mechanism behind the cluster formation after multiplexing (Fig. 5.6(a)) as observed for the isolated networks [57, 58], while at the intermediate and strong couplings the connection density of the second layer plays an important role. In this coupling regime, multiplexing may lead to a change in the mechanism of cluster formation. For example, for the isolated sparse networks mixed or dominant D is the main mechanism behind the cluster formation [57], while upon multiplexing there is transition to the dominant SO mechanism for a certain limit of $\langle k_2 \rangle$. The 1-d lattice of $\langle k_1 \rangle = 4$ exhibits a transition from the dominant D to dominant SO mechanism upon multiplexing with random network for $\langle k_2 \rangle \lesssim 10$ (Fig. 5.6(b)). SF networks exhibit the transition from the mixed clusters state to dominant SO clusters state upon multiplexing with the random network for $\langle k_2 \rangle \lesssim 8$ at the intermediate cou-

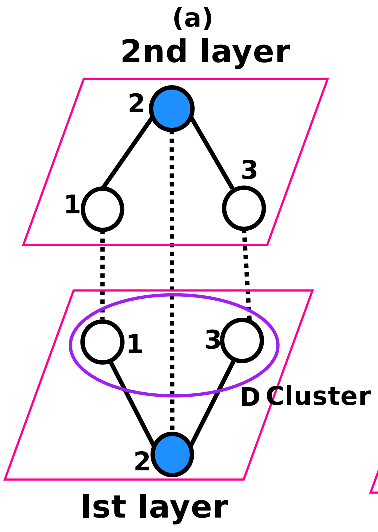

Figure 5.9: Schematic diagrams depicting a multiplex network with three nodes in each layer. (a) formation of D cluster (nodes within the circle) when node 2 is synchronized with its counter part (denoted with same color, (b) complete suppression in synchronization due to synchronization between the all the nodes (denoted with same color).

plings (Fig. 5.7(a)) and transition from the dominant D clusters state to dominant SO clusters state for $\langle k_2 \rangle \lesssim 10$ at the strong couplings (Fig. 5.7(b)). The multiplexing with the dense networks leads to a suppression in cluster synchronization but the mechanism behind cluster formation remains the same (Fig. 5.6(b)).

Using a simple multiplex network having three nodes in each layer, we provide an understanding to this impact of multiplexing on the mechanism behind the cluster formation. Numerical simulation of three nodes multiplex network (Fig.5.9) indicates that the synchronization among the nodes in the same layer is suppressed due to an enhancement in the synchronization between the nodes of the different layers. What follows that the suppression in the SO synchronization at the strong couplings occurs due to the synchronization between nodes which are counter part of each other in different layers, whereas the D synchronization between a pair of node remains unaffected due to the same coupling environment they receive. As in Fig. 5.9(a), occurrence of synchronization between node 2 in first layer with its counter part in the second layer suppresses the synchronization between nodes 2, 3 and 2, 1 while the nodes 1 and 3 remain synchronized as these nodes still receive a common coupling from node 2.

Further, in order to demonstrate the impact of size and robustness of the phenomena discussed above for large network size, we present results for $N = 500$. At the weak coupling range, the cluster synchronization always enhances with the dominant D being the mechanism behind the cluster formation (Fig.5.8(a)) and at the strong coupling the multiplexing with the sparse networks enhances the cluster synchronization with the dominant SO being the mechanism behind the cluster formation (Fig.5.8(a)). The network parameters for which the multiplexing imposes a change in the dynamical behavior may change with an increase in the network size but the results remain same. For example, the limit of $\langle k_2 \rangle$, for which there is an enhancement in the synchronization at the strong couplings, depends on the network properties such as the average degree and the size of the network. For 1-d lattice with $N = 500$ and $\langle k_1 \rangle = 6$, there is an enhancement in the synchronization upto $\langle k_2 \rangle < 8$ (Fig. 5.8) upon multiplexing with the random network, while for the 1-d lattice of $N = 100$ and $\langle k_1 \rangle = 4$ the enhancement occurs for $\langle k_2 \rangle < 10$ (Fig. 5.2) upon multiplexing.

5.4 Conclusion

To conclude, we have studied the impact of multiplexing on the cluster synchronizability and mechanism behind the synchronization of a layer in the simplest multiplex network consisting of two layers. We find that at weak couplings, the multiplexing enhances the cluster synchronizability, while at the strong couplings this enhancement depends on the architecture as well as the connection density of the another layer. The cluster synchronizability of a layer is enhanced when another layer has a moderate connection density. Moreover, multiplexing favors to the enhancement in the cluster synchronization when multiplexed with the random network. The enhancement in the cluster synchronization is also associated with the change in the mechanism of the cluster formation. The multiplexing primarily influences the synchronization between the nodes which are directly connected while leaving the synchronization between other pairs of nodes unaffected.

Our work demonstrates that in a multiplex network, the activity in a layer (sub-network) is significantly influenced by the structural properties of another layer (sub-network). If connection density in one layer increases above a certain limit, it may spoil the synchronization in the another layer. The results presented here, about dynamical behavior of multiplex networks, may provide a guidance for the construction of a better model networks with multiplex architecture, such as the airport networks composing different airline companies [185].

Bibliography

[1] Pikovsky A., Rosenblum M., Kurths J., Hilborn R. C. (2002), Synchronization: A universal concept in nonlinear sciences, Vol. 2, Cambridge University Press, Cambridge (ISBN: 9780511074417).

[2] Huygens C. (1673), Horologium Oscillatorium sive De Motu Pendulorum ad Horologia aptato Demostrationes Geometricae, Pars Tertia. Oeuvres Complétes de Christiaan Huygens, 18.

[3] Aldridge J., Pye E. K. (1976), Cell density dependence of oscillatory metabolism, Nature, **259**, 670-671 (DOI: 10.1038/259670a0).

[4] Strogatz S. H., Stewart I. (1993), Coupled oscillators and biological synchronization, Sci. Am., **269**, 102-109 (DOI: 10.1038/scientificamerican1293-102).

[5] Varela F., Lachaux J. P., Rodriguez E., Martinerie J. (2001), The brainweb: phase synchronization and large-scale integration, Nat. Rev. Neurosciene, **2(4)**, 229-239 (DOI: 10.1038/35067550).

[6] Malinen S., Hlushchuk Y., Hari R. (2007), Towards natural stimulation in fMRI-issues of data analysis, Neuroimage, **35(1)**, 131-139 (DOI: 10.1016/j.neuroimage.2006.11.015).

[7] Kauppi J. P., Jääskeläinen I. P., Sams M., Tohka J. (2010), Inter-subject correlation of brain hemodynamic responses during watching a movie: localization in space and frequency, Frontiers in Neuroinformatics, **4**, 5 (DOI: 10.3389/fninf.2010.00005).

[8] Nummenmaa L., Glerean E., Viinikainen M., Jääkeläinen I. P., Hari R., Sams M. (2012), Emotions promote social interaction by synchronizing brain activity across individuals, Proc. Natl. Acad. Sci. USA, **109(24)**, 9599-9604 (DOI: 10.1073/pnas.1206095109).

[9] Gellings C. W., Yeager K. E. (2004), Transforming the electric infrastructure, Phys. Today, **57(12)**, 45-51 (DOI: 10.1063/1.1878334).

[10] Strogatz, S., (2003) Sync: The emerging science of spontaneous order, Hyperion Press, Vol. 51, No. 3, pp. 312-319 (ISBN: 0-7868-6844-9).

[11] Lozano S., Buzna L., Díaz-Guilera A. (2012), Role of network topology in the synchronization of power systems, Eur. Phys. J. B, **85(7)**, 1-8 (DOI: 10.1140/epjb/e2012-30209-9).

[12] Rohden M., Sorge A., Timme M., Witthaut D. (2012), Self-organized synchronization in decentralized power grids, Phys. Rev. Lett., **109(6)**, 064101 (DOI: 10.1103/PhysRevLett.109.064101).

[13] Motter A. E., Myers S. A., Anghel M., Nishikawa T. (2013), Spontaneous synchrony in power-grid networks, Nature Phys., **9**, 191-197, (DOI: 10.1038/NPHYS2535).

[14] Boccaletti, S., (2008) The synchronized dynamics of complex systems, Vol. 6, Elsevier, Amsterdam, (ISBN: 9780444527431).

[15] Strogatz S. H., Abrams D. M., McRobie A., Eckhardt B., Ott E. (2005), Theoretical mechanics: Crowd synchrony on the Millennium Bridge, Nature, **438(7064)**, 43-44 (DOI: 10.1038/438043a).

[16] Buck J. (1988), Synchronous rhythmic flashing of fireflies. II, Quarterly review of biology, **63(3)**, 265-289 (DOI: 10.1086/394562).

[17] Strogatz S. H. (2001), Exploring complex networks, Nature, **410(6825)**, 268-276 (DOI:10.1038/35065725).

[18] Eckhouse V., Fridman M., Davidson N., Friesem A. A. (2008), Loss enhanced phase locking in coupled oscillators, Phys. Rev. Lett., **100(2)**, 024102 (DOI: 10.1103/PhysRevLett.100.024102).

[19] Fridman M., Nixon M., Davidson N., Friesem A. A. (2010), Passive phase locking of 25 fiber lasers, Opt. Lett., **359**, 1434-1436 (DOI: 10.1364/OL.35.001434).

[20] Boccaletti S., (2008) The Synchronized Dynamics of Complex Systems, Elsevier Science Ltd., Vol. 6. (ISBN: 978-0-444-52743-1).

[21] Arenas A., Díaz-Guilera A., Kurths J., Moreno Y., Zhou C. (2008), Synchronization in complex networks, Phys. Rep., **469(3)**, 93-153 (DOI: 10.1016/j.physrep.2008.09.002).

[22] Blasius B., Huppert A., Stone L. (1999), Complex dynamics and phase synchronization in spatially extended ecological systems, Nature, **399(6734)**, 354-359 (DOI: 10.1038/20676).

[23] Nixon M., Friedman M., Ronen E., Friesem A. A., Davidson N., Kanter I. (2011), Synchronized cluster formation in coupled laser networks, Phys. Rev. Lett., **106(22)**, 223901 (DOI: 10.1103/PhysRevLett.106.223901).

[24] Newman M. E. J., Strogatz S. H., Watts D. J. (2001), Random graphs with arbitrary degree distributions and their applications, Phys. Rev. E, **64**, 026118 (DOI: 10.1103/PhysRevE.64.026118).

[25] Redner S. (1998), How popular is your paper? An empirical study of the citation distribution, Eur. Phys. J. B, **4**, 131-134 (DOI: 10.1007/s100510050359).

[26] Newman M. E. J., (2010) Networks: an introduction, first ed., Oxford University Press, London, (ISBN: 978-0199206650).

[27] Albert R., Barabási A. L. (2002), Statistical mechanics of complex networks, Rev. of Mod. Phys., **74**, 47-97 (DOI: 10.1103/RevModPhys.74.47).

[28] Goh K. I., Cusick M. E., Valle D., Childs B., Vidal M., Barabási A. L. (2007), The human disease network, Proc. Natl. Acad. Sci. USA, **104(21)**, 8685-8690 (DOI: 10.1073/pnas.0701361104).

[29] Rai A., Menon A. V., Jalan S. (2014), Randomness and preserved patterns in cancer network, Sci. Rep., **4**, 6368 (DOI: 10.1038/srep06368).

[30] Castellano C., Pastor-Satorras R. (2010), Thresholds for epidemic spreading in networks, Phys. Rev. Lett., **105**, 218701 (DOI: 10.1103/PhysRevLett.105.218701).

[31] Pastor-Satorras R., Vespignani A. (2001), Epidemic spreading in scale-free networks, Phys. Rev. Lett., **86**, 3200 (DOI: 10.1103/PhysRevLett.86.3200).

[32] Schnettler S. (2009), A structured overview of 50 years of small-world research, Social Networks, **31(3)**, 165-178 (DOI: 10.1016/j.socnet.2008.12.004).

[33] Watts D. J., Strogatz S. H. (1998), Collective dynamics of ‘small-world networks, Nature, **393(6684)**, 440-442 (DOI: 10.1038/30918).

[34] Abello J., Pardalos P. M., Resende M. G. C., (1999), in External Memory Algorithms, edited by J. Abello and J. Vitter, DIMACS Series in Discrete Mathematics Theoretical Computer Science (American Mathematical Society), p. 119.

[35] Lawrence S., Giles C. L. (1998), Searching the world wide web, Science, **280(5360)**, 98-100 (DOI: 10.1126/science.280.5360.98).

[36] Barabási A. L., Albert R. (1999), Emergence of scaling in random networks, Science, **286**, 509-512 (DOI: 10.1126/science.286.5439.509).

[37] Gade P. M., Cerdeira H. A., Ramaswamy R. (1995), Coupled maps on trees, Phys. Rev. E, **52**, 2478 (DOI: 10.1103/PhysRevE.52.2478).

[38] Van Santen R. A. (1982), Localisation criterion in the Cayley tree without electron-electron interactions, J. Phys. C:Solid State Phys., **15(16)**, L513 (DOI: 10.1088/0022-3719/15/16/001).

[39] Hasegawa T., Nemoto K. (2007), Ising model on the scale-free network with a cayley-tree-like structure, Phys. Rev. E, **75**, 026105 (DOI: 10.1103/PhysRevE.75.026105).

[40] Anderson R. W., Neumann A. U., Perelson A. S. (1993), A Cayley tree immune network model with antibody dynamics, Bull Math Biol, **55**, 1091-1131 (DOI: 10.1007/BF02460701).

[41] Allegra M., Giorda P. (2012), Topology and energy transport in networks of interacting photosynthetic complexes, Phys. Rev. E, **85**, 051917 (DOI: 10.1103/PhysRevE.85.051917)

[42] Fidaleo F. (2012), Harmonic analysis on Cayley Trees II: the Bose Einstein condensation, Infin. Dimens. Anal. Quantum. Probab. Relat. Top., **15(04)**, 1250024 (DOI: 10.1142/S0219025712500245).

[43] Pan R. K., Sinha S., Kaski K., Saramäki J. (2012), The evolution of interdisciplinarity in physics research, Sci. Rep., **2**, 551 (DOI: 10.1038/srep00551).

[44] Mehta D. P., Sahni S., (2004) Handbook of data structures and applications, Chapman and Hall/CRC Press (ISBN: 9781584884354).

[45] Fujisaka H., Yamada T. (1983), Stability Theory of Synchronized Motion in Coupled-Oscillator Systems, Prog. Theor. Phys., **69**, 32-47 (DOI: 10.1143/PTP.69.32).

[46] Boccalettia S., Kurthsc J., Osipovd G., Valladaresb D.L., Zhouc C.S (2002), The synchronization of chaotic systems, Phys. Rep., **366**, 1-101, (DOI: 10.1016/S0370-1573(02)00137-0).

[47] Rosenblum M. G., Pikovsky A. S., Kurths J. (1997), From Phase to Lag Synchronization in Coupled Chaotic Oscillators, Phys. Rev. Lett., **78(22)**, 4193-4196 (DOI: 10.1103/PhysRevLett.78.4193).

[48] Rosenblum M. G., Pikovsky A. S., Kurths J. (1995), Phase Synchronization of Chaotic Oscillators, Phys. Rev. Lett., **76**, 1804-1807 (DOI: 10.1103/PhysRevLett.76.1804).

[49] Rulkov F., Sushchik M.M., Tsimring Lev S. (1995), Generalized synchronization of chaos in directionally coupled chaotic systems, Phys. Rev. E, **51**, 980-994 (DOI: 10.1103/PhysRevE.51.980).

[50] Dolby A. S., Grubb T. C. (1998), Benefits to satellite members in mixed species foraging groups: an experimental analysis, Anim. Behav., **56**, 501509 (DOI: 10.1006/anbe.1998.0808).

[51] Blasius B., Huppert A., Stone, L. (1999), Complex dynamics and phase synchronization in spatially extended ecological systems, Nature, **399(6734)**, 354-359 (DOI: 10.1038/20676).

[52] Schnitzler A., Gross J. (2005), Normal and pathological oscillatory communication in the brain, Nat. Rev. Neurosci, **6(4)**, 285-296 (DOI:10.1038/nrn1650).

[53] Hegselmann R., Krause U. (2002), Opinion dynamics and bounded confidence: models, analysis and simulation, J. Artif. Soc. Soc. Simulat., **5**, 1-24 (DOI: 10.1006/anbe.1998.0808).

[54] Xia W., Cao, M. (2010), Cluster synchronization algorithms, ACC, 6513-6518 (DOI: 10.1109/ACC.2010.5531433).

[55] Xia W., Cao M. (2011), Clustering in diffusively coupled networks, Automatica, **47(11)**, 2395-2405 (DOI: 10.1016/j.automatica.2011.08.043).

[56] Jalan S., Amritkar R. E. (2003), Self-organized and driven phase synchronization in coupled maps, Phys. Rev. Lett., **90(1)**, 014101 (DOI: 10.903/PhysRevLett.90.014101).

[57] Jalan S., Amritkar R. E., Hu C. K. (2005), Synchronized clusters in coupled map networks. I. Numerical studies, Phys. Rev. E, **72(1)**, 016211 (DOI: 10.1103/PhysRevE.72.016211).

[58] Amritkar R. E., Jalan S., Hu C. K. (2005), Synchronized clusters in coupled map networks. II. Stability analysis, Phys. Rev. E, **72(1)**, 016212 (DOI: 10.1103/PhysRevE.72.016212).

[59] Ji P., Peron T. K. D., Menck P. J., Rodrigues F. A., Kurths, J. (2013), Cluster explosive synchronization in complex networks, Phys. Rev. Lett., **110**, 218701 (DOI: 10.1103/PhysRevLett.110.218701).

[60] Osipov G. V., Pikovsky A. S., Rosenblum M. G., Kurths, J. (1997), Phase synchronization effects in a lattice of nonidentical Rössler oscillators, Phys. Rev. E, **55**, 2353 (DOI: 10.1103/PhysRevE.55.2353).

[61] Manrubia S. C., and Mikhailov A. S. (1999), Mutual synchronization and clustering in randomly coupled chaotic dynamical networks, Phys. Rev. E., **60(2)**, 1579 (DOI: 10.1103/PhysRevE.60.1579).

[62] Zhao, M., Zhou, C., L$\ddot{u}$, J., Lai, C. H. (2011). Competition between intra-community and inter-community synchronization and relevance in brain cortical networks. Physical Review E, **84(1)**, 016109 (DOI: 10.1103/PhysRevE.84.016109)

[63] Strogatz S. H. (1998), Nonlinear dynamics: Death by delay, Nature, **394**, 316-317 (DOI: 10.1038/28488).

[64] Lakshmanan, M., Senthilkumar, D. V., (2011) Dynamics of nonlinear time-delay systems, Springer Science and Business Media, New York (ISBN: 9783642149375).

[65] Kandel, E. R., Schwartz, J. H., T. M. Jessell, (1991) Principles of neural science, 3rd edn. Elsevier, New York (ISBN: 0444015620).

[66] Dhamala M., Jirsa V. K., Ding M. (2004), Enhancement of neural synchrony by time delay, Phys. Rev. Lett., **92**, 074104 (DOI: 10.1103/PhysRevLett.92.074104).

[67] Ng T. E., Zhang, H. (2002), Predicting Internet network distance with coordinates-based approaches, IEEE, **39**, 1482-1493 (DOI: 10.1109/26.103043).

[68] Stahlhut J. W., Browne T. J., Heydt G. T., Vittal V. (2008), Latency viewed as a stochastic process and its impact on wide area power system control signals, IEEE, **23**, 84-91 (DOI: 10.1109/TPWRS.2007.913210).

[69] Ali H., Dasgupta D. (2012), Effects of Time Delays in the Electric Power Grid, IFIP Advances, **390**, 139-154 (DOI: 10.1007/978-3-642-35764-0-11).

[70] Eurich C. W., Thiel A., Fahse L. (2005), Distributed delays stabilize ecological feedback systems, Phys. Rev. Lett., **94**, 158104 (DOI: 10.1103/PhysRevLett.94.158104).

[71] Wall E., Guichard F., Humphries A. R. (2013), Synchronization in ecological systems by weak dispersal coupling with time delay, Theoretical Ecology, **6(4)**, 405-418 (DOI: 10.1007/s12080-013-0176-6).

[72] Wünsche H. J., Bauer S., Kreissl J., Ushakov O., Korneyev N., Henneberger F., Wille E., Erzgräber H., Peil, M. Elsäer, W. Fischer, I. (2005), Synchronization of delay-coupled oscillators: A study of semiconductor lasers, Phys. Rev. Lett., **94(16)**, 163901 (DOI: 10.1103/PhysRevLett.94.163901).

[73] Carr T. W., Schwartz I. B., Kim M. Y., Roy R. (2006), Delayed-mutual coupling dynamics of lasers: scaling laws and resonances, SIAM J. Appl. Dyn. Syst., **5(4)**, 699-725 (DOI: 10.1137/050647918).

[74] Shahverdiev E. M., Shore, K. A. (2008), Chaos synchronization regimes in multiple-time-delay semiconductor lasers, Phys. Rev. E, **77(5)**, 057201 (DOI: 10.1103/PhysRevE.77.057201).

[75] Ramana Reddy D. V., Sen A., Johnston G. L. (1998), Time delay induced death in coupled limit cycle oscillators, Phys. Rev. Lett., **80(23)**, 5109 (DOI: 10.1103/PhysRevLett.80.5109).

[76] Bhowmick S. K., Ghosh D., Roy P., Dana S. K., Murali K., Sinha S., (2014), Targeting Temporal Patterns in Time-Delay Chaotic Systems, IJBC **24**, 1450014 (DOI: 10.1142/S021812741450014X).

[77] Punetha N., Karnatak R., Prasad A., Kurths J., Ramaswamy R. (2012), Frequency discontinuity and amplitude death with time-delay asymmetry, Phys. Rev. E, **85**, 046204 (DOI: 10.1103/PhysRevE.85.046204).

[78] Atay F. M., Karabacak (2006), Stability of coupled map networks with delays, SIAM J. Appl. Dyn. Sys., **5(3)**, 508-527 (DOI: 10.1137/060652531).

[79] Atay F. M. (2012), On delay-induced stability in diffusively coupled discrete-time systems, Afrika Matematika, **23**, 109-119 (DOI: 10.1007/s13370-011-0024-z).

[80] Atay F. M., Jost J., Wende A. (2004), Delays, connection topology, and synchronization of coupled chaotic maps. Phys. Rev. Lett., **92**, 144101 (DOI: 10.1103/PhysRevLett.92.144101).

[81] Schöll E., Hiller G., Hövel P., Dahlem M. A. (2009), Time-delayed feedback in neurosystems, Phil Trans. R. Soc. A, **367**, 1079-1096 (DOI: 10.1098/rsta.2008.0258).

[82] Dhamala M., Jirsa V. K., Ding M. (2004), Enhancement of neural synchrony by time delay, Phys. Rev. Lett., **92**, 074104 (DOI: 10.1103/PhysRevLett.92.074104).

[83] Shrii M. M., Senthilkumar D. V., Kurths J. (2012), Delay coupling enhances synchronization in complex networks, EPL, **98**, 10003 (DOI: 10.1209/0295-5075/98/10003).

[84] Sen M. K., Bag B. C., Petrosyan K. G., Hu C. K. (2010), Effect of time delay on the onset of synchronization of the stochastic Kuramoto model, J. Stat. Mech. **10**, P08018 (DOI: 10.1088/1742-5468/2010/08/P08018).

[85] Sethia G. C., Sen A., Atay F. M. (2008), Clustered chimera states in delay-coupled oscillator systems, Phys. Rev. Lett., **100**, 144102 (DOI: 10.1103/PhysRevLett.100.144102).

[86] Jalan S., Jost J., Atay F. M. (2006), Symbolic synchronization and the detection of global properties of coupled dynamics from local information, Chaos, **16(3)**, 033124 (DOI: 10.1063/1.2336415).

[87] Sethia G. C., Sen A., Atay F. M. (2008), Clustered chimera states in delay-coupled oscillator systems, Phys. Rev. Lett., **100**, 144102 (DOI: 10.1103/PhysRevLett.100.144102).

[88] Shiau Y. H., Peng Y. F., Cheng Y. C., Hu C. K. (2003), Multistability and chaos in a semiconductor microwave device with timedelay feedback, J. Phys. Soc. Japan, **72**, 801-804 (DOI: 10.1143/JPSJ.72.801).

[89] Dahms T., Lehnert J., and Schöll E. (2012), Cluster and group synchronization in delay-coupled networks, Phys. Rev. E, **86**, 016202 (DOI: 10.1103/PhysRevE.86.016202).

[90] Williams C. R., Murphy T. E., Roy R., Sorrentino F., Dahms T., Schöll, E. (2013), Experimental observations of group synchrony in a system of chaotic optoelectronic oscillators, Phys. Rev. Lett., **110**, 064104 (DOI: 10.1103/PhysRevLett.110.064104).

[91] Kinzel W. , Englert A. , Kanter I. (2009), On chaos synchronization and secure communication, Phil. Trans. R. Soc. A **368**, 379 (DOI: 10.1098/rsta.2009.0230).

[92] Prasad A., Kurths J., Ramaswamy R. (2008), The effect of time-delay on anomalous phase synchronization, Phys. Lett. A, **372**, 6150-6154 (DOI: 10.1016/j.physleta.2008.08.043).

[93] Höfener J. M., Sethia G. C., Gross T. (2013), Amplitude death in networks of delay-coupled delay oscillators, Phil. Trans. R. Soc. A, **371**, 1999 (DOI: 10.1098/rsta.2012.0462).

[94] Tank D. W., Hopfield J. J. (1987) Proc. Natl. Acad. Sci. USA **84**, 1896; *Epilepsy as a Dynamic Disease*, edited by J. Milton and P. Jung (Springer, Berlin, 2003). Tank, D. W., and Hopfield, J. J. (1987), Neural computation by concentrating information in time, PNAS, **84**, 1896-1900. Milton, J., and Jung, P. (Eds.). (2002). Epilepsy as a dynamic disease. Springer Science and Business Media. ISSN 1618-7210.

[95] Socolar J. E., Gauthier D. J. (1998), Analysis and comparison of multiple-delay schemes for controlling unstable fixed points of discrete maps, Phys. Rev. E, **57**, 6589 (DOI: 10.1103/PhysRevE.57.6589).

[96] Rosenblum M., Pikovsky A. (2004), Delayed feedback control of collective synchrony: an approach to suppression of pathological brain rhythms, Pikovsky, Phys. Rev. E, **70(4)**, 041904 (DOI: 10.1103/PhysRevE.70.041904)

[97] Ahlborn A., Parlitz U. (2007), Controlling spatiotemporal chaos using multiple delays, Phys. Rev. E, **75**, 065202 (DOI: 10.1103/PhysRevE.75.065202).

[98] Shahverdiev E. M., Shore K. A. (2008), Chaos synchronization regimes in multiple-time-delay semiconductor lasers, Phys. Rev. E, **77**, 057201 (DOI: 10.1103/PhysRevE.77.057201).

[99] Atay F. M., Jalan S., Jost J. (2010), Symbolic dynamics and synchronization of coupled map networks with multiple delays, Phys. Lett. A, **375**, 130-135 (DOI: 10.1016/j.physleta.2010.10.044).

[100] Masoller C., Atay F. M. (2011), Complex transitions to synchronization in delay-coupled networks of logistic maps, EPJ D, **62**, 119-126 (DOI: 10.1140/epjd/e2011-10370-7).

[101] Zigzag M., Butkovski M., Englert A., Kinzel W., Kanter I. (2010), Zero-lag synchronization and multiple time delays in two coupled chaotic systems, Phys. Rev. E, **81**, 036215 (DOI: 10.1103/PhysRevE.81.036215).

[102] Szalai R., Orosz G. (2013), Decomposing the dynamics of heterogeneous delayed networks with applications to connected vehicle systems, Phys. Rev. E, **88(4)**, 040902 (DOI: 10.1103/PhysRevE.88.040902).

[103] Rosin D. P., Rontani D., Gauthier D. J., Schöll E. (2013). Control of synchronization patterns in neural-like Boolean networks. Phys. Rev. Lett., **110**, 104102 (DOI: 10.1103/PhysRevLett.110.104102).

[104] Hong Y. *et al*, 1215 (2004). Hong Y., Lee M. W., Spencer P. S., Shore K. A. (2004), Synchronization of chaos in unidirectionally coupled vertical-cavity surface-emitting semiconductor lasers, Opt. Lett., **29**, 1215-1217 (DOI: 10.1364/OL.29.001215).

[105] May R. M., (2001) Stability and complexity in model ecosystems, Vol. 6, Princeton University Press, Oxfordshire, (ISBN: 0691081301).

[106] Bartlett M. S., Stochastic Population Models (Methuen and Co., London, 1960). Chesson P. (1991), Stochastic population models, In Ecological heterogeneity, pp. 123-143). Springer New York. (DOI: 10.1007/978-1-4612-3062-57) (Print ISBN 978-1-4612-7781-1)

[107] MacFadyen A., (1963) Animal Ecology: Aims and Methods, Pitman and Sons, London. Macfadyen A., Macfadyen A. (1957). Animal Ecology: aims and methods (pp. 215-218). Pitman and Sons, London.

[108] Atay F. M. (2003), Distributed delays facilitate amplitude death of coupled oscillators, Phys. Rev. Lett., **91**, 094101 DOI: 10.1103/PhysRevLett.91.094101).

[109] Kyrychko Y. N., Blyuss K. B., Schöll, E. (2013), Amplitude and phase dynamics in oscillators with distributed-delay coupling, Phil. Trans. R. Soc. A, **371**, 20120466 (DOI: 10.1098/rsta.2012.0466).

[110] Masoller C., Marti A. C. (2005), Random delays and the synchronization of chaotic maps, Phys. Rev. Lett., **94**, 134102 (DOI: 10.1103/PhysRevLett.94.134102).

[111] [107] Kaneko K. (1984), Period-Doubling of Kink-Antikink Patterns, Quasiperiodicity in Antiferro-Like Structures and Spatial Intermittency in Coupled Logistic Lattice Towards a Prelude of a Field Theory of Chaos, Prog. Theo. Phys., **72**, 480-486 (DOI: doi: 10.1143/PTP.72.480).

[112] Waller I., Kapral R. (1984), Spatial and temporal structure in systems of coupled nonlinear oscillators, Phys. Rev. A, **30**, 2047 (DOI: 10.1103/PhysRevA.30.2047).

[113] Kaneko K. (1986), Lyapunov analysis and information flow in coupled map lattices, Physica D, **23**, 436-447 (DOI: 10.1016/0167-2789(86)90149-1).

[114] Kaneko K. (1989), Pattern dynamics in spatiotemporal chaos: Pattern selection, diffusion of defect and pattern competition intermettency. Physica D, **34**, 1-41 (DOI: 10.1016/0167-2789(89)90227-3).

[115] Kaneko K. (1989), Chaotic but regular posi-nega switch among coded attractors by cluster-size variation, Phys. Rev. Lett., **63**, 219 (DOI: 10.1103/PhysRevLett.63.219).

[116] Kaneko K. (1990), Globally coupled chaos violates the law of large numbers but not the central-limit theorem, Phys. Rev. Lett., **65**, 1391 (DOI: 10.1103/PhysRevLett.65.1391).

[117] Kaneko K. (1990), Clustering, coding, switching, hierarchical ordering, and control in a network of chaotic elements, Physica D, **41**, 137-172 (DOI: 10.1016/0167-2789(90)90119-A).

[118] Kaneko K. (1998). On the strength of attractors in a high-dimensional system: Milnor attractor network, robust global attraction, and noise-induced selection. Physica D, **124**, 322-344 (DOI: 10.1016/S0167-2789(98)00205-X).

[119] Kaneko K. Formation, Dynamics and Statistics of Pattern, Edited by K. Kawasaki et al. (World Sci., Singapore, 1990); Chaos **2**, 279 (1992).

[120] Kessler D. A., Levine H. L., Reynolds W. N. (1990), Coupled-map lattice model for crystal growth, Phys. Rev. A, **42**, 6125 (DOI: 10.1103/PhysRevA.42.6125).

[121] Hendry R. J., McGlade J. M., Weiner, J. (1996), A coupled map lattice model of the growth of plant monocultures, Ecological modelling, **84**, 81-90 (DOI: 10.1016/0304-3800(94)00128-6).

[122] Aref, H. (1983), Integrable, chaotic, and turbulent vortex motion in two-dimensional flows, Ann. Rev. Fluid Mech., **15**, 345-389 (DOI: 10.1146/annurev.fl.15.010183.002021).

[123] Tsallis C., de Souza A. M. C., Curado E. M. F. (1995), Stock exchange: A statistical model, Chaos, Solitons and Fractals, **6**, 561-567 (DOI: 10.1016/0960-0779(95)80063-M).

[124] Palaniyandi P., Muruganandam P., Lakshmanan M. (2005), Desynchronized wave patterns in synchronized chaotic regions of coupled map lattices, Phys. Rev. E **72**, 037205 (DOI: 10.1103/PhysRevE.72.037205).

[125] Omelchenko I., Maistrenko Y., Hövel P., Schöll E., (2011), Loss of Coherence in Dynamical Networks: Spatial Chaos and Chimera States Phys. Rev. Lett. **106**, 234102 (DOI: 10.1103/PhysRevLett.106.234102).

[126] Bauer F., Atay F. M., (2010), Synchronized chaos in networks of simple units, EPL **89**, 20002 (DOI: 10.1029/0295-5075/89/20002).

[127] Grassberger P., (1999) Synchronization of coupled systems with spatiotemporal chaos, Phys. Rev. E **59**, R2520(R) (DOI: 10.1103/PhysRevE.59.R2520).

[128] Chaté H., Manneville P., (1988), Continuous and Discontinuous Transition to Spatio-Temporal Intermittency in Two-Dimensional Coupled Map Lattices, EPL **6**, 591 (DOI: 10.1209/0295-5075/6/7/004).

[129] Chaté H., Chaté P. M. H., Manneville P., (2001), Spatio-temporal intermittency in coupled map lattices, Physica D **32**, 409422 (DOI: 10.1016/0167-2789(88)90065-6).

[130] Hilborn R. C., (2000) Chaos and nonlinear dynamics: an introduction for scientists and engineers, Oxford university press, Oxford, (ISBN: 9780198507239).

[131] Ott E., (2002). Chaos in Dynamical Systems, 2nd edition, Cambridge Univ. Press, (ISBN : 0521811961).

[132] San Roman F.S.de S., Boccaletti S., Maza D., Mancini H., (1998), Erratum: Weak Synchronization of Chaotic Coupled Map Lattices, Phys. Rev. Lett. **81**, 3639 (DOI: http://dx.doi.org/10.1103/PhysRevLett.82.674).

[133] Zhao M., Zhou C., Chen Y., Hu B., Wang B., (2010), Complexity versus modularity and heterogeneity in oscillatory networks: Combining segregation and integration in neural systems, Phys. Rev. E., **82**, 046225 (DOI: 10.1103/PhysRevE.82.046225).

[134] Girvan M., Newman M. E. J. (2001), Community structure in social and biological networks, Proc. Natl. Acad. Sci. USA, **99**, 7821-7826 (DOI: 10.1073/Proc. Natl. Acad. Sci. U.S.A..122653799).

[135] Clauset A., Newman M. E. J., Moore C., (2004), Finding community structure in very large networks, Phys. Rev. E., **70**, 066111 (DOI: http://dx.doi.org/10.1103/PhysRevE.70.066111).

[136] Newman M.E.J., (2005), A measure of betweenness centrality based on random walks, Soc. Net., **27**, 39-54 (DOI:10.1016/j.socnet.2004.11.009).

[137] Newman M.E.J, (2006), Modularity and community structure in networks, Proc. Natl. Acad. Sci. USA, **103**, 8577-8582 (DOI: 10.1073 Proc. Natl. Acad. Sci. U.S.A..0601602103).

[138] Ravasz E., Somera A. L., Mongru D. A., Oltvai Z. N., Barabási A. L. (2002), Hierarchical organization of modularity in metabolic networks, Science, **297**, 1551-1555 (DOI: 10.1126/science.1073374); Guimera R., Amaral L. A. N. (2005), Functional cartography of complex metabolic networks, Nature, **433**, 895-900 (DOI: 10.1038/nature03288).

[139] Zhou C., and Kurths J. (2006), Hierarchical synchronization in complex networks with heterogeneous degrees, Chaos, **16**, 015104 (DOI: 10.1063/1.2150381).

[140] Arenas A., Díaz-Guilera A., Pérez-Vicente C. J. (2006), Synchronization reveals topological scales in complex networks, Phys. Rev. Lett., **96**, 114102 (DOI: 10.1103/PhysRevLett.96.114102).

[141] Gardeńes J.G., Moreno Y., Arenas A. (2007), Paths to synchronization on complex networks, Phys. Rev. Lett., **98**, 034101 (DOI: 10.1103/PhysRevLett.98.034101).

[142] Zhou C., Zemanová L., Zamora G., Hilgetag C. C., Kurths J. (2006), Hierarchical organization unveiled by functional connectivity in complex brain networks, Phys. Rev. Lett., **97**, 238103 (DOI: 10.1103/PhysRevLett.97.238103).

[143] Timme M. (2006), Does dynamics reflect topology in directed networks?, EPL, **76**, 367 (DOI: 10.1209/epl/i2006-10289-y).

[144] Nandi A., Santhosh G., Singh R. B., Ramaswamy R. (2007), Effective mechanisms for the synchronization of stochastic oscillators, Phys. Rev. E, **76**, 041136 (DOI: 10.1103/PhysRevE.76.041136).

[145] Amritkar R. E., Jalan S. (2005), Coupled dynamics on networks, Physica A, **346**, 13-19 (DOI: 10.1016/j.physa.2004.08.044).

[146] Jalan S., Jost J., Atay F. M. (2006), Symbolic synchronization and the detection of global properties of coupled dynamics from local information, Chaos, **16**, 033124 (DOI: 10.1063/1.2336415).

[147] Wiggins S. (2003) Introduction to applied nonlinear dynamical systems and chaos, Vol. 2, Springer Science and Business Media, Berlin, (ISBN: 0387001778).

[148] He R., Vaidya P. G. (1992), Analysis and synthesis of synchronous periodic and chaotic systems, Phys. Rev. A, **46(12)**, 7387 (DOI: 10.1103/PhysRevA.46.7387).

[149] Amritkar R. E., Hu C. K. (2006), Synchronized state of coupled dynamics on time-varying networks, Chaos, **16**, 015117 (DOI: 10.1063/1.2168395).

[150] Kestler J., Kinzel W., Kanter I. (2007), Sublattice synchronization of chaotic networks with delayed couplings, Phys. Rev. E, **76(3)**, 035202 (DOI: 10.1103/PhysRevE.76.035202).

[151] Kanter I., Kopelowitz E., Vardi R., Zigzag M., Kinzel W., Abeles M., Cohen D. (2011), Nonlocal mechanism for cluster synchronization in neural circuits, Europhys. Lett., **93(6)**, 66001 (DOI: 10.1209/0295-5075/93/66001).

[152] Motter A. E., Myers S. A., Anghel M., Nishikawa, T. (2013), Spontaneous synchrony in power-grid networks, Nature Phys., **9(3)**, 191-197 (DOI: 10.1038/nphys2535).

[153] Varela F., Lachaux J. P., Rodriguez E., Martinerie J. (2001), The brainweb: phase synchronization and large-scale integration, Nat. Rev. Neuroscience, **2(4)**, 229-239 (DOI: 10.1038/35067550).

[154] Suresh R., Senthilkumar D. V., Lakshmanan M., Kurths J. (2012), Global and Partial Phase Synchronizations in Arrays of Piecewise Linear Time-Delay Systems, IJBC, **22(07)** (DOI: 10.1142/S0218127412501787).

[155] Franović I., Todorović K., Vasović N., Burić N. (2012), Spontaneous formation of synchronization clusters in homogenous neuronal ensembles induced by noise and interaction delays, Phys. Rev. Lett., **108(9)**, 094101 (DOI: 10.1103/PhysRevLett.108.094101).

[156] Hf̈ener J. M., Sethia G. C., Gross T. (2011), Stability of networks of delay-coupled delay oscillators, EPL, **95(4)**, 40002 (DOI: 10.1209/0295-5075/95/40002).

[157] Ares S., Morelli L. G., Jörg D. J., Oates A. C., Jülicher F. (2012), Collective modes of coupled phase oscillators with delayed coupling, Phys. Rev. Lett., **108(20)**, 204101 (DOI: 10.1103/PhysRevLett.108.204101).

[158] Owens R. (1971), Industrialization and the Indian joint family, Ethnology, **10(2)**, 223-250.

[159] Vicente R., Gollo L. L., Mirasso C. R., Fischer I., Pipa G. (2008), Dynamical relaying can yield zero time lag neuronal synchrony despite long conduction delays, Proc. Natl. Acad. Sci. U.S.A., **105(44)**, 17157-17162 (DOI: 10.1073/Proc. Natl. Acad. Sci. U.S.A..0809353105).

[160] Busche M. A., Chen X., Henning H. A. *et. al.* (2012) Critical role of soluble amyloid-β for early hippocampal hyperactivity in a mouse model of Alzheimer's disease, Proc. Natl. Acad. Sci. U.S.A., **109(22)**, 8740-8745 (DOI: 10.1073/Proc. Natl. Acad. Sci. U.S.A..1206171109).

[161] Denison D., Lief C., Ward J. L. (2004), Culture in Family-Owned Enterprises: Recognizing and Leveraging Unique Strengths, Fam. Bus. Rev., **17**, 61-70 (DOI: 10.1111/j.1741-6248.2004.00004.x).

[162] Poutziouris P. Z., Smyrnios K. X., Klein S. B., (2008) Handbook of Research on Family Business, second ed. Edward Elgar Publishing (ISBN: 9781848443228).

[163] Zhou J., Liu Z. (2008), Synchronized patterns induced by distributed time delays, Phys. Rev. E, **77(5)**, 056213 (DOI: 10.1103/PhysRevE.77.056213).

[164] Barahona M., Pecora L. M. (2002), Synchronization in small-world systems, Phys. Rev. Lett., **89(5)**, 05410 (DOI: 10.1103/PhysRevLett.89.05410).

[165] Menck P. J., Heitzig J., Marwan N., Kurths J. (2013), How basin stability complements the linear-stability paradigm, Nature Physics, **9(2)**, 89-92 (DOI: 10.1038/nphys2516).

[166] Singh A., Jalan S., Kurths J. (2013), Role of delay in mechanism of cluster formation, Phys. Rev. E **87**, 030902(R) (DOI: 10.1103/PhysRevE.87.030902).

[167] Ashwin P., Buescu J., Stewart I. (1994), Bubbling of attractors and synchronisation of chaotic oscillators, Phys. Lett. A, **193(2)**, 126-139 (DOI: 10.1016/0375-9601(94)90947-4).

[168] Venkataramani S. C., Hunt B. R., Ott E. (1996), Bubbling transition, Phys. Rev. E, **54(2)**, 1346 (DOI: 10.1103/PhysRevE.54.1346).

[169] Acharyya S., Amritkar R. E. (2012), Synchronization of coupled nonidentical dynamical systems, EPL, **99(4)**, 40005 (DOI: 10.1209/0295-5075/99/40005).

[170] Cheng R., Peng M., Yu W., Sun B., Yu J. (2013), Stability analysis and synchronization in discrete-time complex networks with delayed coupling, Chaos, **23(4)**, 043108 (DOI: 10.1063/1.4825095).

[171] Buchner T., Źebrowski J. J. (2000), Logistic map with a delayed feedback: Stability of a discrete time-delay control of chaos, Phys. Rev. E, **63(1)**, 016210 (DOI: 10.1103/PhysRevE.63.016210).

[172] Singh A., Jalan S. (2013), Delay-induced cluster patterns in coupled Cayley tree networks, EPJ-ST, **222(3-4)**, 885-893 (DOI: 10.1140/epjst/e2013-01891-2).

[173] Pais-Vieira M., Lebedev M., Kunicki C.*et al* (2013) A brain-to-brain interface for real-time sharing of sensorimotor information, Sci. Rep., **3** (DOI: 10.1038/srep01319).

[174] Dumas G., Nadel J., Soussignan R. *et al* (2010) Inter-brain synchronization during social interaction, PloS one, **5(8)**, e36414 (DOI: 10.1371/journal.pone.0012166).

[175] Braak H., Braak E., Yilmazer D. *et al* (1996), Pattern of brain destruction in Parkinson's and Alzheimer's diseases, J. Neural. Transm., **103(4)**, 455-490 (DOI: 10.1007/BF01276421).

[176] Garzarelli F., Cristelli M., Pompa G., Zaccaria A., Pietronero L. (2014), Memory effects in stock price dynamics: evidences of technical trading, Sci. Rep., **4**, 4487 (DOI: 10.1038/srep04487).

[177] Grönlund A., Yi I. G., Kim B. J. (2012), Fractal profit landscape of the Stock Market, PloS one, **7(4)**, e33960 (DOI: 10.1371/journal.pone.0033960).

[178] Boccaletti S., Bianconi G., Criado R., Del Genio C. I., Gómez-Gardeñes J., Romance M., Sendiña-Nadal I., Wang Z., Zanin M. (2014), The structure and dynamics of multilayer networks, Phys. Rep., **544(1)**, 1-122 (DOI: 10.1016/j.physrep.2014.07.001).

[179] Szell M., Lambiotte R., Thurner S. (2010), Multirelational organization of large-scale social networks in an online world, Proc. Natl Acad. Sci., **107(31)**, 13636-13641 (DOI: 10.1073/Proc. Natl. Acad. Sci. U.S.A.).

[180] Barthélemy M. (2011), Spatial networks, Phys. Rep., **499(1)**, 1-101 (DOI: 10.1016/j.physrep.2010.11.002).

[181] Gómez-Gardenes J., Reinares I., Arenas A., Floría L. M. (2012), Evolution of cooperation in multiplex networks, Sci. Rep., **2**, 620 (DOI: 10.1038/srep00620).

[182] Granell C., Gómez S., Arenas A. (2013), Dynamical interplay between awareness and epidemic spreading in multiplex networks, Phys. Rev. Lett., **111**, 128701 (DOI: 10.1103/PhysRevLett.111.128701).

[183] Aguirre J., Sevilla-Escoboza R., Gutiérrez R., Papo D., Buldú J. M. (2014), Synchronization of interconnected networks: the role of connector nodes, Phys. Rev. Lett., **112**, 248701 (DOI: 10.1103/PhysRevLett.112.248701).

[184] Bogojeska A., Filiposka S., Mishkovski I., Kocarev L. (2013), On opinion formation and synchronization in multiplex networks, Telecommunications Forum (TELFOR), **2013 21st**, 172-175 (DOI: 10.1109/TELFOR.2013.6716200).

[185] Cardillo A., Gómez-Gardees J., Zanin M., Romance M., Papo D., del Pozo F., Boccaletti S. (2013), Emergence of network features from multiplexity, Sci. Rep., **3**, 1344 (DOI: 10.1038/srep01344).